LBL-22720 c.2

Lawrence Berkeley Laboratory
UNIVERSITY OF CALIFORNIA

EARTH SCIENCES DIVISION

RECEIVED
LAWRENCE
BERKELEY LABORATORY
MAR 2 1987
LIBRARY AND
DOCUMENTS SECTION

THE EFFECT OF CO_2 ON RESERVOIR BEHAVIOR FOR GEOTHERMAL SYSTEMS

S.W. Gaulke
(M.S. Thesis)

December 1986

TWO-WEEK LOAN COPY
This is a Library Circulating Copy
which may be borrowed for two weeks.

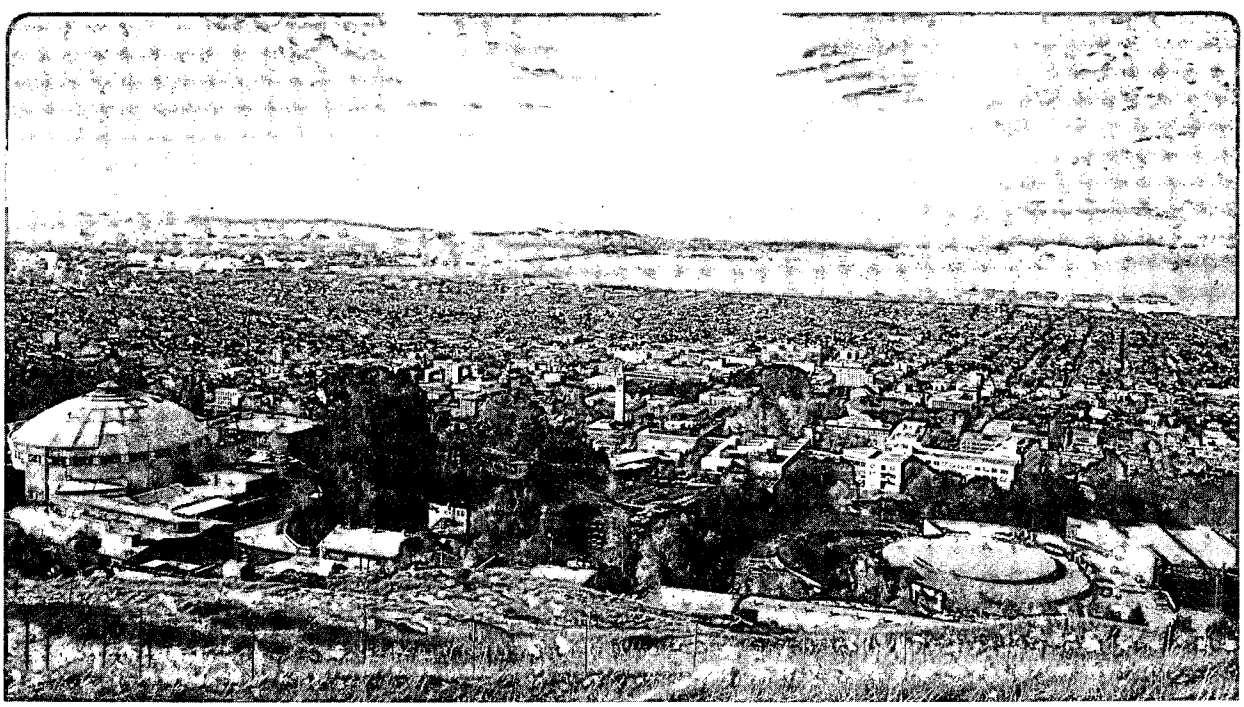

LBL-22720 c.2

Prepared for the U.S. Department of Energy under Contract DE-AC03-76SF00098

DISCLAIMER

This document was prepared as an account of work sponsored by the United States Government. While this document is believed to contain correct information, neither the United States Government nor any agency thereof, nor the Regents of the University of California, nor any of their employees, makes any warranty, express or implied, or assumes any legal responsibility for the accuracy, completeness, or usefulness of any information, apparatus, product, or process disclosed, or represents that its use would not infringe privately owned rights. Reference herein to any specific commercial product, process, or service by its trade name, trademark, manufacturer, or otherwise, does not necessarily constitute or imply its endorsement, recommendation, or favoring by the United States Government or any agency thereof, or the Regents of the University of California. The views and opinions of authors expressed herein do not necessarily state or reflect those of the United States Government or any agency thereof or the Regents of the University of California.

LBL-22720

THE EFFECT OF CO_2 ON RESERVOIR BEHAVIOR FOR GEOTHERMAL SYSTEMS

Scott W. Gaulke

Earth Sciences Division
Lawrence Berkeley Laboratory
University of California
Berkeley, California 94720

M.S. Thesis

December 1986

This work was supported by the U.S. Department of Energy under Contract Number DE-AC03-76SF00098.

Table of Contents

LIST OF FIGURES iv

LIST OF TABLES ix

NOMENCLATURE x

ACKNOWLEDGMENTS xi

1.0 INTRODUCTION 1

2.0 LITERATURE SURVEY 4

2.1 The Use of Gases to Analyze Geothermal Systems 4

2.2 The Use of Flowing Enthalpy to Characterize Geothermal Systems 10

3.0 ENTHALPY AND CO_2 TRANSIENTS IN FRACTURED RESERVOIRS 15

3.1 Introduction 15

3.2 Background 15

3.3 Approach 17

3.4 The Base Case 21

3.5 Initial Partial Pressure of CO_2 26

3.6 Bottomhole Pressure 32

3.7 Fracture Porosity 36

3.8 Matrix Porosity 40

3.9 Fracture Permeability-Thickness 44

3.10 Matrix Permeability 48

3.11 Initial Gas Saturation 54

3.12 Thermal Conductivity 58

3.13 Fracture Spacing 63

3.14 Relative Permeability Curves 68

3.15 Summary 73

4.0 FRACTURE-MATRIX INTERACTION AND FLUID RECOVERY FROM GAS-RICH RESERVOIRS 76

4.1 Introduction 76

4.2 Approach 76

4.3 Results 79

4.4 Radial Cases 90

4.5 Chemical Effects and/or Backflow 99

4.6 Injection Effects 100

4.7 Summary 105

5.0 FIELD EXAMPLE - WELL BR21, OHAAKI, NEW ZEALAND 107

5.1 Introduction 107

5.2 Reservoir and Well Description 109

5.3 The Well Data 112

5.4 Summary 118

6.0 CONCLUSION 120

REFERENCES 124

APPENDIX A 129

APPENDIX B 132

APPENDIX C 134

LIST OF FIGURES

Figure (3-1).	Relative permeability curves used in this study (S_{gr}=0.4, S_{lr}=0.05).	20
Figure (3-2).	Flowing enthalpy and formation pressure transients for the base case.	22
Figure (3-3).	Total kinematic mobility curves for matrix relative permeability curves with S_{gr}=0.4 and S_{lr}=0.05.	23
Figure (3-4).	Flowing enthalpy and flowing mass fraction of CO_2 transients for the base case.	24
Figure (3-5).	Mass fraction of CO_2 in liquid and gaseous phases (O'Sullivan et al, 1985).	25
Figure (3-6).	Effect of initial partial pressure of CO_2 on flowing enthalpy transients.	27
Figure (3-7).	Comparison of flowing enthalpy and formation pressure transients for initial partial pressures of CO_2 of 0.01 and 10 bars.	28
Figure (3-8).	Effect of initial partial pressure of CO_2 on mass flowrate transients.	29
Figure (3-9).	Effect of initial partial pressure of CO_2 on transients of the total flowing mass fraction of CO_2.	30
Figure (3-10).	Effect of initial partial pressure of CO_2 on the stable flowing mass fraction of CO_2.	31
Figure (3-11).	Effect of bottomhole pressure on mass flowrate transients with 10 bars initial partial pressure of CO_2 present.	33
Figure (3-12).	Effect of bottomhole pressure on flowing enthalpy transients with 10 bars initial partial pressure of CO_2 present.	34
Figure (3-13).	Effect of bottomhole pressure on transients of total flowing mass fraction of CO_2 with 10 bars initial partial pressure of CO_2 present.	35
Figure (3-14).	Effect of fracture porosity on flowing enthalpy transients with 10 bars initial partial pressure of CO_2 present.	37
Figure (3-15).	Effect of fracture porosity on transients of formation pressure with 10 bars initial partial pressure of CO_2 present.	38
Figure (3-16).	Effect of fracture porosity on transients of total flowing mass fraction of CO_2 with 10 bars initial partial pressure of CO_2 present.	39

Figure (3-17).	Effect of matrix porosity on flowing enthalpy transients with 10 bars initial partial pressure of CO_2 present.	41
Figure (3-18).	Effect of matrix porosity on flowing enthalpy transients without CO_2 present (Lippmann et al, 1985).	42
Figure (3-19).	Effect of matrix porosity on transients of total flowing mass fraction of CO_2 with 10 bars initial partial pressure of CO_2 present.	43
Figure (3-20).	Effect of fracture permeability-thickness product on flowing enthalpy transients with 10 bars initial partial pressure of CO_2 present.	45
Figure (3-21).	Effect of fracture permeability-thickness product on transients of total flowing mass fraction of CO_2 with 10 bars initial partial pressure of CO_2 present.	46
Figure (3-22).	Effect of fracture permeability-thickness product on mass flowrate transients with 10 bars initial partial pressure of CO_2 present.	47
Figure (3-23).	Effect of fracture permability-thickness product on flowing enthalpy transients without CO_2 present (Lippmann et al, 1985)	49
Figure (3-24).	Effect of matrix permeability on flowing enthalpy transients with 10 bars initial partial pressure of CO_2 present.	50
Figure (3-25).	Effect of matrix permeability on transients of total flowing mass fraction of CO_2 with 10 bars initial partial pressure of CO_2 present.	52
Figure (3-26).	Effect of matrix permeability on mass flowrate transients with 10 bars initial partial pressure of CO_2 present.	53
Figure (3-27).	Effect of initial gas saturation on flowing enthalpy transients with 10 bars initial partial pressure of CO_2 present.	55
Figure (3-28).	Effect of initial gas saturation on transients of total flowing mass fraction of CO_2 with 10 bars initial partial pressure of CO_2 present.	56
Figure (3-29).	Effect of initial gas saturation on mass flowrate transients with 10 bars partial pressure of CO_2 present.	57
Figure (3-30).	Effect of matrix thermal conductivity on flowing enthalpy transients without CO_2 present (Lippmann et al, 1985).	59

Figure (3-31).	Effect of matrix thermal conductivity on flowing enthalpy trasients with 10 bars initial partial pressure of CO_2 present.	60
Figure (3-32).	Effect of matrix thermal conductivity on transients of total flowing mass fraction of CO_2 with 10 bars initial partial pressure of CO_2 present.	61
Figure (3-33).	Effect of matrix thermal conductivity on mass flowrate transients with 10 bars initial partial pressure of CO_2 present.	62
Figure (3-34).	Effect of fracture spacing on flowing enthalpy transients with 10 bars initial partial pressure of CO_2 present.	64
Figure (3-35).	Effect of fracture spacing on formation pressure transients with 10 bars initial partial pressure of CO_2 present.	65
Figure (3-36).	Effect of fracture spacing on transients of total flowing mass fraction of CO_2 with 10 bars initial partial pressure of CO_2 present.	66
Figure (3-37).	Effect of fracture spacing on mass flowrate transients with 10 bars initial partial pressure of CO_2 present.	67
Figure (3-38).	Effect of fracture relative permeability curves on flowing enthalpy transients without CO_2 present (Lippmann et al, 1985).	69
Figure (3-39).	Effect of fracture relative permeability curves on flowing enthalpy transients with 10 bars initial partial pressure of CO_2 present.	70
Figure (3-40).	Effect of matrix relative permeability curves on flowing enthalpy transients with 10 bars initial partial pressure of CO_2 present.	71
Figure (3-41).	Effect of matrix relative permeability curves on transients of flowing mass fraction of CO_2 with 10 bars initial partial pressure of CO_2 present.	72
Figure (4-1).	Simple model of a matrix block surrounded by a fracture.	77
Figure (4-2).	Effect of initial partial pressure of CO_2 on recovery transients normalized by the by the initial mass in the matrix.	80
Figure (4-3).	Schematic results of changes in pressure, gas saturation, temperature, and CO_2 partial pressure with time for cases with and without chemical buffers in the matrix.	81
Figure (4-4).	Effect of gas saturation in the fracture on backflow of fluid to the matrix.	84

Figure (4-5).	Effect of total flowing mass fraction of CO_2 on the amount of backflow per unit pore volume for various final matrix gas saturations.	85
Figure (4-6).	Effect of flowing enthalpy on the amount of backflow per unit pore volume for various final matrix gas saturations.	86
Figure (4-7).	Effect of initial pressure gradient on intermittent recovery and recovery after backflow. Backflow is normalized by the mass necessary to fully saturate the matrix for various initial partial pressures of CO_2.	88
Figure (4-8).	Effect of initial gas saturation on recovery normalized by the mass necessary to fully saturate the matrix for various initial partial pressures of CO_2.	89
Figure (4-9).	Changes in gas saturation with time for various fracture and matrix elements without CO_2 present.	92
Figure (4-10).	Changes in gas saturation with time for various fracture and matrix elements with 10 bars of CO_2 present.	93
Figure (4-11).	Variations in the average matrix gas saturation with radial distance from the well.	95
Figure (4-12).	Changes in mass flowrate with time for the cases of no CO_2 and 10 bars initial CO_2 partial pressure.	96
Figure (4-13).	Changes in flowing enthalpy with time for the cases of 0 and 10 bars initial CO_2 partial pressure.	97
Figure (4-14).	Changes in gas saturation with time for various fracture and matrix elements with 10 bars initial partial pressure of CO_2 present and gaseous diffusion included.	98
Figure (4-15).	Changes in the flowing mass fraction of CO_2 in the steam phase with time for Krafla geothermal field, Iceland (Steingrimsson et al, 1984).	101
Figure (4-16).	Sketch of CO_2 distribution used to approximate conditions during injection of pure water into a reservoir with 10 bars initial partial pressure of CO_2.	102
Figure (4-17).	Changes in mass flowrate and total mass fraction of CO_2 with time.	104
Figure (5-1).	Changes in the downhole pressure, flowing mass fraction of CO_2, and flowing enthalpy for well BR21, Broadlands, New Zealand (Grant and Glover, 1984).	108
Figure (5-2).	Location map for Broadlands geothermal field on the north island of New Zealand. years.	110

Figure (5-3).	Location map of wells including temperature contours in Broadlands geothermal field, New Zealand (Ministry of Works and Development, Wellington).	111
Figure (5-4).	Cross section showing the geology surrounding well BR21, Broadlands geothermal field, New Zealand (Ministry of Works and Development, Wellington).	113
Figure (5-5).	Comparison of best fit model to measured results of changes in downhole pressure, flowing mass fraction of CO_2, and flowing enthalpy with time (Grant and Glover, 1984).	116
Figure (5-6).	Diagram of best fit model including important reservoir and fluid parameters.	119

LIST OF TABLES

Table (2-1).	Gas Content in Fluids From Various Geothermal Fields.	4
Table (3-1).	Constant Reservoir Parameters for Sensitivity Study.	18
Table (3-2).	Reservoir Parameters Varied in Sensitivity Study.	18
Table (4-1).	Reservoir Parameters Used to Study Recovery and Fracture-Matrix Interaction in Gas-Rich Geothermal Systems.	78
Table (5-1).	Parameters used to model the preformance of well BR21, Broadlands, New Zealand.	115

NOMENCLATURE

h_f	-	flowing enthalpy
h_g	-	enthalpy of the gas phase
h_l	-	enthalpy of the liquid phase
k_{rg}	-	gas phase relative permeability
k_{rl}	-	liquid phase relative permeability
M	-	total mass of fluid backflow
$M_{c,tot}$	-	total mass flow of CO_2
P	-	pressure adjacent to well for deliverability model
P_{wb}	-	bottomhole pressure for deliverability model
P.I.	-	productivity index
Q	-	mass flowrate of the total discharge
q_g	-	mass flowrate of the gas phase
q_l	-	mass flowrate of the liquid phase
S_g	-	gas saturation
S_{gr}	-	residual gas saturation
S_l	-	liquid saturation
S_{lr}	-	residual liquid saturation
S^*	-	variable for SGB relative permeability functions
V	-	total volume of rock in which backflow occurs
W_g	-	mass fraction of the gas phase
W_l	-	mass fraction of the liquid phase
X_c	-	total mass fraction of CO_2
X_{cg}	-	mass fraction of CO_2 in the gas phase
X_{cl}	-	mass fraction of CO_2 in the liquid phase
α (T)	-	temperature dependent Henry's coefficient
μ_g	-	viscosity of the gas phase
μ_l	-	viscosity of the liquid phase
ν_t	-	(total kinematic mobility)$^{-1}$
ρ_c	-	density of CO_2
ρ_g	-	density of the gas phase
ρ_l	-	density of the liquid phase
ρ_v	-	density of water vapor

Acknowledgments

I would like to thank my advisor, Dr. Paul A. Witherspoon, for his encouragement during my graduate studies. I am greatly indepted to Dr. G. S. Bodvarsson for his patient guidence and support throughout this research.

I am grateful to Cindy Lou Yates for her help and patience during the preparation of this manuscript.

This work was supported through U. S. Department of Energy Contract No. DE-AC03-76SF00098 by the Assistant Secretary for Conservation and Renewable Energy, Office of Renewable Technology, Division of Geothermal Technology.

1.0 Introduction

Since Italy first started producing electricity from geothermal steam in 1904, fourteen other countries have begun to harness it for the same purpose. The continuing instability in the world oil market has helped provide the impetus so that more than forty countries have become actively involved in geothermal energy exploration (Donovan, 1984). A substantial percentage of the energy requirements of Iceland, the Phillipines, and El Salvador are provided by the exploitation of geothermal resources (Barbier, 1985).

An economically successful exploitation of a geothermal reservoir is dependent on the proper characterization of the reservoir system. The rock characteristics can be determined through a combination of production tests and drilling data. However, due to the heterogeneity of reservoir systems it is necessary to use all the information available in understanding a system.

Most high-temperature geothermal reservoirs are highly fractured (DiPippo, 1980). They can differ substantially in behavior from homogeneous porous medium reservoirs (Kasameyer and Schroeder, 1976; Pruess and Narasimhan, 1982; Bodvarsson and Witherspoon, 1985; Lippmann et al, 1985). In a fractured reservoir, the early transients will be controlled by fluid stored within the fractures. Then, after a short initial period, the matrix will begin to contribute fluid to the fractures and production conditions will stabilize. This is because the fracture porosity represents just a small fraction of the total void space, so that overall fracture contribution of fluid and energy to the recovery is small. The rock matrix has a low flow capability, but it stores most of the heat and mass for the reservoir. Therefore, prolonged recovery is possible only if the rock matrix provides fluid to the fractures at a rate sufficient to sustain production. Using the conventional homogeneous porous medium techniques to evaluate a fractured reservoir is equivalent to assuming instantaneous equilibrium between fracture and matrix. This ignores the importance of fracture-matrix interactions on longterm well preformance. Therefore, techniques are needed to characterize

both fracture and matrix parameters in order to accurately predict the longevity of a reservoir.

Many geothermal reservoirs contain significant amounts of noncondensible gases. The concentration of gas ranges from 0.1 to 10 percent by mass of steam at separator conditions. The most abundant noncondensible gas in geothermal systems is CO_2 which typically accounts for more than 90 percent of the gas present (Kestin et al, 1980). Other significant gases include H_2S, N_2, NH_3, H_2, and CH_4. Appendix A provides a brief outline of the types of gases in geothermal systems and their primary sources.

Noncondensible gases can have large effects on conditions within a reservoir (Ellis, 1959; Sutton, 1976, O'Sullivan et al., 1985). Because CO_2 is poorly soluble in the liquid phase of water most of it resides in the gas phase. Therefore, the presence of CO_2 will expand two-phase zones within a reservoir. The total pressure in the gas phase is basically the sum of the partial pressures of water vapor and CO_2. Consequently, when CO_2 is present in a two-phase system, the saturation temperature is lower than that for a pure water system for the same total pressure.

Non-condensible gases can provide important information about a reservoir system. Many studies have shown that the gases within reservoir can be used to indicate the thermodynamic conditions, flow patterns, and to map recharge areas.

Reservoir rocks will react with reservoir fluids so that noncondensible gases can be valuable tools for characterizing the thermodynamic state of a system. Many publications have examined the chemically reactive constituents; CO_2, H_2S, NH_3, H_2, N_2, and CH_4. Since these constituents are subject to the influence of equilibration processes, their study has been shown to provide useful information on the deep temperature and pressure conditions within an unexploited reservoir where conditions have stabilized (Ellis, 1957; D'Amore and Nuti, 1977; Giggenbach, 1980; D'Amore and Panichi, 1980; Arnorsson and Gunnlaugsson, 1983; Andrews, 1983; Nehring and D'Amore, 1984; D'Amore and Truesdell, 1985; Marini et al, 1986). In a producing reservoir, where conditions are rapidly changing, studies have shown that non-reactive gases are

valuable as tracers for flow patterns within the reservoir (Mazor et al, 1982; Nuti, 1984; Mazor and Truesdell, 1984; D'Amore and Truesdell, 1984).

The purpose of this study is to gain further understanding of the effects of noncondensible gases (CO_2) in fractured two-phase geothermal systems. A thorough review of previous work on noncondensible gases is carried out. In addition, since the flowing mass fraction of CO_2 is strongly controlled by the flowing saturation, the flowing enthalpy literature is also reviewed. Numerical techniques are employed to examine how noncondensible gases (CO_2) affect well transients and to determine the value of these effects as tools to evaluate in situ reservoir parameters. Simplified reservoir models are used to define the effects of CO_2 in the reservoir and the resulting transient behavior at the feedzones to the well. Futhermore, fracture-matrix interaction is studied in detail to identify the effects of CO_2 on recovery and flow patterns within the reservoir. Finally, the insight gained from the sensitivity studies for enthalpy and CO_2 transients is applied to interpret transient data from well BR21 at the Broadlands geothermal field of New Zealand.

2.0 Literature Survey

2.1 The Use of Gases to Analyze Geothermal Systems

Reservoir systems are complex. Non-condensible gases, which are found in significant quantities in many geothermal reservoirs (see Table (2-1)), are increasingly being employed to help understand and explain the behavior of these systems.

Table (2-1). Gas Content in Fluids From Various Geothermal Fields

Location	Gas Content
Ahuachapan, El Salvador	0.05 percent of the total flow by mass with CO_2 accounting for 90 percent (Kestin et al., 1980).
Krafla, Iceland	Gas content rose to 7 percent of the steam by mass during 1975 eruption, but fell to 3 percent after activity stopped (Steingrimsson et al., 1984).
Namafjall, Iceland	1.0 percent gases in the steam by mass, 52 percent H_2S and 32 percent CO_2 (Kestin et al., 1980).
Nesjavellir, Iceland	1300-2700 mg/kg CO_2 concentration (Stefansson, 1985).
Kamojang, Indonesia	1-2 percent gas by mass (Grant et al., 1982).
Bagnore, Italy	Initially produced 90 percent carbon dioxide, but dropped to 7-20 percent since the removal of the gas cap (Kestin et al., 1980).
Larderello, Italy	3-10 percent gas by mass, 95 percent of which is CO_2 (Pruess et al., 1985). Other gases present include helium, methane, nitrogen and hydrogen (D'Amore and Truesdell, 1984).
Mofete, Italy	1-5 percent CO_2 by mass (Carella and Guglielminetti, 1983).
Matsukawa, Japan	0.5 percent gas by mass in the steam (Kestin et al., 1980).
Onikobe, Japan	0.5 percent gas by mass in the steam (Kestin et al., 1980).

Table (2-1). Gas Content in Fluids From Various Geothermal Fields

Location	Gas Content
East Olkaria, Kenya	noncondensible gas content of 500 millimoles per kg. of steam (Bjornsson and Bodvarsson, 1986).
Cerro Prieto, Mexico	0.2-1.0 percent gas by weight with 90 percent CO_2. Other gases present are hydrogen sulfide, nitrogen, hydrogen, ammonia, argon and methane (Nehring and D'Amore, 1984).
Los Azufres, Mexico	0.2-7.0 percent by mass of steam, primarily carbon dioxide and hydrogen sulfide (Kruger et al., 1985).
Broadlands, New Zealand	0.7-2.77 percent by mass with carbon dioxide comprising 95 percent (Brown and Ellis, 1970). Other gases present are hydrogen sulfide, hydrogen, nitrogen, ammonia and methane.
Kawerau, New Zealand	2.5 percent gas by mass in the steam of which 91 percent is carbon dioxide and 8 percent is hydrogen sulfide (Kestin et al., 1980).
Ngawha, New Zealand	1.1 percent gas by mass (Bjornsson and Bodvarsson, 1986).
Wairakei, New Zealand	0.5 percent gas by mass of steam (Kestin et al., 1980).
Palimpinon, Phillipines	0.2-1.0 percent carbon dioxide by mass (Klein et al., 1982)
Kizildere, Turkey	2 percent gas by mass in the steam (Tan, 1984)
Baca, New Mexico, USA	0.4-1.5 percent gas by mass primarily carbon dioxide. Other gases present include hydrogen sulfide, nitrogen, hydrogen, ethane, and methane (Riney and Garg, 1982).
Desert Peak, Nevada, USA	0.02-0.04 percent gas by mass of steam (Goyal et al., 1983)
Pauzhetka, USSR	0.6 percent gas by mass of which 92 percent is carbon dioxide (Kestin et al., 1980)

The presence of a large amount of noncondensible gas can have significant effects on the phase distribution within both exploited and unexploited reservoirs. In general,

the partial pressures of gases have been shown to cause a gas-water mixture to boil at a lower temperature than pure water (Ellis, 1959; Ellis and Golding, 1963; Takenouchi and Kennedy, 1964; Sutton, 1976; Sutton and McNabb, 1977; Pritchett et al, 1981; O'Sullivan et al, 1985). Since the work of Ellis (1959) it is well known that the higher the sum of partial pressures of gases present, the lower the boiling temperature will be (Ellis studied CO_2 effects in particular). In addition, Pritchett et al (1981) noted that although the boiling temperature changes significantly, the temperature at which condensation first occurs remains almost unaffected by the presence of gas. Udell (1986) indicates that gas will affect both the temperature of boiling and of condensation.

At Ohaki-Broadlands reservoir, New Zealand, pressures are substantially higher than would be typically found in a boiling water system. In some of the earliest work using gases in a reservoir fluid analysis, Sutton and McNabb (1977) showed that this pressure-temperature data could be fitted closely by a boiling curve of a CO_2-water mixture (4.4 percent CO_2 by mass). Grant (1977a) confirmed this by incorporating CO_2 in a simple model of the Ohaki-Broadlands reservoir and obtaining a reasonable match with field data (See also Zyvoloski and O'Sullivan, 1978a). Later, Pritchett et al (1981) used CO_2 in the analysis of the natural state of Baca reservoir, New Mexico. They concluded that the reservoir could be either single-phase liquid or two-phase depending on the amount of gas in the reservoir and that more accurate measurement of the gas would be required to determine the exact state of the system. O'Sullivan et al (1981) explains the conclusions of Pritchett et al by stating that if a sufficiently large amount of CO_2 is introduced into liquid water at fixed temperature and pressure, the mixture must boil and evolve a gas phase to accomodate the increase in CO_2. Pritchett et al (1981) found that in order to match the pressure-temperature conditions within the reservoir a gas-water mixture in the range of 0.4-1.5 percent gas by mass was necessary.

Ellis and Golding (1963) have shown that only a small amount of CO_2 (noncondensible gas) can be dissolved in the liquid phase of water, so that most of the CO_2 resides in the vapor phase at conditions typical in geothermal systems (see also

Takenouchi and Kennedy, 1964). In addition, Ellis and Golding (1963) have shown similiar results with sodium chloride solutions typical of geothermal brines.

O'Sullivan et al (1983) used the work of Ellis and Golding to conclude that if the partial pressure of CO_2 is held constant, an increase in the CO_2 mass fraction can only be accomodated by an expansion of the vapor phase. In the expansion from liquid to vapor, Straus and Schubert (1979) found that the large fluid volume changes that occur as gas leaves solution have large positive effects on the bouyancy of geothermal fluids.

Atkinson et al (1978) used the solubility imbalance noted by Ellis and Golding (1963) to explain the development of a large gas cap in the Bagnore reservoir, Italy. With the reservoir in equilibrium, cooling by conduction through the impervious cover created a situation akin to a heat pipe. The heat is provided for conduction by a counter-flow of ascending vapor and descending water formed by condensation. Since much more gas was carried up with the rising vapor due to bouyancy than could be removed by the descending liquid, a net accumulation of gas resulted at the top of the reservoir. A similiar situation at Alfina field, Northern Latium, Italy, is described by Barelli et al (1978).

Grant and Glover (1984) obtained an estimate of the steam saturation within Ohaki-Broadlands reservoir by using the solubility imbalance of CO_2 and a measure of pressure transients from well BR-21. They found that CO_2–H_2S ratios are particularly sensitive to the initial steam saturation.

Several investigators have examined the effects of CO_2 on the dynamics of reservoirs under exploitation. However, much of the work has centered around the assumption of a homogeneous porous medium while geothermal reservoirs are typically in fractured rocks. Grant (1977a) used a lumped parameter model of Ohaki-Broadlands to examine the transient behavior of gassy reservoirs. Grant (1977a) found that the presence of CO_2 gas led to a "degassing" phenomena in liquid dominated reservoirs. He showed that almost all the total pressure drop during early exploitation was produced by a change in the partial pressure of CO_2. Therefore, a substantial pressure drop

may occur without significant boiling since the vapor pressure of water is not greatly affected. Futhermore, if no CO_2 is present, much larger saturation changes are required to produce similiar pressure drops. Grant also noted that the presence of CO_2 made Ohaki-Broadlands reservoir two-phase.

Zyvoloski and O'Sullivan (1978b,1980) used a simple two dimensional model of a homogeneous porous medium to show that the "degassing" phenomena that Grant recognized was important only when the liquid saturation is low and/or production is from the vapor phase. At high liquid saturations, they suggested that discharge is mainly from the liquid phase in which CO_2 content is low. Therefore, the primary effect of the presence of CO_2 on the system is in reducing compressibility of the fluid which leads to faster propagation of pressure transients.

Pritchett et al (1981) studied CO_2 transients in a homogeneous porous medium during a constant rate test. They showed that the CO_2 content under the reservoir conditions could not be correlated with pressure-temperature measurements made on flowing wells and that the measured CO_2 content may be either higher or lower than that in situ. They found that the flowing ethalpy was strongly dependent on CO_2 content; the higher the CO_2 content, the higher the initial fluid enthalpy. However, this was attributed to variations in saturation caused by the increasing CO_2 content at a constant pressure and temperature by O'Sullivan et al (1985). Finally, Pritchett et al (1981) showed that interpretation of the drawdown data from a gassy field will infer smaller permeabilities than exists in a reservoir and that this discrepancy will increase with increasing CO_2 content. This is shown by the steeper slope on a graph of sandface pressure versus the logarithm of time for cases with high CO_2 content.

O'Sullivan et al (1985) found that the presence of CO_2 significantly affects the results of transient well tests in a homogeneous porous medium reservoir. They used a productivity index to simulate a well producing at a constant bottomhole pressure. They found that the early pressure decline is much faster due to the degassing phenomena, but the decline is much slower at late times because of the reduced flowing enthalpy. The heat capacity of CO_2 is substantially less than that of water

vapor. Therefore, the reduced flowing enthalpy due to the presence of CO_2 causes a slower decline in temperature and consequently, in pressure at later times. O'Sullivan et al outlined a technique to determine the in situ vapor saturation from the measurement of the stable flowing CO_2 content provided the relative permeabilities are known. They determined that after an initial short transient period flowing CO_2 content will reach a stable value as indicated by the asymptotic method outlined by O'Sullivan (1981). They also show that the stable flowing CO_2 content primarily depends on the relative permeability functions, the intial vapor saturation, and the initial partial pressure of CO_2 while smaller effects are due to the flowrate and porosity.

Bodvarsson (1984) examined CO_2 transients in a composite porous media reservoir for both constant rate and constant pressure productions. It was found that the flowing CO_2 content is highly dependent on the vapor saturation due to the solubility variation between the phases of water (see also Grant and Glover, 1984). Bodvarsson also noted, as O'Sullivan et al (1985) had, that porosity and permeability had little affect on the stable flowing CO_2 content. From these results, it was concluded that the monitoring of CO_2 content in conjunction with the flowing enthalpy could provide information about radial changes in vapor saturation and hydrologic parameters. Bodvarsson found that if only enthalpy changed that it was representive of a variation in porosity or permeabilty since the gas content is independent of these. However, if both enthalpy and gas content changed, this could indicate a variation in saturation within the reservoir since both transients are highly dependent on saturation.

Pruess et al (1985) used a fracture model to determine the origin of CO_2 in the Larderello vapor-dominated reservoir, Italy (see Pruess and Narasimhan, 1982, for a discussion on MINC). It was concluded from the tremendous amount of fluid that has been recovered from this field (estimated at 400 X 10^9 kg) that the fluid was originally stored as a liquid. Since the solubility of CO_2 in liquid water is very low, he suggested that CO_2 is supplied to the system by an external source or by a mineral buffer (see Appendix A for a brief discussion of mineral buffers and Appendix B for a discussion of techniques to determine controlling mineral buffers) and could not have been stored

within the reservoir. Pruess et al (1985) noted that the gas-steam ratio had remained relatively constant since early production and concluded from this that mineral buffers were a much more likely source. Numerical simulations were preformed to study CO_2 discharge from the matrix with a prehnite/clinozoisite mineral buffer present. They found that the CO_2 concentration trends were similiar to those found at Larderello, however, field values were somewhat higher suggesting more than one mineral buffer is present. From this work Pruess et al concluded that mineral buffers are an important source of CO_2 in producing reservoirs where flowing concentrations do not vary substantially.

2.2 Use of Flowing Ethalpy to Characterize Geothermal Systems

Analysis of flowing enthalpy transients has recieved increasing attention as a tool to determine reservoir characteristics. Although many geothermal reservoirs are controlled by fracture flow, much of the work that has been done has examined enthalpy transients in a homogeneous porous medium. Grant (1977b) suggested that steam/water relative permeabilities of the Wairakei field could be inferred from the production history. He considered the enthalpy and discharge histories to obtain a curve of steam permeability versus water saturation. His result was a "regional curve" with substantial leeway for the permeability reduction factors, however, it did indicate that the reduction factors differed substantially from those used previously.

Horne and Ramey (1978) improved on the shortcomings of the Grant curve. They accounted for heat loss from the wellbore. They normalized total discharge by bottomhole pressure to filter out changes due to overall pressure decline and used downhole enthalpy values calulated from downhole temperatures rather then to assume an overall mean temperature. They used the downhole enthalpy in conjunction with the normalized pressure to produce a pair of steam/water relative permeability curves which suggest that steam is unaffected by the presence of water except at very high water saturations.

Grant (1979) developed a quasi-analytical solution for constant discharge which is formulated with pressure and flowing enthalpy as dependent variables. This method assumed a homogeneous porous media. The solution indicated that flowing enthalpy changes depend on the well discharge divided by the permeability thickness, porosity, initial reservoir pressure and initial saturation. He found an inverse relationship between enthalpy and porosity. For solutions with a constant porosity ranging from 0.10 to 0.30, the pressure response varied little but the rise in enthalpy ranged from 510 to 260 kJ/kg respectively.

Using the work of Grant (1979), Sorey et al (1980) developed a series of graphs by which porosity of the reservoir can be determined. A enthalpy versus flowrate plot was used (since enthalpy transients data is scarce) along with information from pressure transient data to provide an estimate of the porosity. They determined that the rise in enthalpy depends strongly on the relative permeability functions. Using this, Sorey et al outlined a method by which measurements of the pressure transient and the stable flowing enthalpy during a two-phase well test can yield information about the relative permeability functions. The well history will give k_{rw} and k_{rs} correct to a constant. In addition, they show that the quasi-analytic solution developed for pressure, saturation, and flowing entalpy transients is a function of the similarity variable t/r^2 only. Finally, Sorey et al showed that in a homogeneous porous medium, flowing enthalpy will increase until the pressure-log time plot becomes linear, after which the enthalpy will remain practically constant.

Grant and Sorey (1979) indicate that measurement of the discharge enthalpy which is equal to the flowing enthalpy at the well face allows saturation to be estimated at at the wellface. They suggest that if the relative permeability is a known function of saturation and the reservoir temperature is known, that the saturation and each relative permeability can be calculated. In addition, they suggest that properties such as density of the flowing mixture, which depends only on the relative permeabilities, can be calculated directly from the enthalpy.

O'Sullivan (1981) confirmed the work of Sorey et al (1980), showing that enthalpy rises to an approximately constant level at a value of t/r^2. He also determined that, for medium initial liquid saturations, the measurement of flowing enthalpy will enable the value of kinematic viscosity to be calculated. However, at high liquid saturations, enthalpy changes very little while the permeability divided by the kinematic viscosity changes substantially, thus yielding an erroneous result.

Bodvarsson et al (1980) made use of the rise in flowing enthalpy to study the sensitivity of reservoir behavior with regards to relative permeability functions. They examined the behavior of a homogeneous porous medium with semi-analytical and numerical techniques. They determined that the change in enthalpy is strongly dependent on the nature of the relative permeability functions (also see Sorey et al, 1980). These functions control the phase mobilities, thus determining the fluid enthalpy. They also found that the rise in enthalpy is dependent on several other factors including initial temperature and saturation, porosity (ϕ), mass flowrate, and the total kinematic mobility. They determined that the saturation changes and, therfore, the enthalpy changes were far greater at lower temperatures because the kinematic mobility is less. Futhermore, enthalpy rise is greater at lower porosity. At low vapor saturations the flowing enthalpy scales linearly with $(1 - \phi)/\phi$, however, at high vapor saturations non-linear effects "are more pronounced." Using these relationships, Bodvarsson et al concluded that the rise in enthalpy can give information regarding the relative permeability functions if permeability-thickness and porosity can be determined from injection and/or interference tests.

Stefansson and Steingrimsson (1980) indicate that thermal contraction can enhance permeability so that enthalpy will not stablize rapidly. Well KG-12 at Krafla, a two phase reservoir, reaches a stable flowing enthalpy "after a few weeks" producing superheated steam. However, well BJ-11 in Namafjall, a liquid dominated field, has reached a constant waterflow but the steamflow and enthalpy continue to rise. Stefansson and Steingrimsson suggest that thermal contraction is expanding fractures around well BJ-11 increasing the flowrate with time.

O'Sullivan et al (1985) used a homogeneous porous medium approximation to determine that there was a linear relationship between flowing enthalpy and flowing CO_2 content. They state that exact correlation depends both on the vapor saturation of the boiling mixture and on the nature of the permeability functions. Futhermore, O'Sullivan et al determine that the presence of noncondensible gases lowers the flowing enthalpy causing a slower temperature decline in a reservoir.

Bodvarsson (1984) examined enthalpy transients in a composite porous medium allowing for both constant and variable rates with a productivity index. For constant rate tests, Bodvarsson concluded that spatial variations in porosity, permeability, and vapor saturation can greatly effect the enthalpy of produced fluids but that distinguishing between effects maybe difficult. It was found that enthalpy increased with both decreasing permeability and with increasing saturation. It was also found that enthalpy increased with decreasing porosity as Sorey et al (1980) had concluded. For constant pressure production, he found that the enthalpy never stablized. Enthalpy had a sharp initial rise followed by a slow decline with time and flowrate typical of many field results. He found that other conclusions were similiar to those for constant rate tests.

Pruess (1983) used numerical and analytical techniques to study nonisothermal flow of steam and water in an idealized fractured porous medium. He determined that the enhancement of flowing enthalpy by conductive heat flux depends upon the ratio of heat conductivity to effective permeability for the liquid phase. A smaller matrix permeability results in stronger enhancement of flowing enthalpy. Pruess shows that with fracture spacings of 5 m and 50 m that there is little difference in enthalpy despite there being 10 times more contact area between the fractures and matrix with the 5 m spacing. He concludes that fractured boiling reservoirs behave quite differently from porous medium-type reservoirs and that the assumption of thermodynamic equilibrium between fracture and matrix can lead to erroneous results.

Grant and Glover (1984) used enthalpy transients in conjuction with pressure transients to evaluate the reservoir around well BR21, Ohaki-Broadlands, New

Zealand. They noted that the pressure transients indicate a transient period of minutes or seconds while the enthalpy variation needed weeks to attain stability. Grant (1983) found that if there is flashing flow in a homogeneous porous medium that the transient period for enthalpy lasted only minutes. Grant and Glover instead assumed that the medium is fractured and that heat, but no mass can be transferred from the matrix to the fracture (see also Moench, 1978). Grant (1982a,1983) determined that the stabilization time for enthalpy is then equal to the relaxation time for conductive equilibrium of the matrix blocks. With these assumptions, Grant and Glover determined that the best fit relaxation times were 400 and 1000 hours. These fits imply that the average matrix block radius is 1-2 meters and that the fissure volume represents a few percent of the total volume

3.0 Enthalpy and CO_2 Transients in Fractured Reservoirs

3.1 Introduction

The enthalpy and CO_2 transients can provide valuable information about the properties of a reservoir. A sensitivity study was performed to determine the important controlling parameters for both enthalpy and CO_2 transients in fractured two-phase geothermal systems. Parameters considered were matrix permeability, fracture permeability-thickness product, matrix and fracture relative permeability functions, initial gas saturation and partial pressure, fracture and matrix porosity, and the fracture spacing.

3.2 Background

The movement of mass and energy in geothermal systems is strongly affected by the total kinematic mobility and the flowing enthalpy (Bodvarsson et al, 1980). For two-phase systems in a porous medium, the mobility of each phase is impeded by the presence of the other phase. The amount interference between phases depends on the volumetric proportion of the phases present. This interference between phases is described mathematically by the saturation dependant relative permeability functions k_{rl} and k_{rg} for the liquid and gas phase, respectively. The total kinematic viscosity (ν_t) is then a function of both the relative permeability and the viscosity of each phase. It is defined as

$$\frac{1}{\nu_t} = \frac{k_{rl}}{\nu_l} + \frac{k_{rg}}{\nu_g} \tag{3-1}$$

The symbols are defined in the nomenclature. The kinematic mobility is then equal to

$$\frac{k}{\nu_t} = k[\frac{k_{rl}}{\nu_l} + \frac{k_{rg}}{\nu_g}] \tag{3-2}$$

where k is the absolute permeability. The flowing enthalpy is defined as

$$h_f = \nu_t[\frac{k_{rl}h_l}{\nu_l} + \frac{k_{rg}h_g}{\nu_g}] \tag{3-3}$$

where h_l and h_g are the liquid and gas phase enthalpies, respectively.

When appreciable amounts of CO_2 are present, the gas can have major effects on the behavior of a reservoir under exploitation. Small changes in the CO_2 content of a reservoir can cause significant changes in enthalpy and CO_2 content of the discharge fluid. Because of the important role of CO_2 in determining the transport parameters and thermodynamic characteristics of a reservoir it is essential to include the effects of CO_2 on these transients. Also, since the CO_2 content of a discharge will not change substantially in the wellbore unless scaling is occuring, the flowing mass fraction of CO_2 can provide valuble information about in situ conditions. The flowing mass fraction of CO_2 is defined as

$$X_c = \frac{X_{cl}q_l + X_{cg}q_g}{Q} \tag{3-4}$$

where q_l, q_g, and Q are the mass flowrate of the liquid phase, the gas phase, and total discharge, respectively. X_{cl} is the mass fraction of CO_2 in the liquid phase and is determined by Henry's law as

$$X_{cl} = \alpha(T)P_c \tag{3-5}$$

and X_{cg} is the mass fraction of CO_2 in the gas phase given by

$$X_{cg} = \frac{\rho_c}{\rho_c + \rho_v} \tag{3-6}$$

The pressure and temperature gradients within a producing reservoir control the rate of energy transfer. Therefore, the properties of the fluid and reservoir rock that affect these gradients will ultimately control the amount of energy that can be recovered from a reservoir. A distributed parameter model was used to examine the

sensitivity of flowing enthalpy and mass fraction of CO_2 to various reservoir and fluid properties.

3.3 Approach

The fractured nature of a geothermal reservoir was represented by an idealized model having three mutually perpindicular planar fracture sets with equal aperature and spacing. The "multiple interacting continua" (MINC) technique for numerically simulating heat and fluid flow in fractured porous media was developed by Pruess and Narasimhan (1982). This method is similiar to the double-porosity model of Warren and Root (1963) except this method allows for fully transient heat and mass flow. The MINC method is implemented in conjunction with the two-phase, multicomponent, non-isothermal geothermal reservoir simulator MULKOM (Pruess, 1982). MULKOM is coded in a general way to model energy and mass with a separate mass balance equation for each component. The H_2O–CO_2 equation of state was developed by O'Sullivan et al (1983), based on the work of Sutton and McNabb (1977). A single-layer radially infinite mesh is developed using the preprocessor program GMINC (Pruess, 1983). In the study, we use a radial grid discretized logarithmically starting with a 0.1 meter well element and increasing outward. There were five elements per log cycle. The mesh is a single layer so that the effects of gravity are neglected and, hence, the initial conditions are the same in the fractures and matrix.

The constant reservoir and fluid properties for the base case and the sensitivity studies can be found in Table (3-1). The rock and fluid parameters which were varied for the sensitivity studies are shown in Table (3-2).

Table (3-1). Constant Parameters for Sensitivity Study.

Parameter	Reservoir Values
reservoir thickness	1000 m
wellbore radius	0.1 m
productivity index	$1.25 \times 10^{-12} m^3$
rock heat capacity	1000 J/kg °C
rock density	2650 kg/m^3
initial pressure	90 bars
diffusion coefficient	$1.38 \times 10^{-5} m^2$
tortuosity	0.25m/m

Table (3-2). Parameters Varied in the Sensitivity Study

Parameter	Base Value	Other Values
bottomhole pressure	40 bars	20, 60 bars
fracture spacing	100 m	20, 500 m
fracture porosity	1%	0.25%, 2%
matrix porosity	5%	0.1%, 10%, 20%
fracture transmissivity	2.0 dm	5.0, 10.0 dm
matrix permeability	0.01 md	0.0, 0.001, 0.1 md
thermal conductivity	2.2 W/m °C	0.0, 4.4 W/m °C
fracture relative permeability	X-curves	SGB-curves
	S_{rl}=.0 S_{rg}=.0	S_{rl}=.0 S_{rg}=.0
matrix relative permeability	SGB curves	Corey curves
	S_{rl}=.05 S_{rg}=.40	S_{rl}=.05 S_{rg}=.40
initial gas saturation	20%	2%, 10%, 30%, 50%
initial partial pressure of CO_2	10 bars	0.01, 2.0, 20.0 bars
intial temperature	≈295 °C	≈295 °C (depends on P_{CO_2})

A deliverability model is used based on constant bottomhole pressure with the total production rate given by

$$Q = \sum_{i=\text{phases}} \frac{k_{ri}}{\mu_i} \rho \, (\text{P.I.}) \, (P - P_{wb}) \tag{3-7}$$

Where (P.I.) is the productivity index, P_{wb} is the bottomhole pressure, and P is the pressure in the element adjacent to the well. The productivity index employed provides flowrates typical of high temperature two-phase geothermal wells (25-35 kg/s). The fracture relative permeability functions are linear without cutoffs and the matrix relative permeability functions are conventional SGB curves (Sorey et al, 1980) with a residual liquid saturation of 0.40 and a residual gas saturation of 0.05 unless otherwise noted (see Figure (3-1)). The fracture curves are

$$k_{rl} = S_l \tag{3-8a}$$

$$k_{rg} = S_g \tag{3-8b}$$

and the relative permeability functions for the matrix are

$$k_{rl} = [S^*]^4 \tag{3-9a}$$

$$k_{rg} = 1 - k_{rl} \tag{3-9b}$$

where

$$S^* = \frac{S_l - S_{lr}}{1 - S_{lr} - S_{gr}} \tag{3-9c}$$

The computed values for flowing enthalpy, flowing mass fraction of CO_2 and pressure reported in this study refer to the inlet conditions at the wellfeeds.

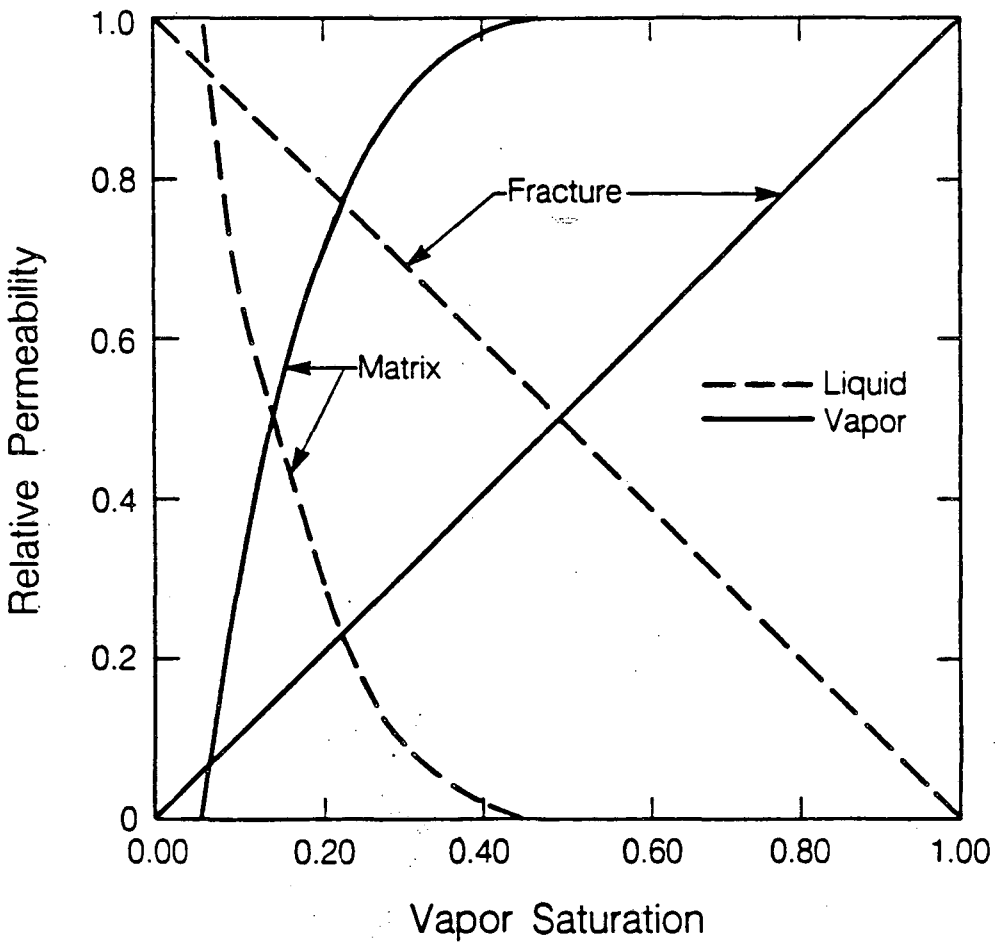

XBL 8612-12800

Figure (3-1). Relative permeability curves used in this study (S_{gr}=0.4, S_{lr}=0.05).

3.4 The Base Case

A base case is first considered in order to develop a basis for comparison in the effects of various parameters on enthalpy and CO_2 transients. The base case considers a reservoir initially at a total pressure of 90 bars including 10 bars of CO_2 gas and a 20 percent gas saturation. It should be noted that the gas phase (gas saturation) includes both water vapor and CO_2 gas. The changes in the downhole pressure and flowing enthalpy for the base case are shown in Figure (3-2). As production begins, the pressure drops rapidly and there is a substantial rise in the flowing enthalpy. The pressure gradient must increase around the well in order to overcome the drop in kinematic mobility of the fluid as the gas saturation increases (Lippmann et al, 1985). Figure (3-3) shows the kinematic mobility versus the gas saturation for both the SGB, linear, and the conventional Corey relative permeability functions. The mobility of fluid drops rapidly as the gas saturation increases from the initial value of 20 percent.

At early time, all of the produced fluids come from the fractures, but with time, the radius of influence increases rapidly, causing increased surface area for flow from the matrix to the fractures. This results in an increase in the rate of heat transfer due to conduction and convection. Because of this fracture-matrix interaction, the transient period for the flowing enthalpy will be large. Futhermore, since the heat stored within the low porosity matrix is much greater than can be removed by the pore fluid, the conductive enhancement of the enthalpy will continue after the matrix has been depleted of fluid. These effects can be observed in the flowing enthalpy in Figure (3-2), where the enthalpy continues to rise after two years of production. This enthalpy enhancement due to fracture-matrix interaction is an important phenomena that is ignored in porous medium models where instantaneous equilibrium between fracture and matrix is assumed (Pruess, 1983).

Figure (3-4) shows the flowing mass fraction of CO_2 and enthalpy versus time. The flowing mass of CO_2 is initially 2 percent of the total mass flowrate, but rises to almost 3 percent after 2 years. The initial rise is due to the rapid degassing of the fractures. Figure (3-5) (O'Sullivan et al, 1983) shows the mass fractions of CO_2 in the

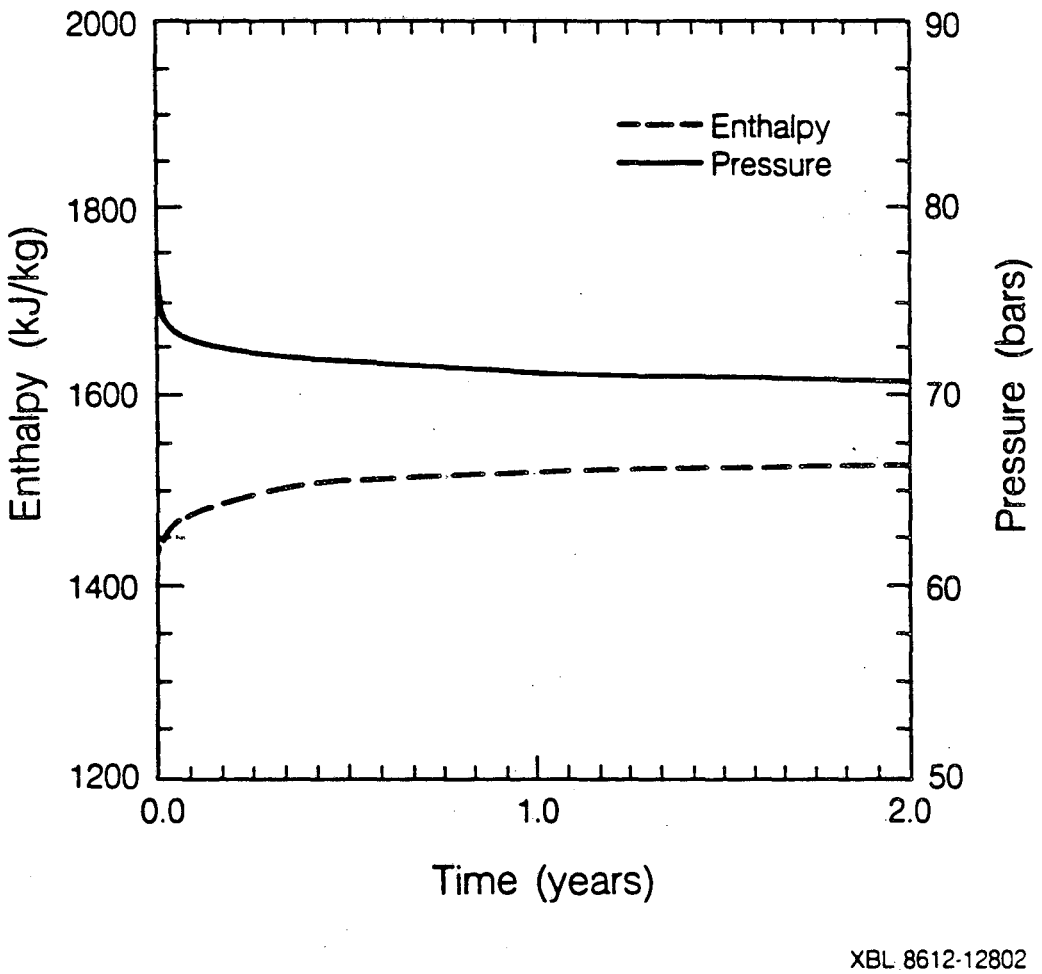

Figure (3-2). Flowing enthalpy and formation pressure transients for the base case.

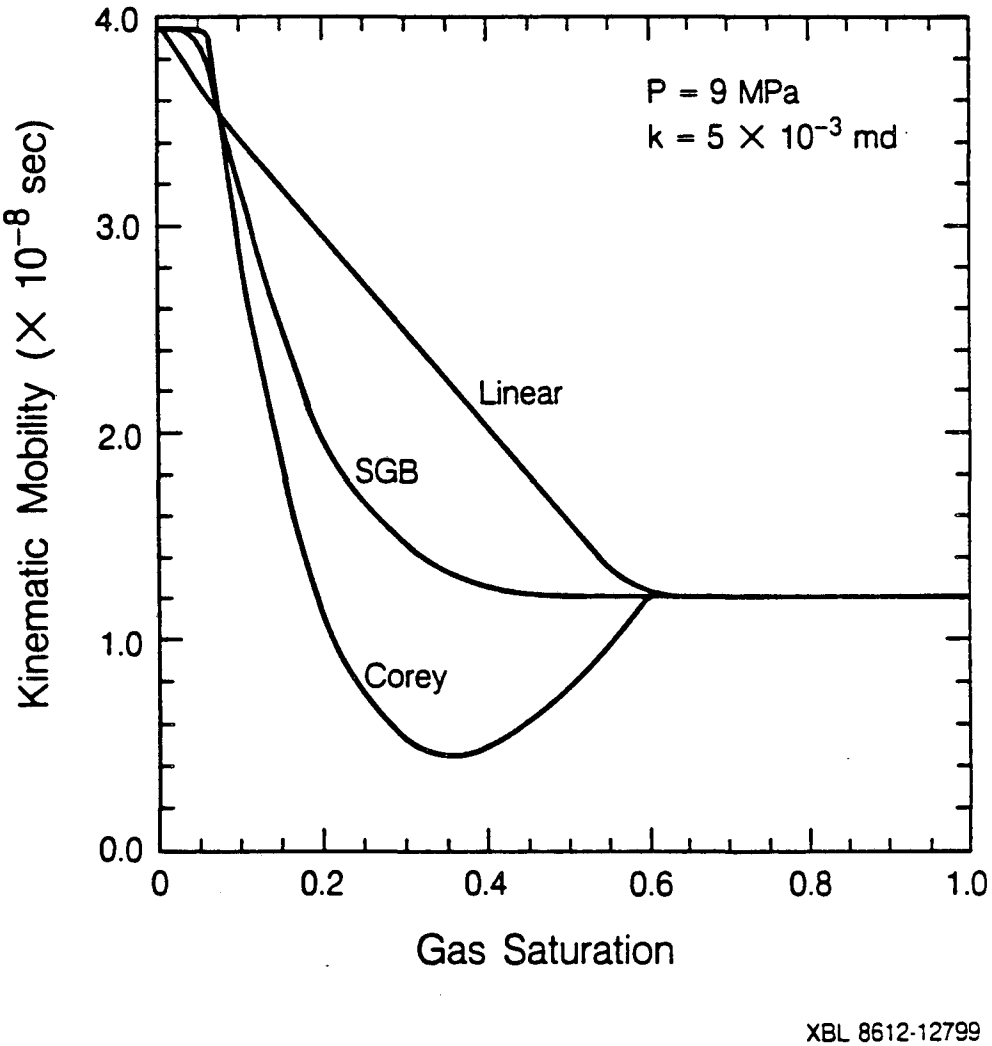

Figure (3-3). Total kinematic mobility curves for matrix relative permebility curves with S_{gr}=0.4 and S_{lr}=0.05.

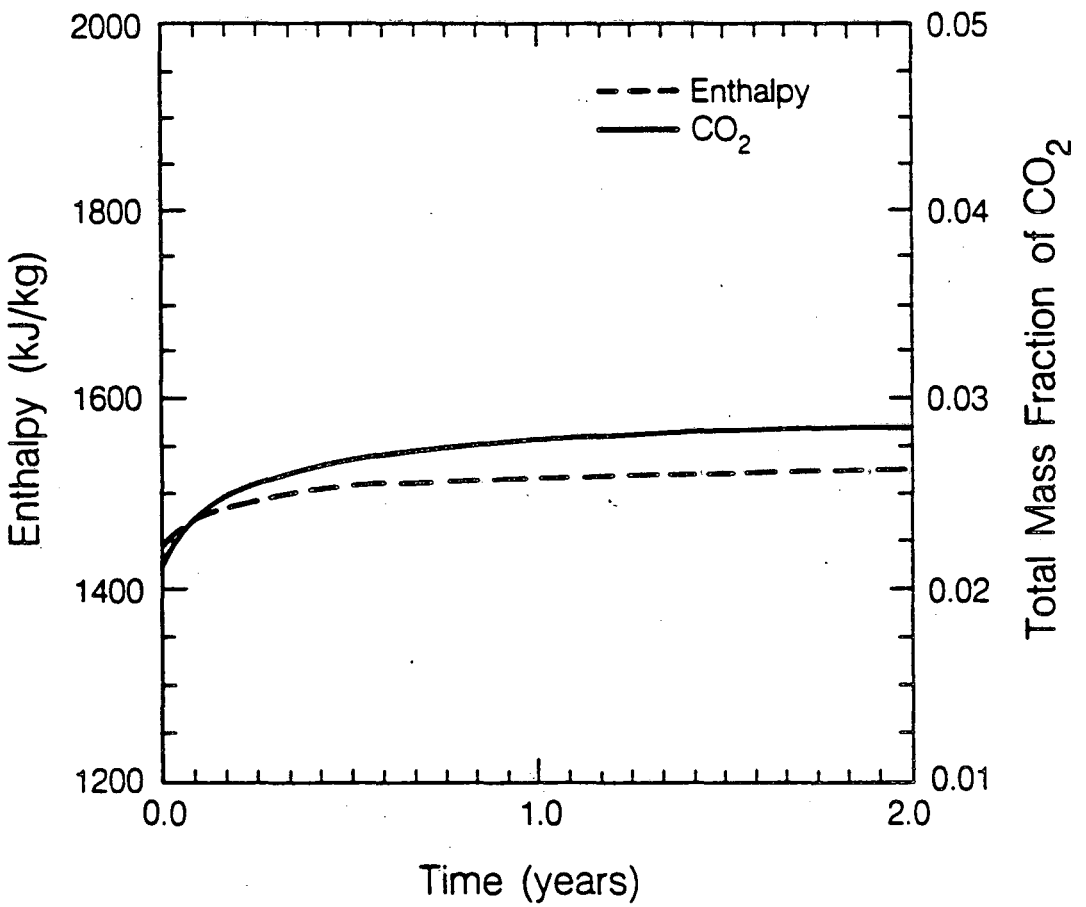

Figure (3-4). Flowing enthalpy and flowing mass fraction of CO_2 transients for the base case.

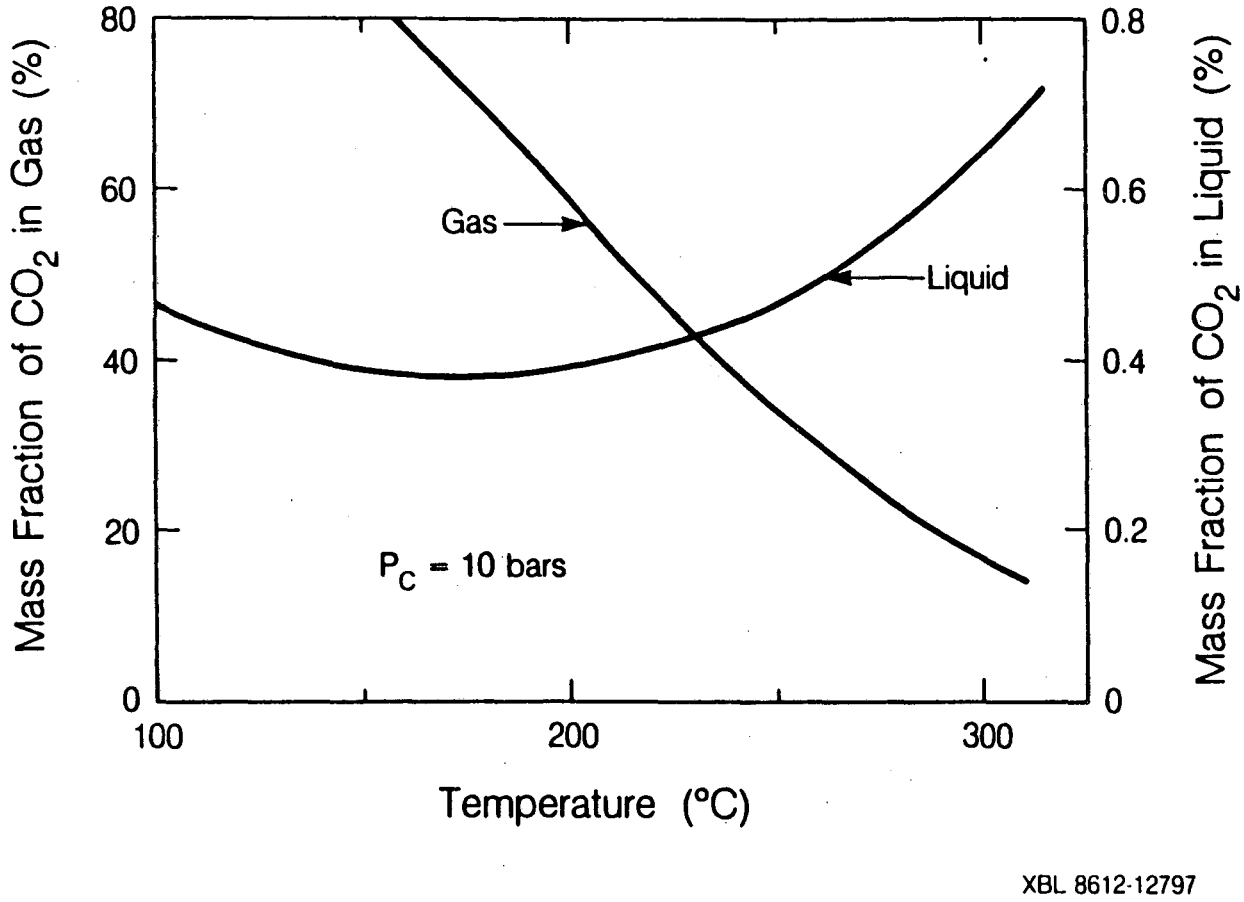

Figure (3-5). Mass fraction of CO_2 in liquid and gaseous phases (O'Sullivan et al, 1985).

liquid and gas phase, respectively, as a function of temperature. This figure indicates that even for high partial pressures of CO_2, the total amount of CO_2 that may be dissolved in the liquid phase is small. Since most of the CO_2 resides in the gas phase, the flowing mass fraction of CO_2 will be strongly controlled by the mobility of the gas phase. The early rise in enthalpy is indicative of the increasing gas phase mobility. Also, the amount of CO_2 that can be dissolved in the liquid phase drops rapidly with temperature, therefore, as the pressure (and temperature under two-phase conditions) drops during production, CO_2 is driven from the liquid phase to the gas phase, further increasing the flowing gas content. Finally, it should be noted that the mass fraction of CO_2 in situ is only 0.9 percent, much lower than the flowing CO_2 content. The flowing CO_2 content is primarily a function of the phase mobilities and can differ substantially from the in situ mass fractions (Pritchett et al, 1981).

3.5 Initial Partial Pressure of CO_2.

The initial partial pressure of CO_2 has large effects on the rise in flowing enthalpy. Figure (3-6) shows the flowing enthalpy transients for initial CO_2 partial pressures of 0.01, 2.0, 10.0, and 20.0 bars with all other parameters remaining the same as in the base case. The initial flowing enthalpy differs for the various cases because the initial temperature for these cases is different, the water vapor pressure is less than the total pressure by the partial pressure of CO_2 present. Thus, the initial temperature for the case with 0.01 bars partial pressure is 303 °C while the temperature is only 285 °C when 20 bars of CO_2 is present. The total initial pressure is maintained at 90 bars. Also, since the heat capacity of CO_2 is only 55 percent of that for steam, as the concentration of CO_2 increases, the enthalpy decreases. The initial enthalpies vary by 150 kJ/kg, ranging from 1300 to 1450 kJ/kg.

Figure (3-7) shows the pressure and flowing enthalpy versus time for 0.01 and 10.0 bars initial partial pressure of CO_2. The total pressure declines by about 1.0 bar more for the case with higher initial partial pressure of CO_2 while the rise in flowing enthalpy is 250 kJ/kg less. This is due to degassing of the reservoir during early time

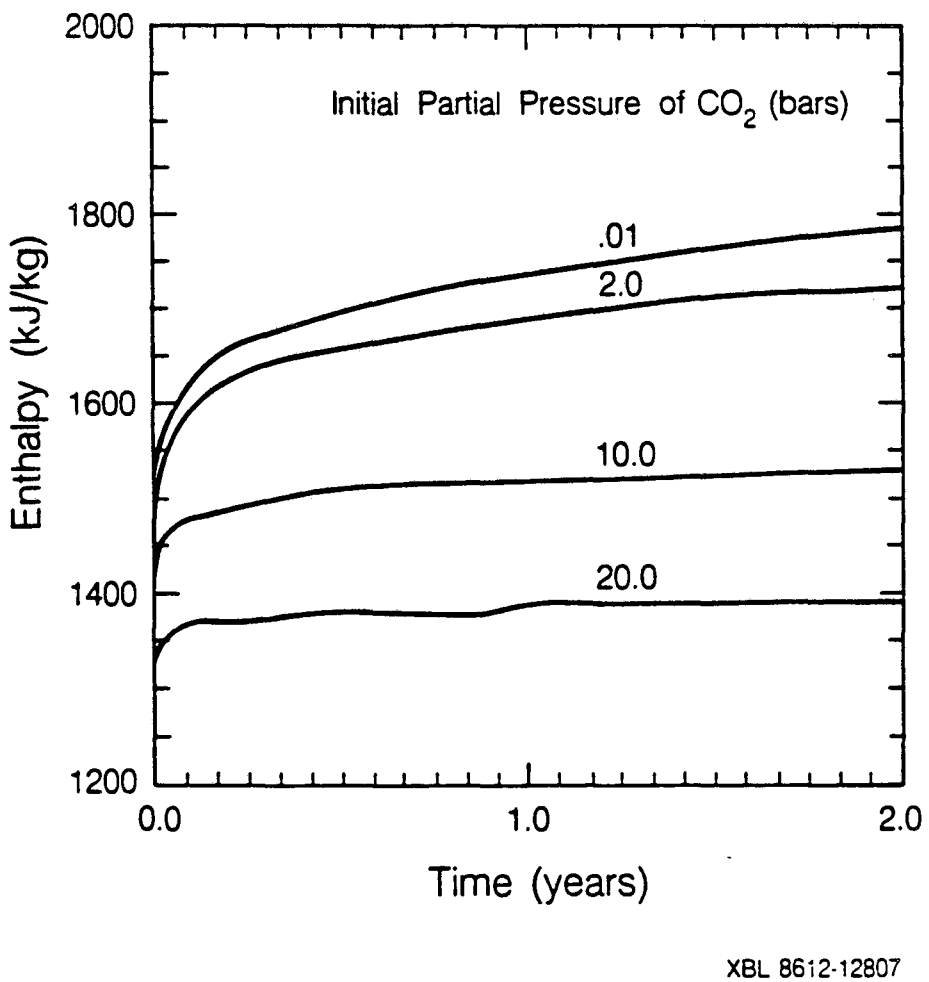

Figure (3-6). Effect of initial partial pressure of CO_2 on flowing enthalpy transients.

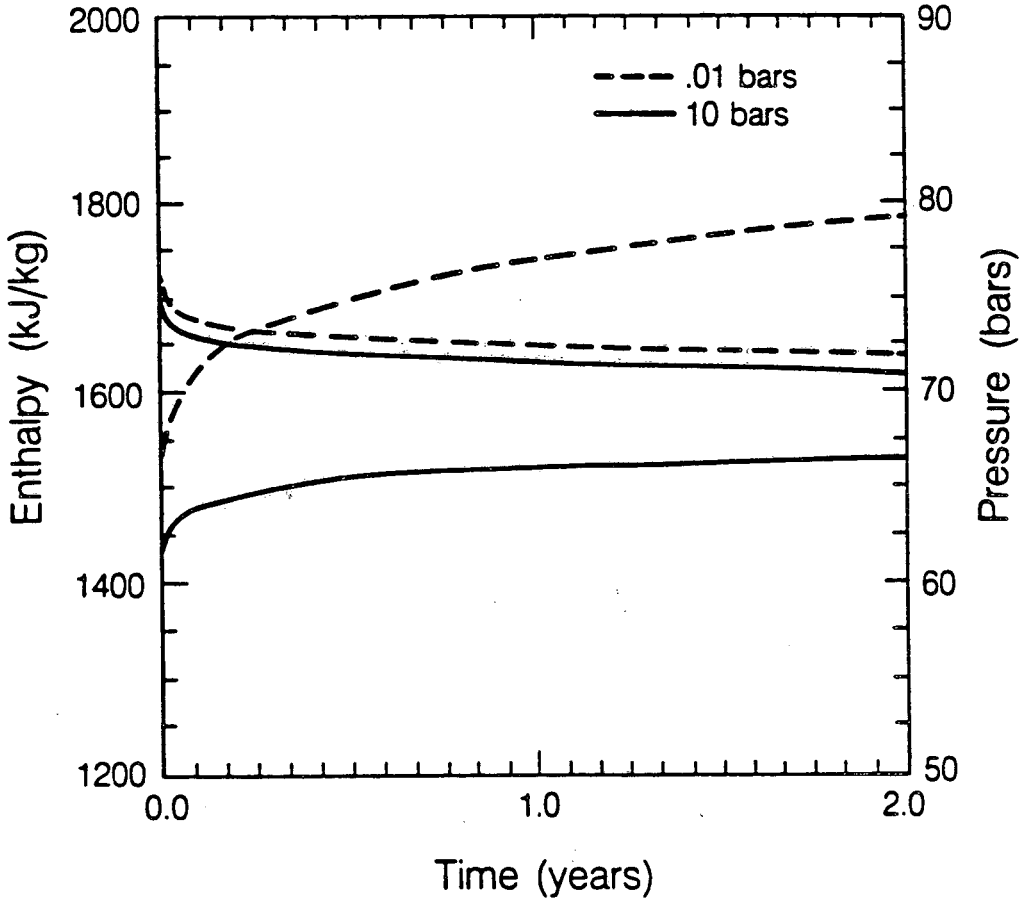

XBL 8612-12801

Figure (3-7). Comparison of flowing enthalpy and formation pressure transients for initial partial pressures of CO_2 of 0.01 and 10 bars.

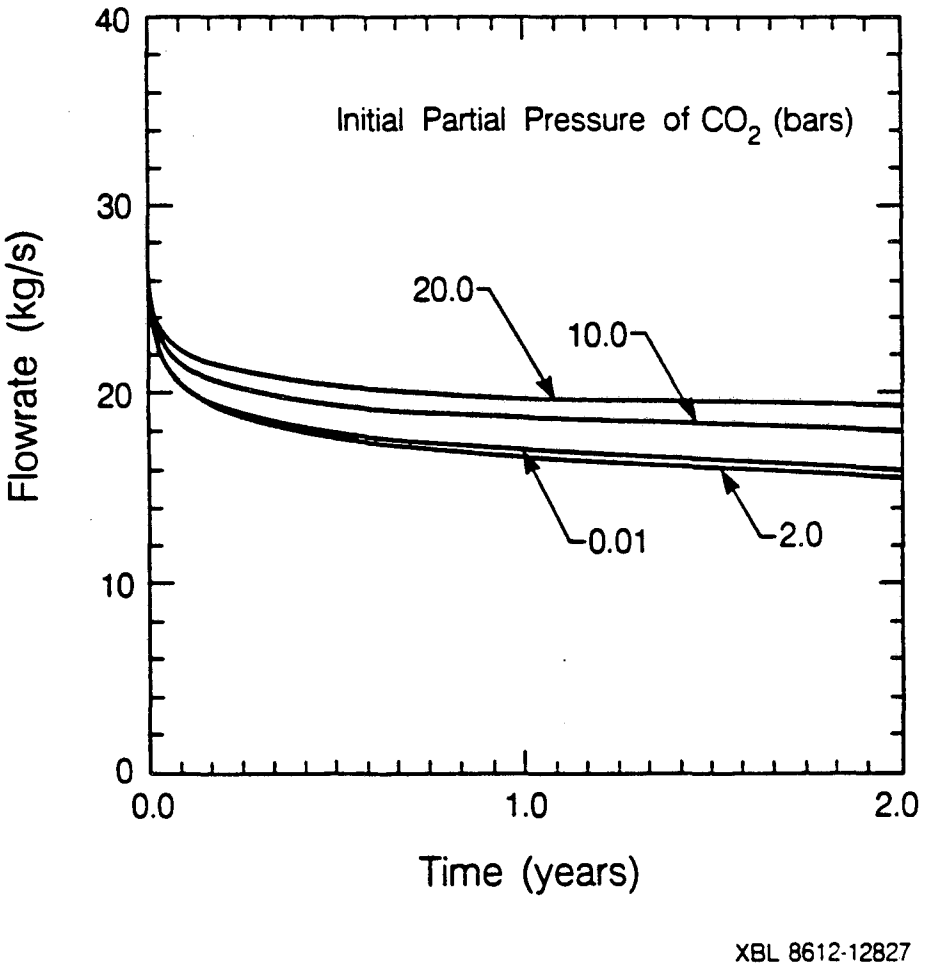

Figure (3-8). Effect of initial partial pressure of CO_2 on mass flowrate transients.

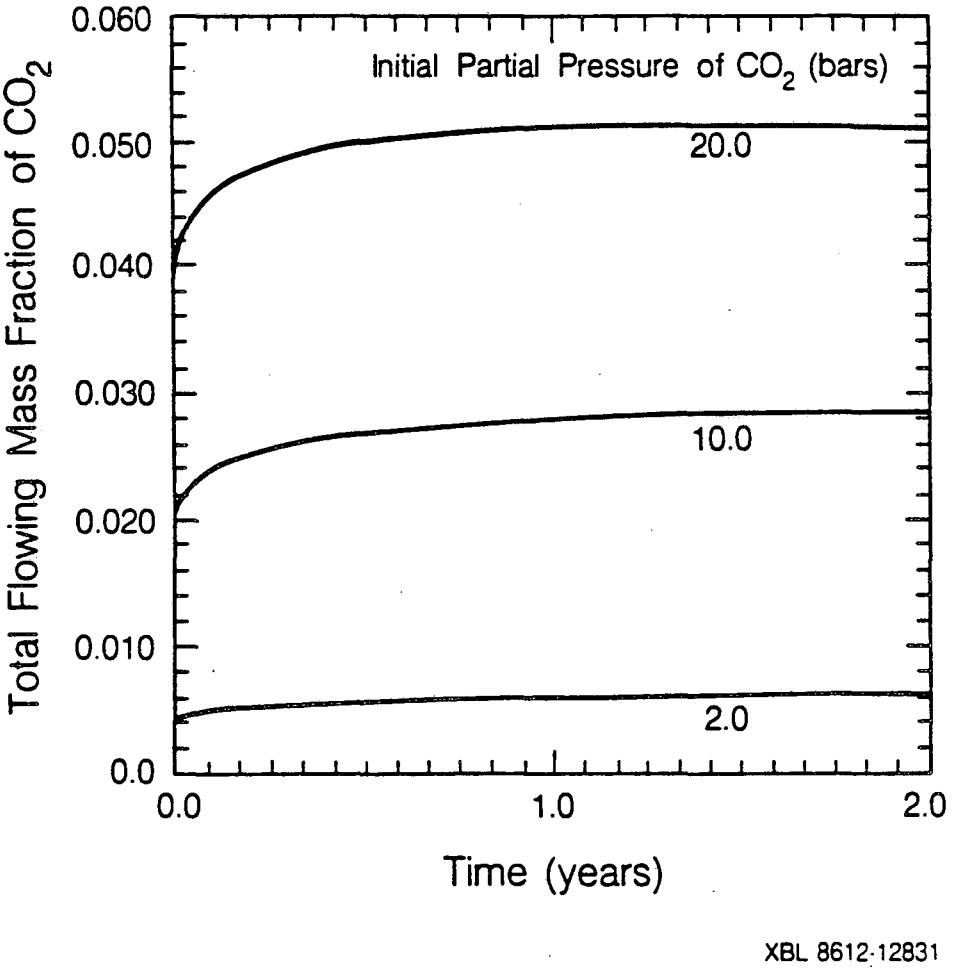

Figure (3-9). Effect of initial partial pressure of CO_2 on transients of the total flowing mass fraction of CO_2.

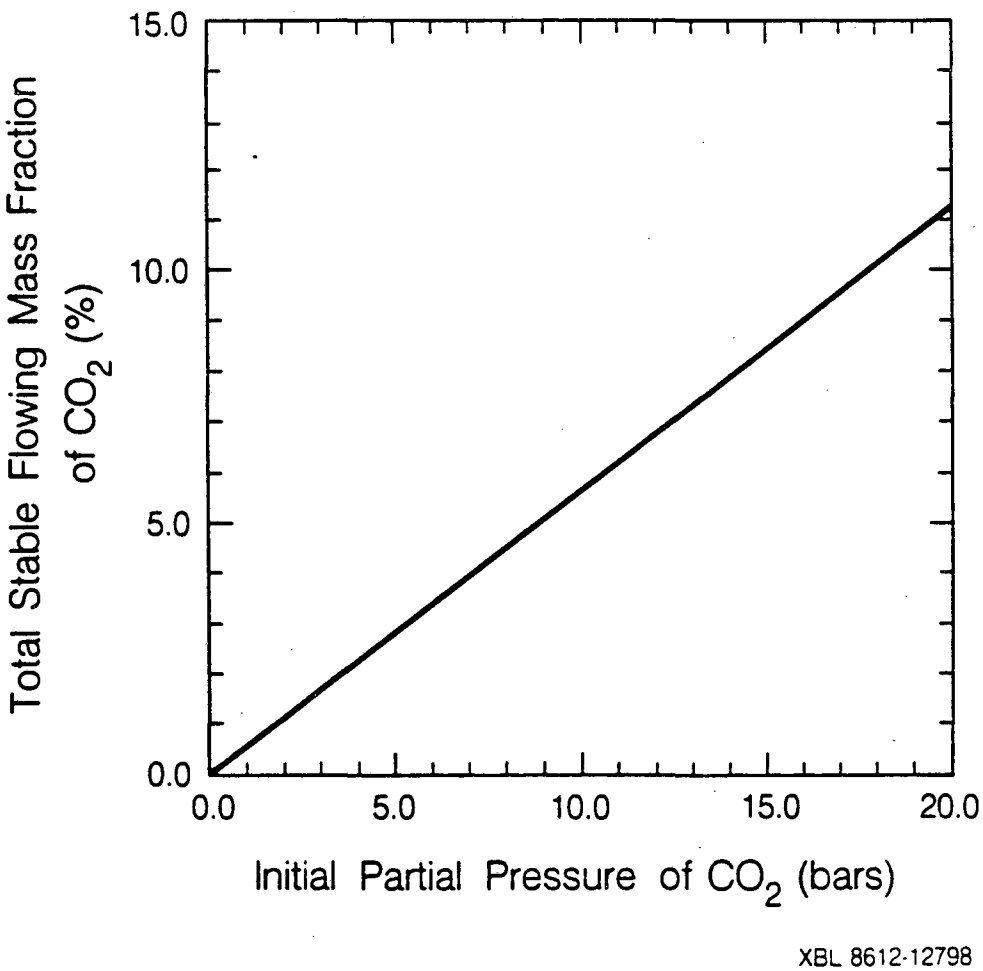

Figure (3-10). Effect of initial partial pressure of CO_2 on the stable flowing mass fraction of CO_2.

production. With CO_2 present, a significant pressure drop can occur without much boiling so that the rise in the flowing enthalpy is reduced. With low partial pressures of CO_2 the variation in enthalpy is much greater. However, since the stable flowing enthalpy (saturation) is lower for high gas concentrations, the liquid phase mobility is larger, leading to an increased mass flowrate as shown in Figure (3-8). The figure shows that the flowrate increases in direct proportion to the amount of gas present.

The flowing mass fraction of CO_2 is strongly dependant on the initial partial pressure of CO_2. Figure (3-9) indicates a direct relationship between initial partial pressure and flowing mass fraction; the higher the initial partial pressure, the higher the flowing mass fraction. By increasing the partial pressure of CO_2, the concentration of CO_2 in each phase will be increased proportionately. This results in a linear increase in the mass fraction with partial pressure of CO_2 as shown in Figure (3-10). The rise in flowing mass fraction of CO_2 is largely due to flow from the matrix since the transient period in the fractures is very short due to the low storage capacity. Therefore, the rise will be linearly related to the initial concentration in the matrix. The stabilization in flowing mass fraction occurs at late time when quasi-steady state flow between fracture and matrix has been established.

3.6 Bottomhole Pressure

The bottomhole pressure is defined here as the wellbore pressure during constant pressure production. The bottomhole pressure has strong effects on the rate of massflow as shown in Figure (3-11) for bottomhole pressures of 20, 40 and 60 bars. Decreasing the bottomhole pressure increases the pressure gradient between the wellbore and the surrounding formation. An increase in the pressure gradient intensifies boiling both in the fracture and the matrix. Figure (3-12) shows the enthalpy transients during the first two years of production. The increase in boiling associated with decreasing bottomhole pressure is indicated by the increase in the stable flowing enthalpy. However, the total increase in stable flowing enthalpy is less than 100 kJ/kg for a 40 bar difference in the bottomhole pressure. The relatively

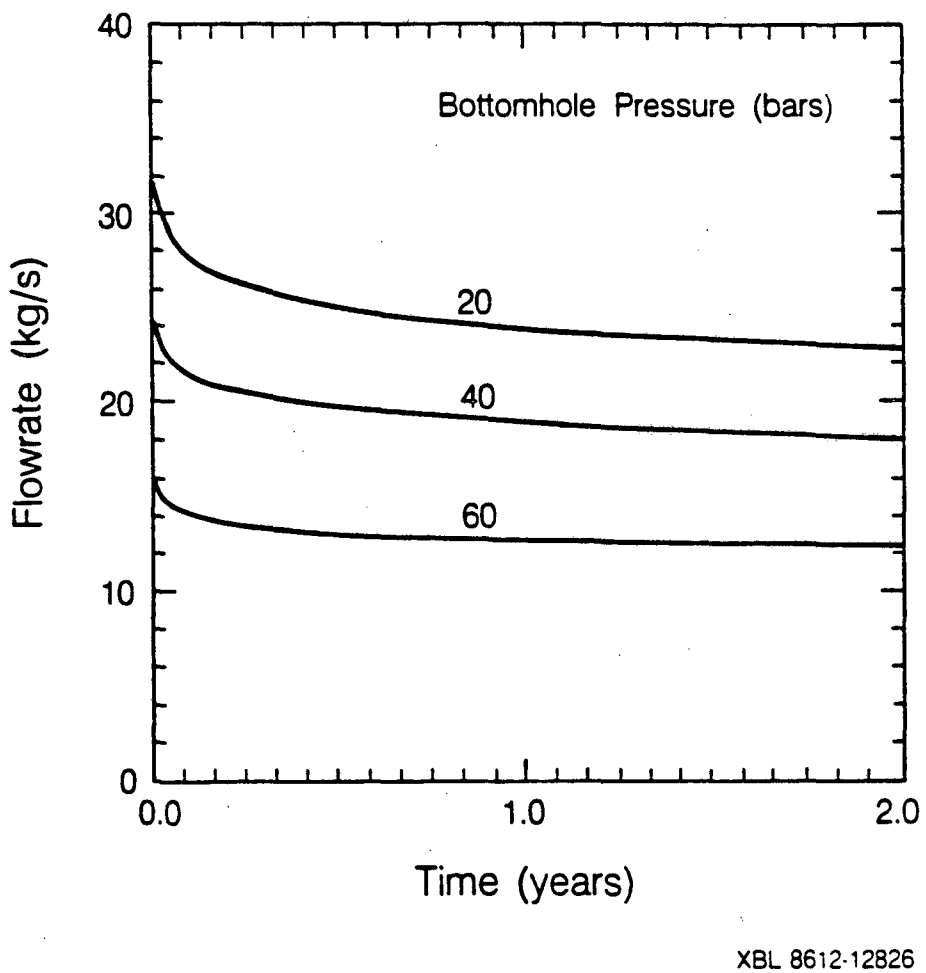

Figure (3-11). Effect of bottomhole pressure on mass flowrate transients with 10 bars initial partial pressure of CO_2 present.

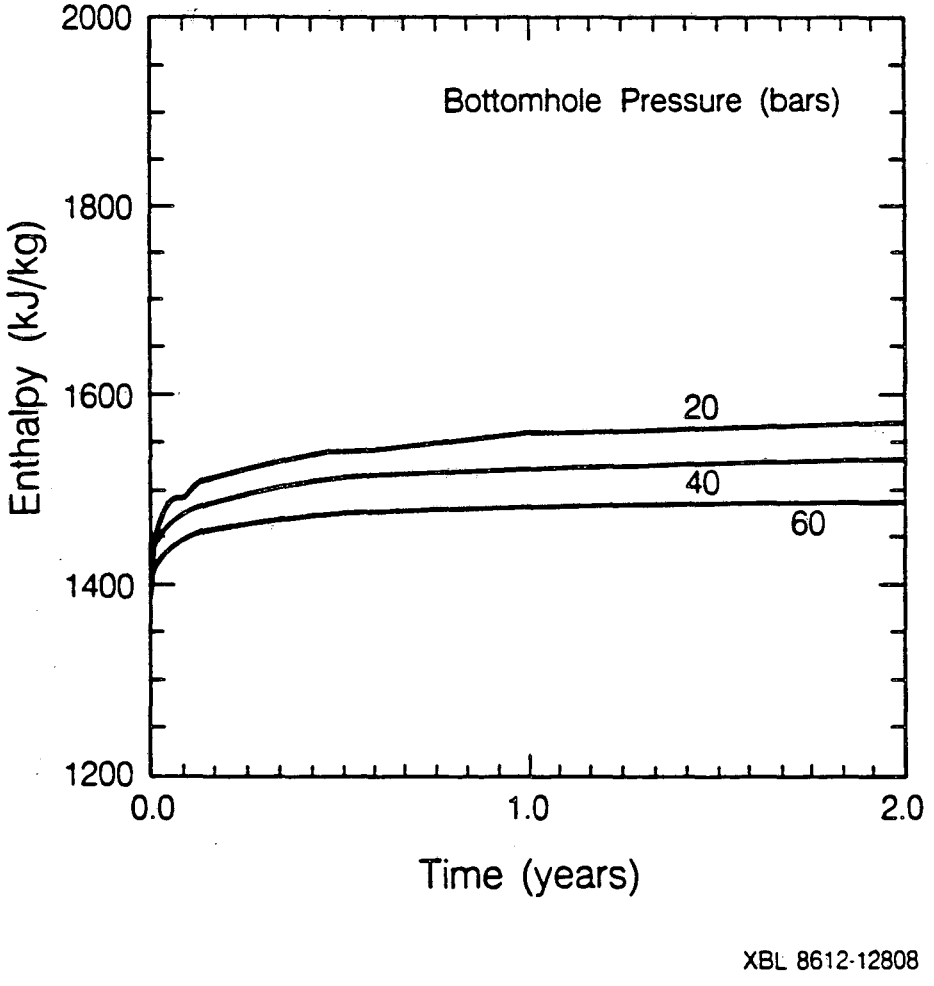

Figure (3-12). Effect of bottomhole pressure on flowing enthalpy transients with 10 bars initial partial pressure of CO_2 present.

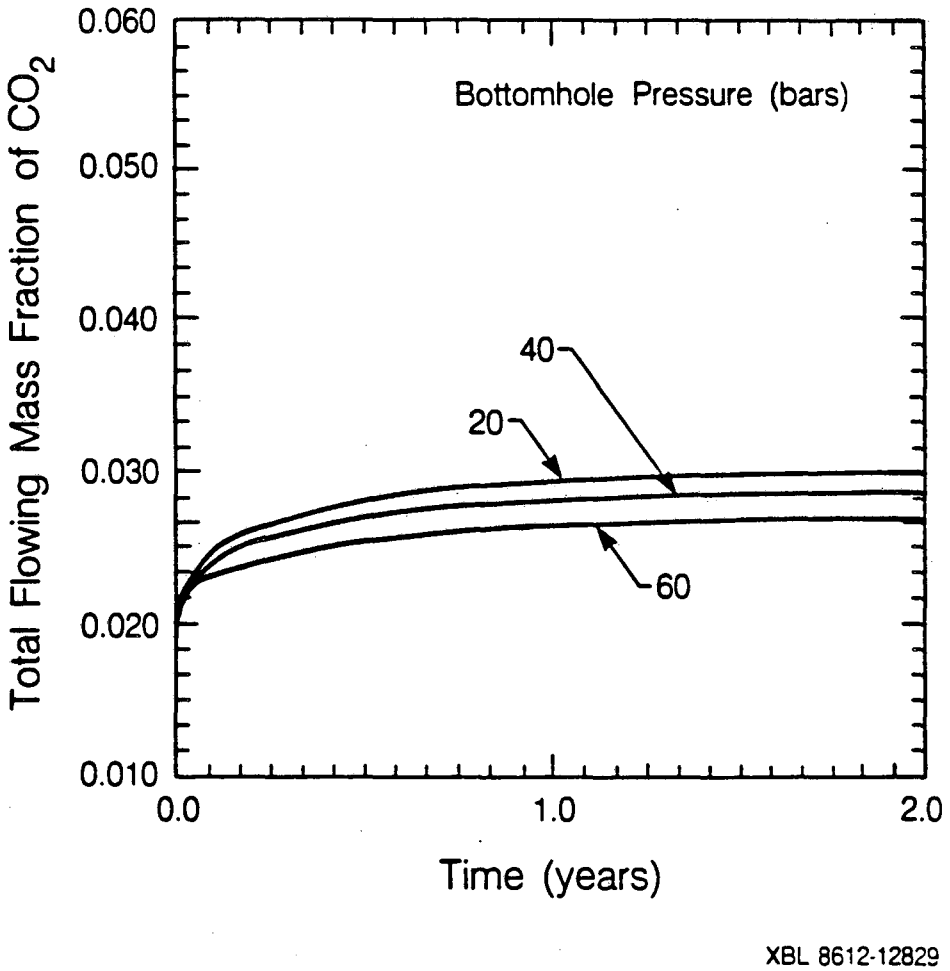

Figure (3-13). Effect of bottomhole pressure on transients of total flowing mass fraction of CO_2 with 10 bars initial partial pressure of CO_2 present.

small difference in the flowing enthalpy is due to the presence of a high concentration of CO_2 in the system. The amount of variation will be much greater at low initial partial pressures of CO_2 as was shown in section 3.5. The rise in flowing mass fraction of CO_2 scales directly with the increasing enthalpy as shown in Figure (3-13) where the flowing mass fraction is shown for different bottomhole pressures. The solubility difference between phases gives rise to the increase in flowing mass fraction of CO_2 as the gas phase mobility increases.

3.7 Fracture Porosity

The fracture porosity is defined here as the fraction of the total volume of rock and pore space which is occupied by the fractures. The fracture porosity has significant effects on the rate of rise in flowing enthalpy (see Figure (3-14)). The rise in flowing enthalpy decreases with increasing fracture porosity. Increasing the fracture porosity increases the amount of fluid in the fractures. The larger volume of fluid available in the fractures reduces the pressure gradient around the well (see Figure (3-15)) which in turn lowers the thermal gradient under two-phase conditions. This reduces both the amount of boiling in the fractures and the amount conductive and convective enhancement from the matrix, thereby reducing the rise in flowing enthalpy.

It has been observed that porous medium system there is a nearly linear relationship between the rise in flowing enthalpy and $(1-\phi)/\phi$ where ϕ is the porosity (Bodvarsson et al, 1980); the lower the porosity the higher the rise in flowing enthalpy. With a low porosity the region around the well becomes depleted rapidly increasing the pressure gradient toward the well and therefore, the amount of boiling. In a fractured medium without CO_2 present it was shown that the fracture porosity had similiar effects; the lower the fracture porosity the higher the rise in flowing enthalpy (Lippmann et al, 1985). When the fracture porosity is high, little recharge occurs from the matrix during the early transients. However, with a small fracture porosity, large gradients of both the pressure and the temperature develop between fracture and

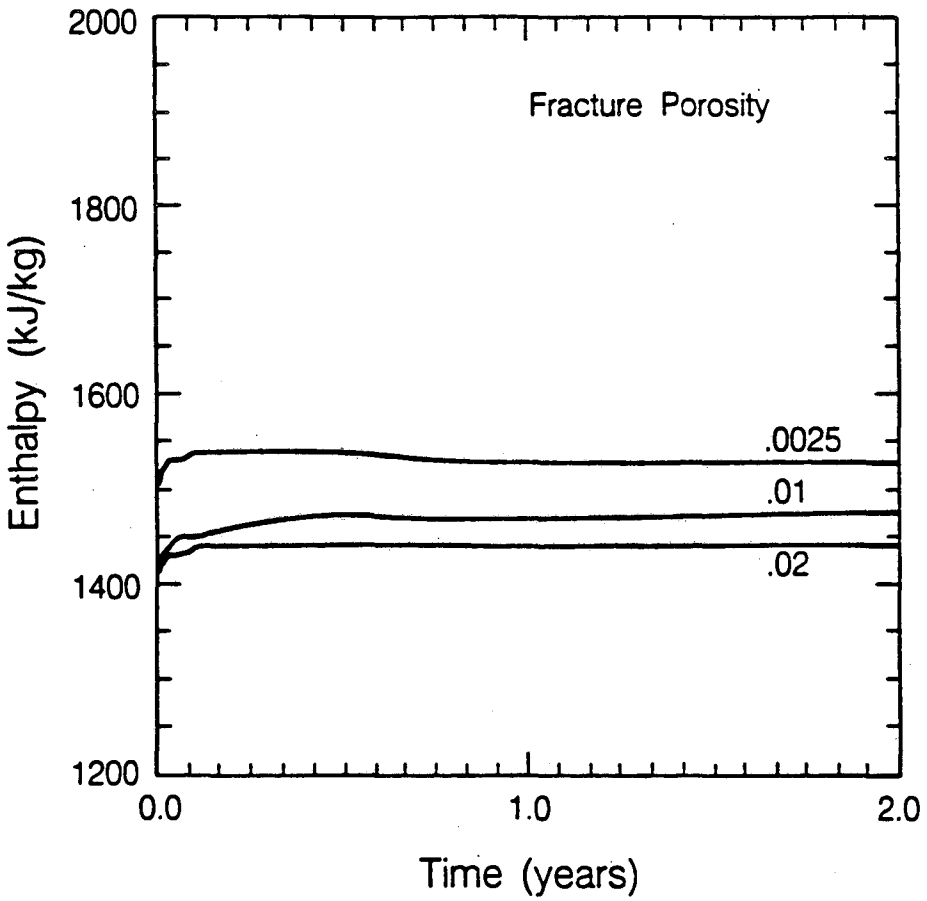

XBL 8612-12804

Figure (3-14). Effect of fracture porosity on flowing enthalpy transients with 10 bars initial partial pressure of CO_2 present.

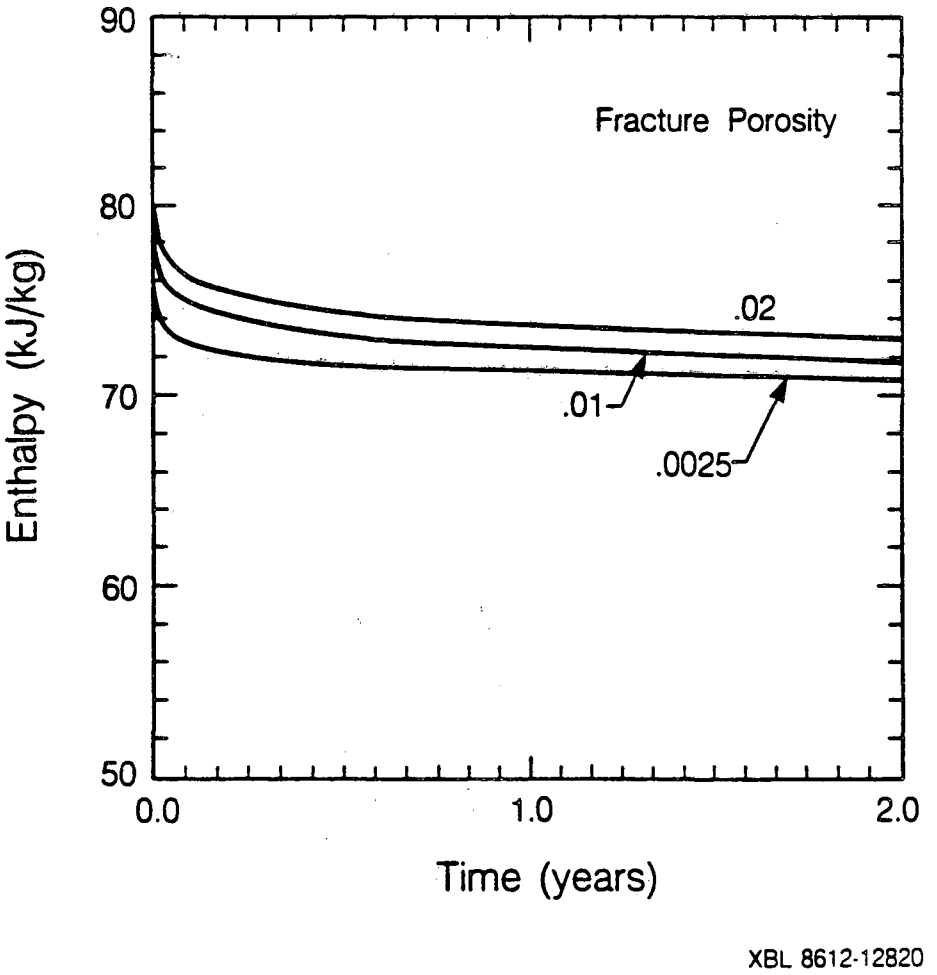

Figure (3-15). Effect of fracture porosity on transients of formation pressure with 10 bars initial partial pressure of CO_2 present.

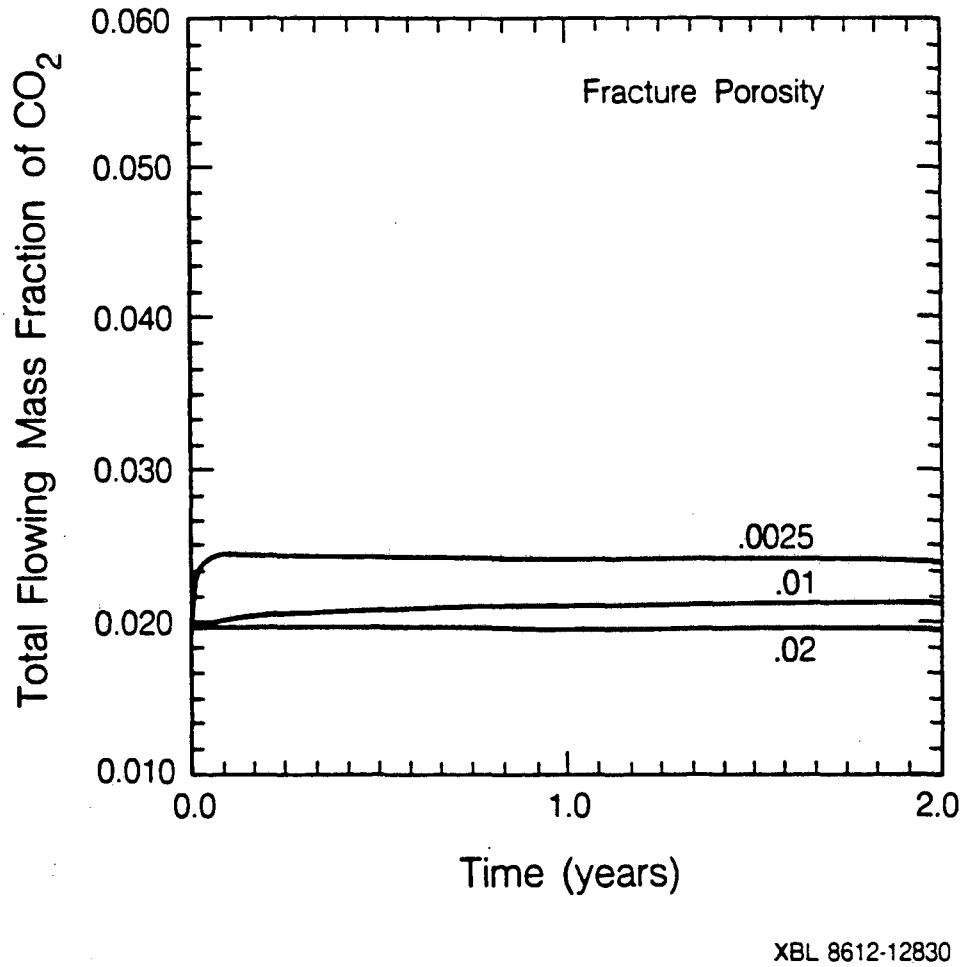

Figure (3-16). Effect of fracture porosity on transients of total flowing mass fraction of CO_2 with 10 bars initial partial pressure of CO_2 present.

matrix, so that the matrix contributes fluid and heat to the fracture rapidly. However, with a large amount of CO_2 present, degassing dominates the pressure decline so that little boiling occurs in the system. Although large pressure gradients may occur between the fracture and matrix the temperature gradient may be small since the pressure difference is strongly influenced by the presence of CO_2 while the boiling temperature of water is not.

Figure (3-16) shows that the flowing mass content of CO_2 increases with decreasing fracture porosity. The larger pressure gradients developed with low fracture porosity drive CO_2-rich fluid from the matrix causing higher flowing mass fraction of CO_2 in the fracture flowing to the well. In addition, the large pressure gradient enhances the effects of solubility imbalance between the phases.

3.8 Matrix Porosity

The matrix porosity has little effect on the flowing enthalpy. Figure (3-17) shows the flowing enthalpy transients for various matrix porosities varying from 0.001 to 0.20. The flowing enthalpy increases directly with matrix porosity; the higher the matrix porosity, the higher the flowing enthalpy. However, the total variation is only 50 kJ/kg after 2 years of production. This result is opposite to the findings of Lippmann et al (1985) for systems without CO_2 present (see Figure (3-18)). In the absence of CO_2, the enthalpy increased significantly with decreasing matrix porosity because of an increase in boiling within the matrix.

In gas-rich reservoirs the amount of CO_2 within the matrix increases linearly with the matrix porosity; the larger the porosity, the more mass of CO_2 in the matrix. Since CO_2 is poorly soluble in the liquid phase, most of the CO_2 is driven to the fractures with the gas phase. With a 0.001 matrix porosity little CO_2 is driven to the fractures since the total amount of fluid available is small, so that the flowing mass fraction of CO_2 remains nearly constant in the fractures (see Figure (3-19)). However, with a larger matrix porosity the total amount of CO_2 driven to the fractures is substantial leading to a significant rise in the flowing mass fraction of CO_2 as is shown in

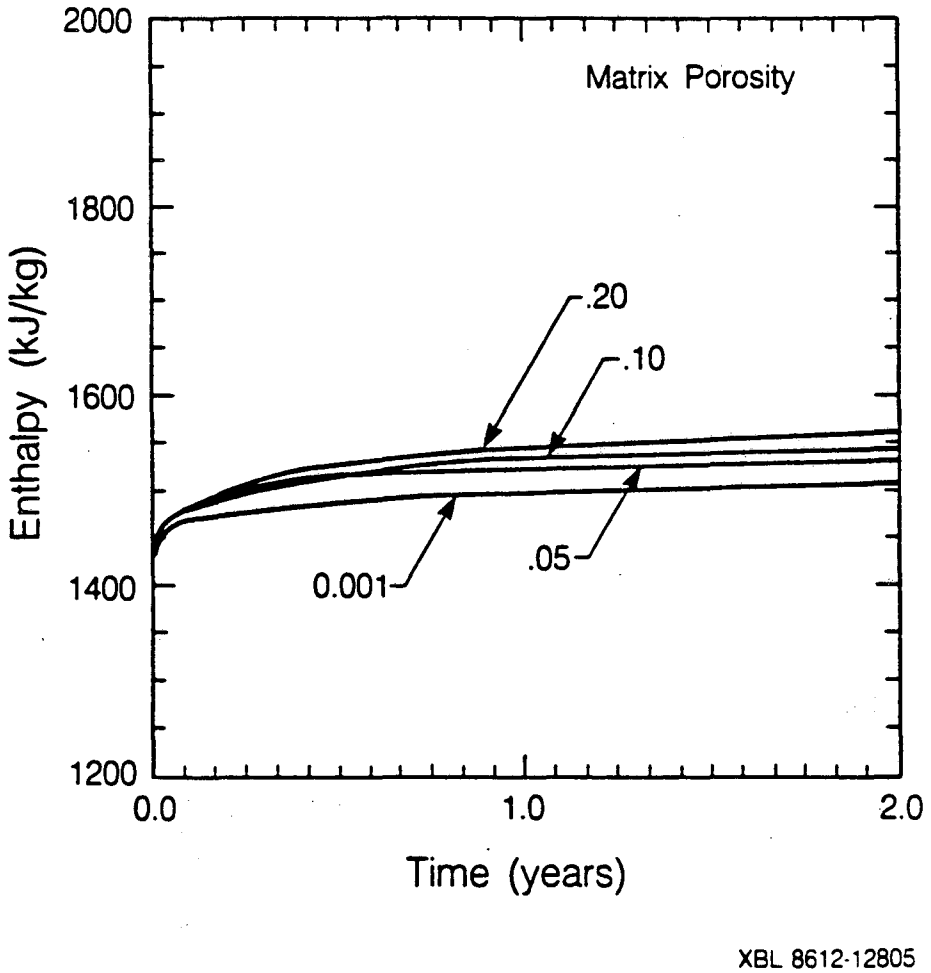

Figure (3-17). Effect of matrix porosity on flowing enthalpy transients with 10 bars initial partial pressure of CO_2 present.

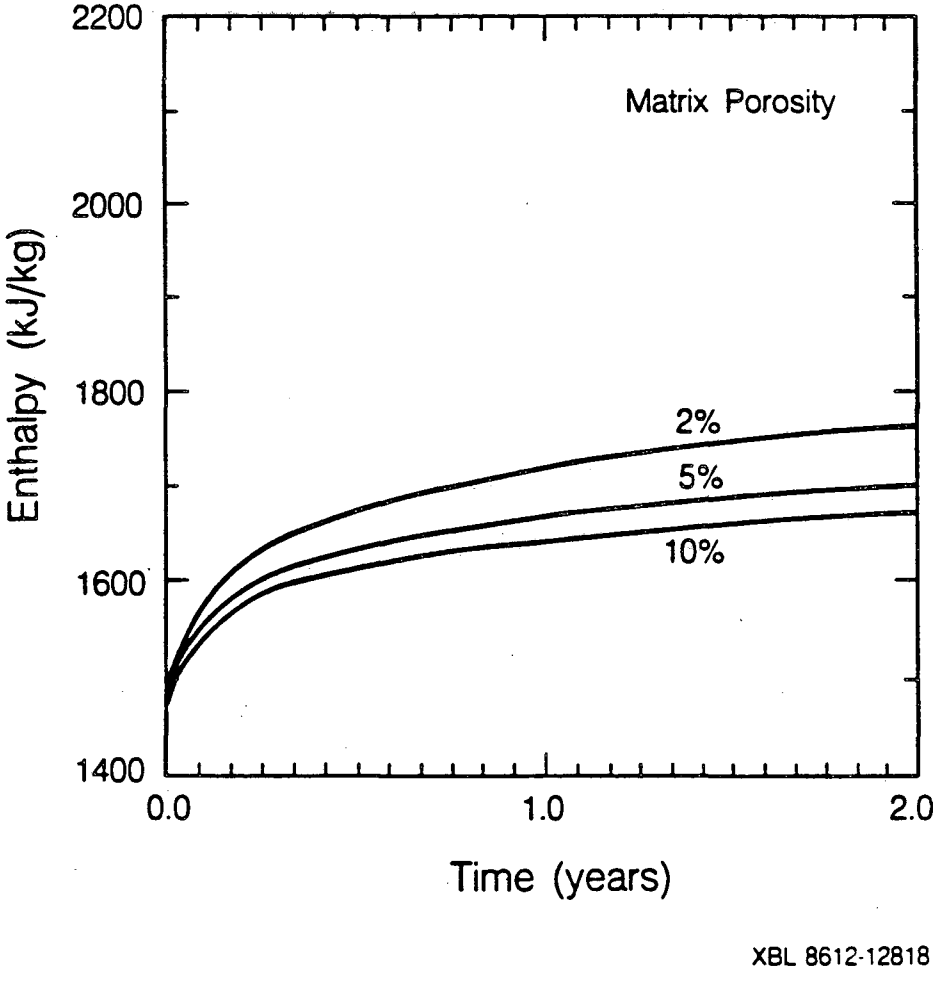

Figure (3-18). Effect of matrix porosity on flowing enthalpy transients without CO_2 present (Lippmann et al, 1985).

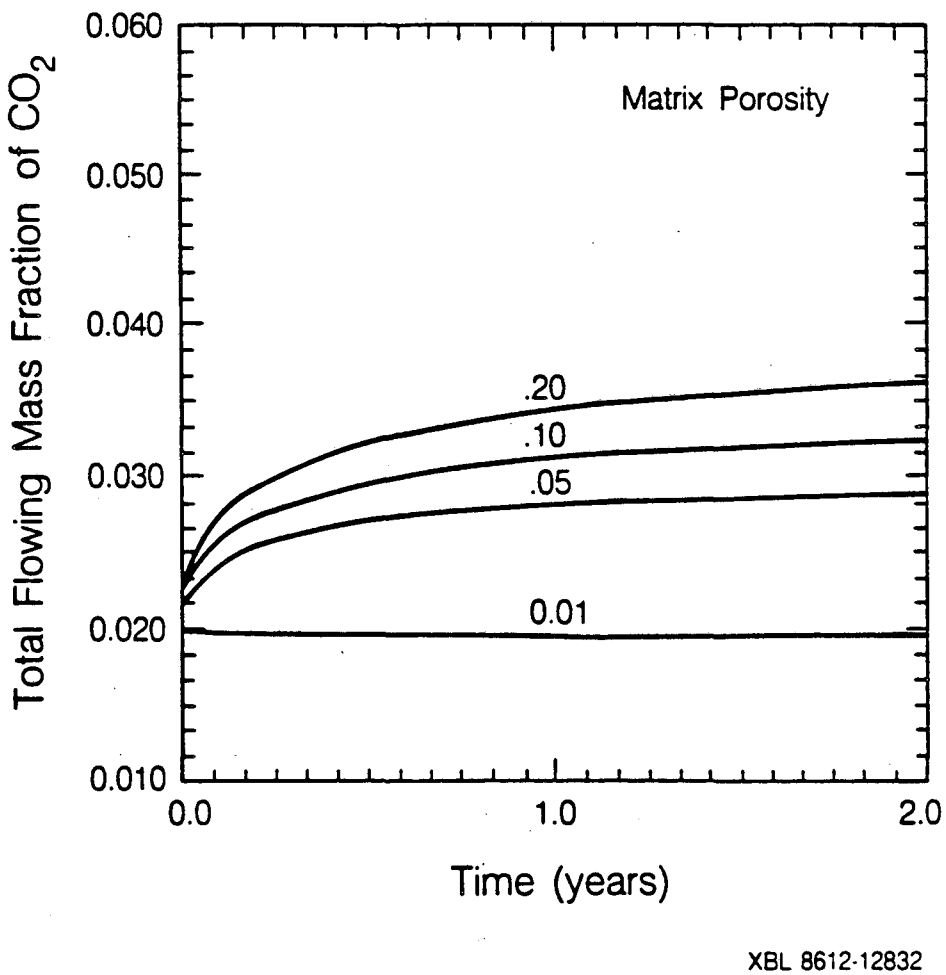

Figure (3-19). Effect of matrix porosity on transients of total flowing mass fraction of CO_2 with 10 bars initial partial pressure of CO_2 present.

Figure (3-19) where the flowing mass fraction of CO_2 increases in direct dependence of the matrix porosity. Since the total pressure in the fractures is nearly equal for all cases (differing by only 0.6 bars for matrix porosities ranging from 0.05 to 0.20), the increase in the mass fraction of CO_2 can only be accomodated by an increase in the gas saturation within the fractures (O'Sullivan, 1983). The increase in the gas saturation results in higher gas phase mobility and, hence, a higher flowing enthalpy. Since the rise in enthalpy is directly related to the amount of CO_2 in the matrix, systems with lower partial pressures will show behavior more like that observed by Lippmann et al (1985).

3.9 Fracture Permeability-Thickness

The fracture permeability-thickness controls the ability of fractures to conduct fluid to the well. The smaller the permeability-thickness product the larger the pressure gradient required to move fluid through the fractures. An increase in the pressure gradient also increases the temperature gradient under two-phase conditions intensifying boiling in the fractures so that flowing enthalpy increases with decreasing permeability-thickness. Figure (3-20) shows the flowing enthalpy transients for various values of the fracture permeability-thickness product. The variation is only 100 kJ/kg after 2 years of production with the largest rise in enthalpy occuring for the case with the lowest permeability-thickness product. This is only 40 percent of the variation Lippmann et al (1985) found without CO_2 present. The presence of a large concentration of CO_2 in a system reduces the amount of boiling so that the enthalpy variation is substantially reduced.

The flowing mass fraction of CO_2 increases as the pressure gradient in the fractures increases (see Figure (3-21)). The gradient increases the fluid contribution from the matrix. Since the matrix relative permeability function provides a much higher gas phase mobility, the fluid recharge from the matrix is CO_2-rich. This increases the flowing mass fraction of CO_2. However, boiling in the fractures produces little CO_2 so that the rise in the flowing mass fraction is not substantial. The variation in the

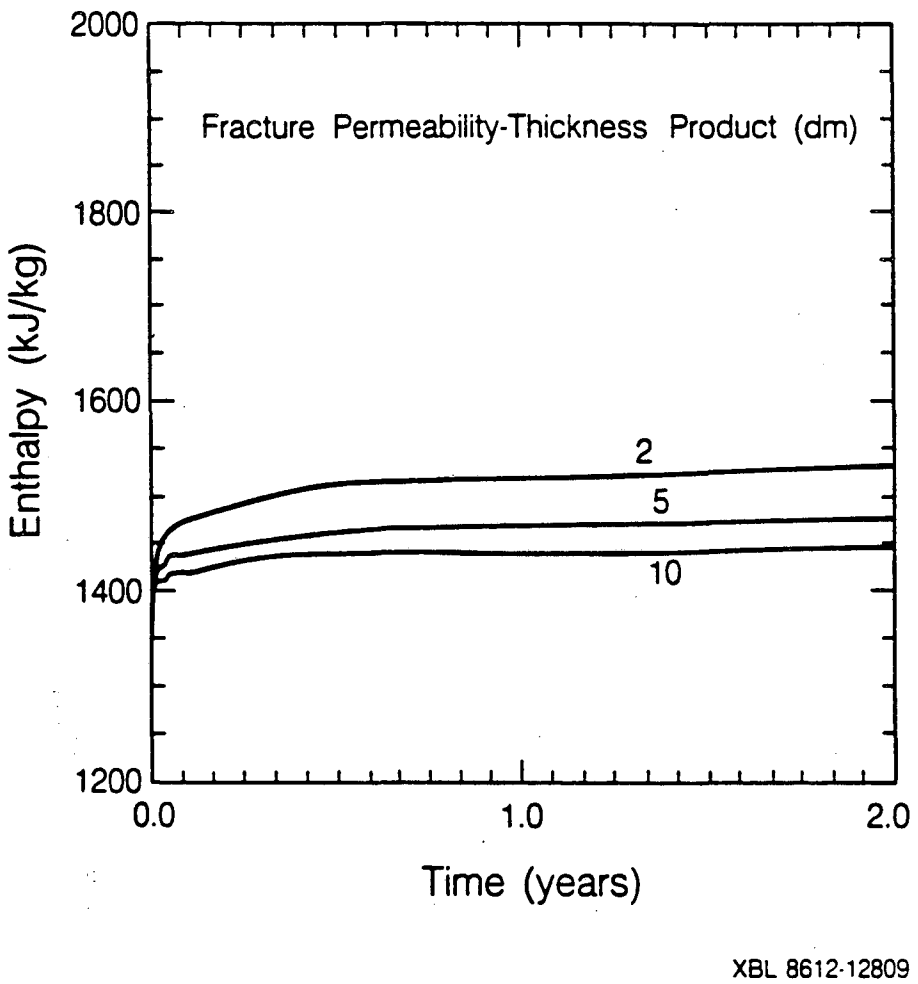

Figure (3-20). Effect of fracture permeability-thickness product on flowing enthalpy transients with 10 bars initial partial pressure of CO_2 present.

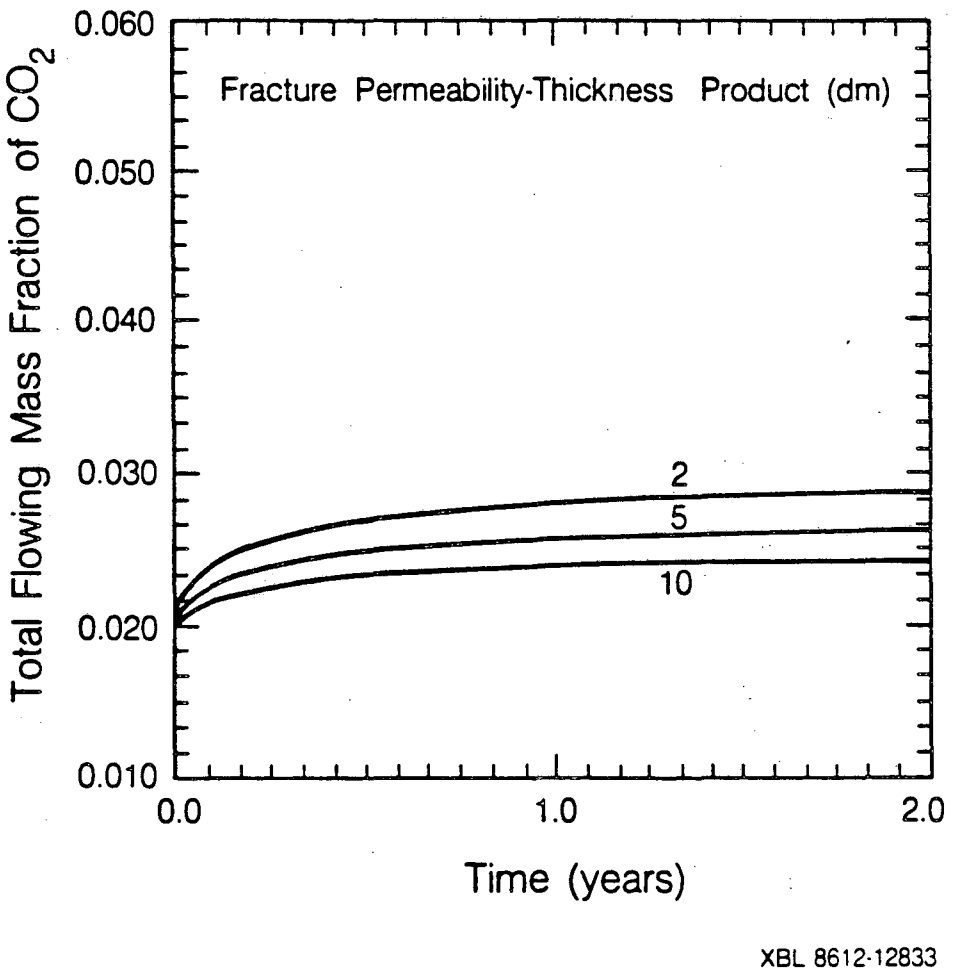

Figure (3-21). Effect of fracture permeability-thickness product on transients of total flowing mass fraction of CO_2 with 10 bars initial partial pressure of CO_2 present.

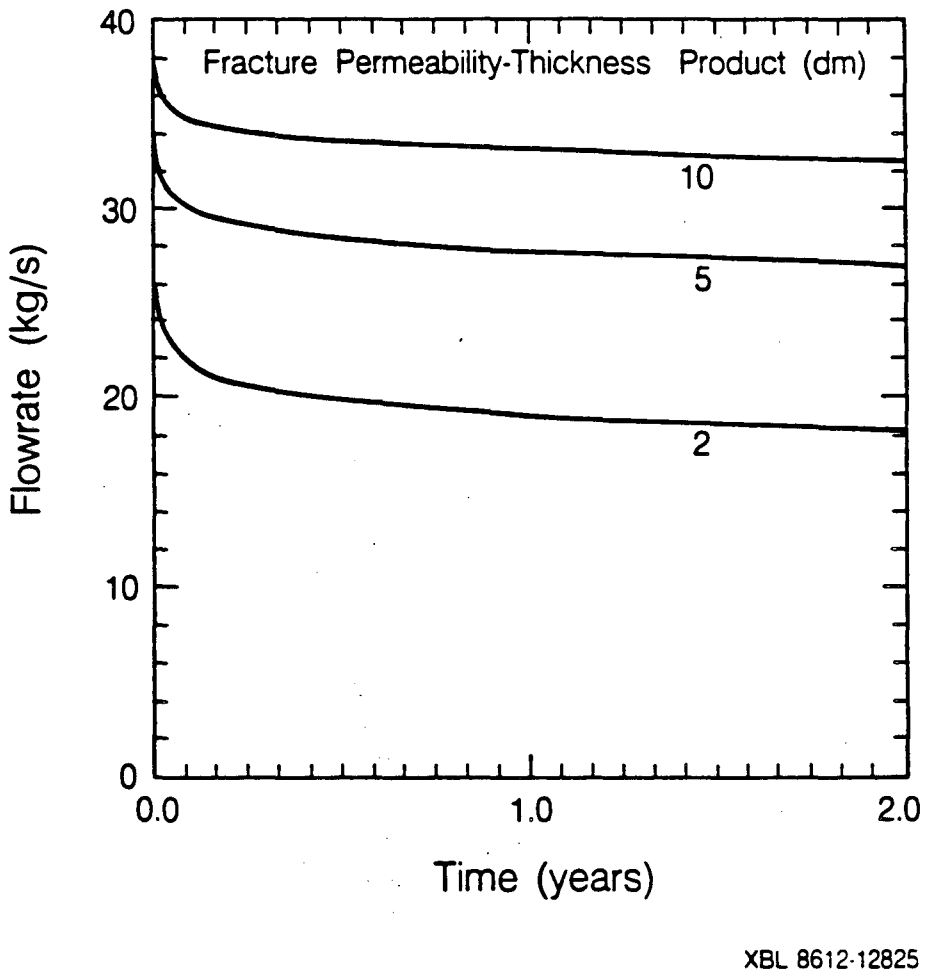

Figure (3-22). Effect of fracture permeability-thickness product on mass flowrate transients with 10 bars initial partial pressure of CO_2 present.

flowing mass fraction of CO_2 is only 0.4 percent after 2 years, primarily resulting from the increased fluid contribution from the matrix.

The production of fluid is strongly controlled by the permeability-thickness product. Decreased boiling combined with a decrease in the flowing mass fraction of CO_2 leads to a large increase in the liquid phase mobilities providing large mass flowrates as shown in Figure (3-22).

3.10 Matrix Permeability

Pruess (1983) determined that the effective matrix permeability has large effects on the flowing enthalpy. Reducing the matrix permeability increases pressure and therefore temperature gradients between matrix and fracture. This causes a large increase in the conductive enhancement of the fracture fluids by the matrix. Lippmann et al (1986) showed that the conductive enhancement was very important when the matrix is nearly impermeable causing a rise in the flowing enthalpy of over 700 kJ/kg (see Figure (3-23)). However, in the presence of a large amount of CO_2, the effects of matrix permeability on the flowing enthalpy are weak. Figure (3-24) shows the the flowing enthalpy versus time for matrix permeabilities of 0.0, 10^{-17}, and 10^{-16} m^2. With an initial partial pressure of CO_2 of 10 bars the total variation in flowing enthalpy is less than 25 kJ/kg after 2 years.

The saturation temperature for a system with CO_2 is less than that for a pure water system under two-phase conditions. The amount of saturation temperature lowering is determined by the partial pressure of CO_2 for a constant total pressure; the larger the partial pressure of CO_2, the lower the vapor pressure of water and therefore the saturation temperature.

With a high matrix permeability, fluid flows rapidly from the matrix. Since most of the CO_2 resides in the vapor phase and substantial boiling occurs, the matrix becomes rapidly depleted in CO_2. Therefore, the matrix has little CO_2 while the fracture has a substantial flowing partial pressure. The higher partial pressure of CO_2 in the fracture indicates a lower vapor pressure of water and, hence, a lower saturation

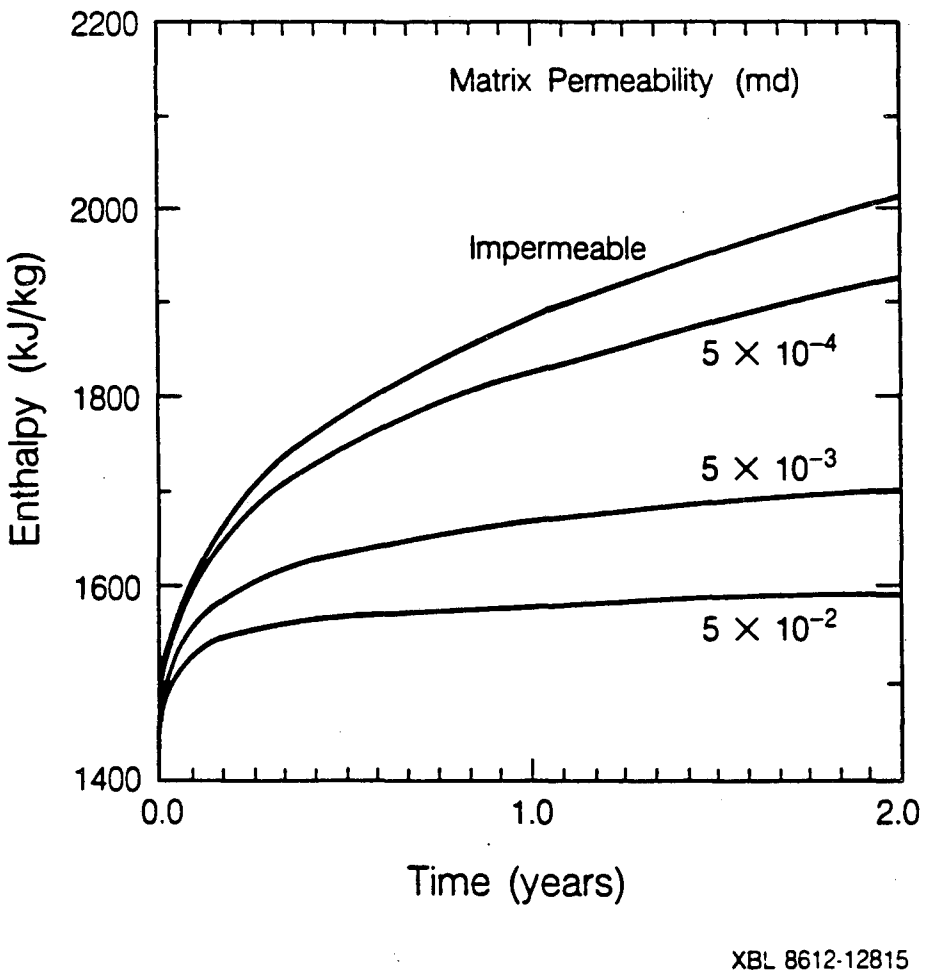

Figure (3-23). Effect of fracture permability-thickness product on flowing enthalpy transients without CO_2 present (Lippmann et al, 1985)

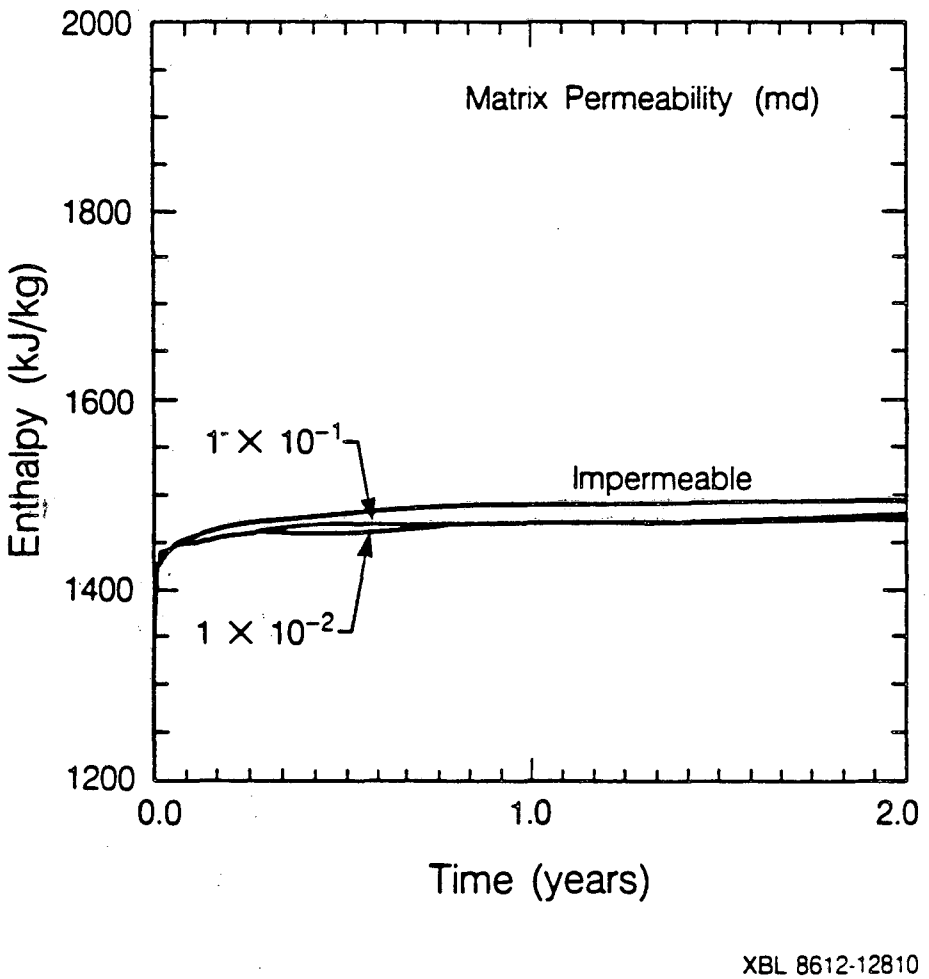

Figure (3-24). Effect of matrix permeability on flowing enthalpy transients with 10 bars initial partial pressure of CO_2 present.

temperature. The difference in temperature between the fracture and the matrix is increased as a result of the disparity in CO_2 partial pressures leading to enhanced thermal conduction.

When the matrix has low permeability, conditions change rapidly in the fractures because the matrix provides little fluid. During production the gas saturation rises in the fractures and the partial pressure of CO_2 drops rapidly. Therefore, the partial pressure of CO_2 is much larger in the matrix than in the fractures because little gas can escape due to the low permeability. The lowering of the partial pressure of CO_2 in the fractures reduces the amount of boiling in the system. Because boiling is reduced, the temperature drops more slowly. The smaller temperature difference between the fracture and the matrix reduces flowing enthalpy enhancement due to conduction.

Therefore, the presence of CO_2 in a system enhances thermal conduction when the matrix permeability is high. However, when the permeability is low, differences in CO_2 partial pressures between the fractures and matrix reduce the temperature gradient by lowering the amount of boiling in the fractures and therefore the amount of enthalpy enhancement due to conduction. However, this effect is directly related to the partial pressure of CO_2 present in the system. If the partial pressure is small, the water vapor pressure will be close to the total pressure for the system and boiling will be significant. This results in a larger temperature gradient, and thus behavior similiar to a reservoir without gas.

The flowing mass fractions of CO_2 for the different permeability cases are shown in Figure (3-25). When the matrix permeability is high the CO_2 mass fraction rises rapidly and stablizes. The flowing mass fraction of CO_2 stabilizes when flow of heat and mass reaches quasi-steady state between fracture and matrix. For lower matrix permeability decreases, there is less rise in the flowing mass fraction, however, the mass fraction continues to rise after two years of production because of the prolonged disequilibrium in the fracture/matrix interaction. There is very little difference in the CO_2 mass fraction between the cases.

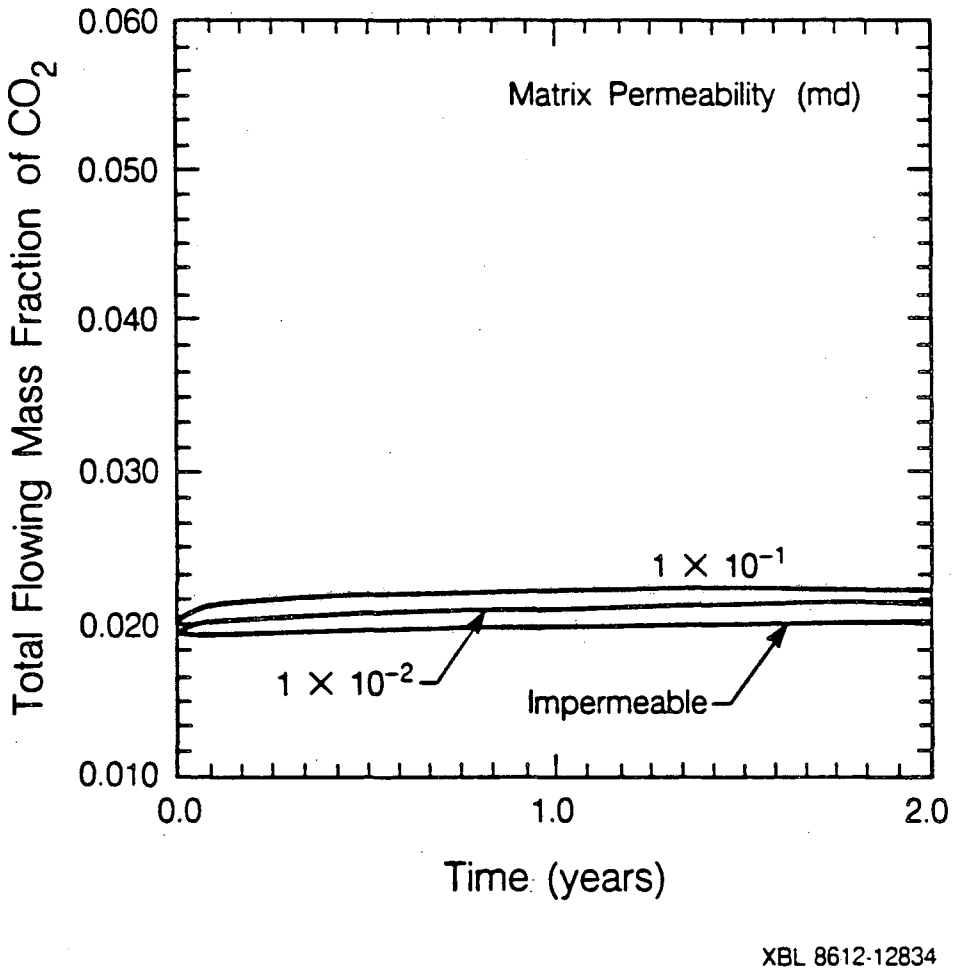

Figure (3-25). Effect of matrix permeability on transients of total flowing mass fraction of CO_2 with 10 bars initial partial pressure of CO_2 present.

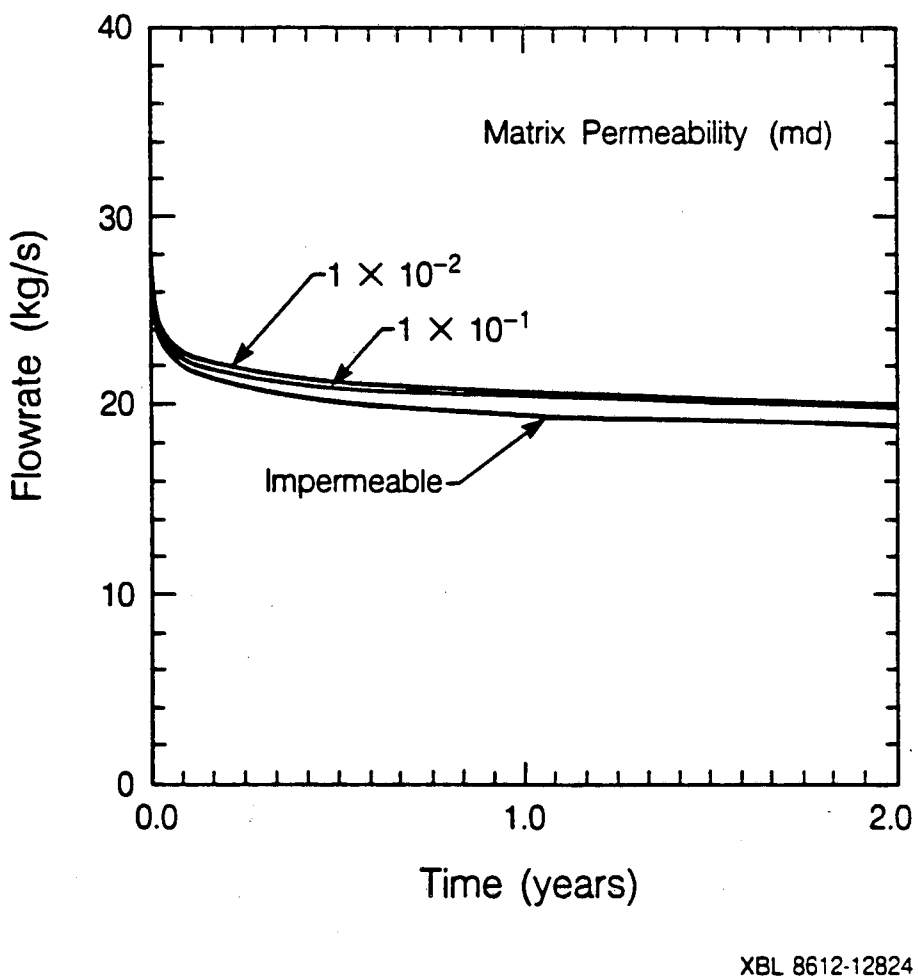

Figure (3-26). Effect of matrix permeability on mass flowrate transients with 10 bars initial partial pressure of CO_2 present.

The total mass flowrate transients for the first 2 years are shown in Figure (3-26). The matrix permeability has little effect on the mass flowrate as the total variation is less than 2 kg/s during the first 2 years. This small variation relates directly to the CO_2 effects on flowing enthalpy. Since there is little enthalpy enhancement with large amounts of CO_2 present, the mobilities for each case are very similiar leading to little variation in mass flowrate.

3.11 Initial Gas Saturation

The initial gas saturation has strong effects on the flowing enthalpy. Figure (3-27) shows the flowing enthalpy transients for initial gas saturations of 0.02, 0.10, 0.20, 0.30, and 0.50. The flowing enthalpy is determined using the saturation dependant relative permeability functions so that the initial and stable flowing enthalpies will increase proportionately with the initial gas saturation. The total variation in the stable flowing enthalpies is 400 kJ/kg (1350-1750kJ/kg) between initial gas saturations ranging from 0.02 to 0.50. This variation is substantially smaller than that observed in a reservoir without CO_2. One would expect that for an initial gas saturation exceeding 0.3, that pure steam would be produced (enthalpy of 2800kJ/kg) if the CO_2 content in the reservoir was low. The rather small enthalpy rise when CO_2 is present is again due to less boiling, as some of the pressure drop is due to degassing, as well as the low enthalpy of CO_2.

The initial gas saturation has large effects on the flowing mass fraction of CO_2 (see Figure (3-28)). Since the amount of CO_2 that can be dissolved in the liquid phase of water is small, most of the CO_2 resides in the vapor phase. Therefore, the flowing mass fraction of CO_2 will practically scale linearly with initial gas saturation of the reservoir. The total variation between gas saturations of 0.02 and 0.50 is more than 4 percent after 2 years of production.

The flowrate varies inversely with the initial gas saturation; a lower gas saturation means increased liquid phase mobility and consequently higher rates (see Figure (3-29)). However, we find that downhole pressure is almost independant of the initial

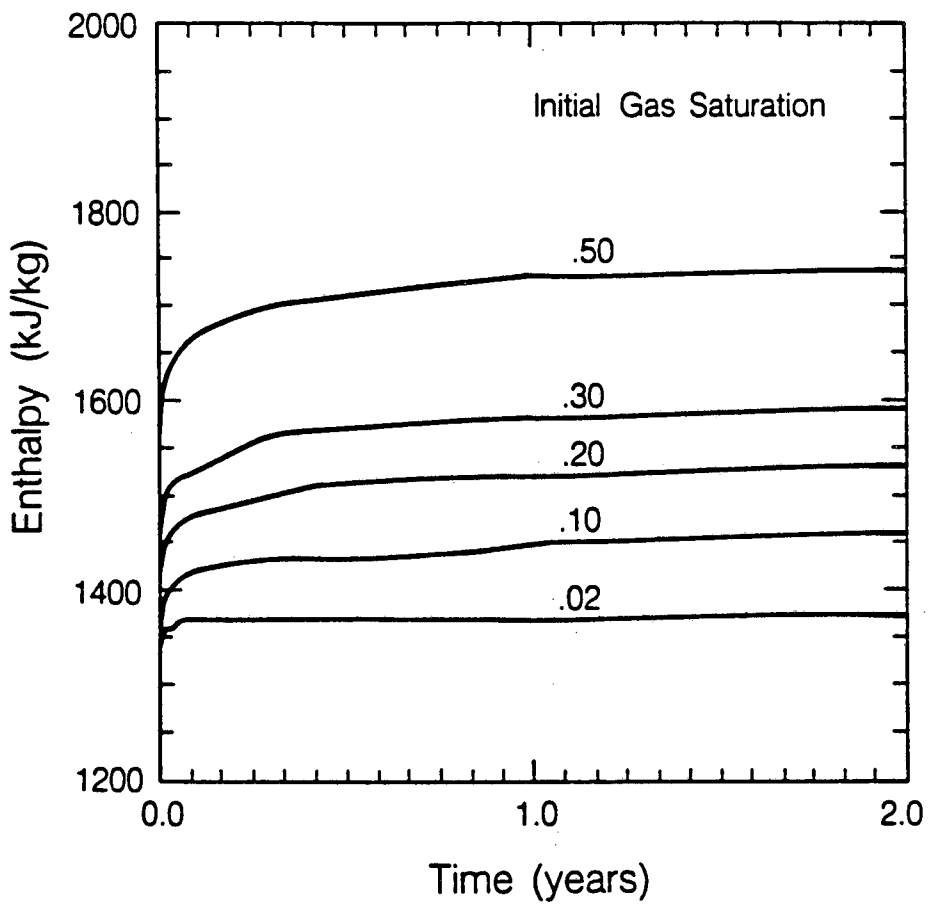

XBL 8612-12811

Figure (3-27). Effect of initial gas saturation on flowing enthalpy transients with 10 bars initial partial pressure of CO_2 present.

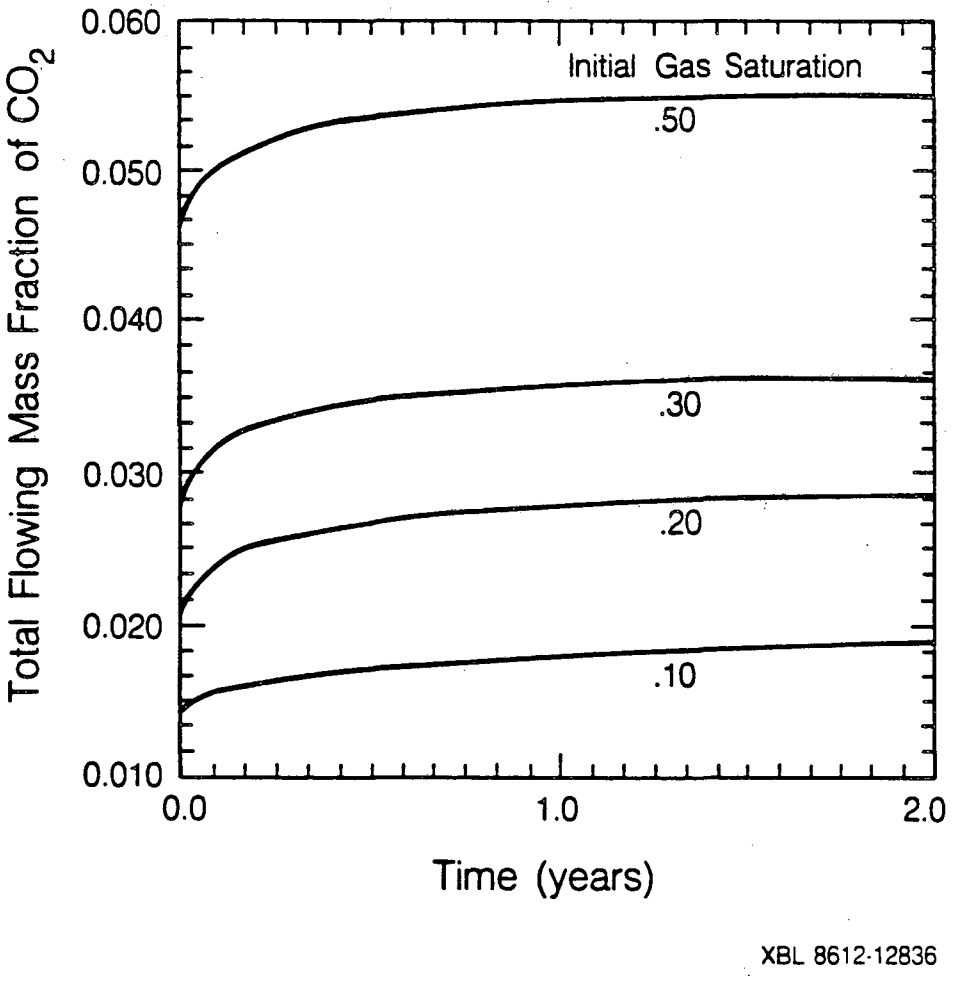

Figure (3-28). Effect of initial gas saturation on transients of total flowing mass fraction of CO_2 with 10 bars initial partial pressure of CO_2 present.

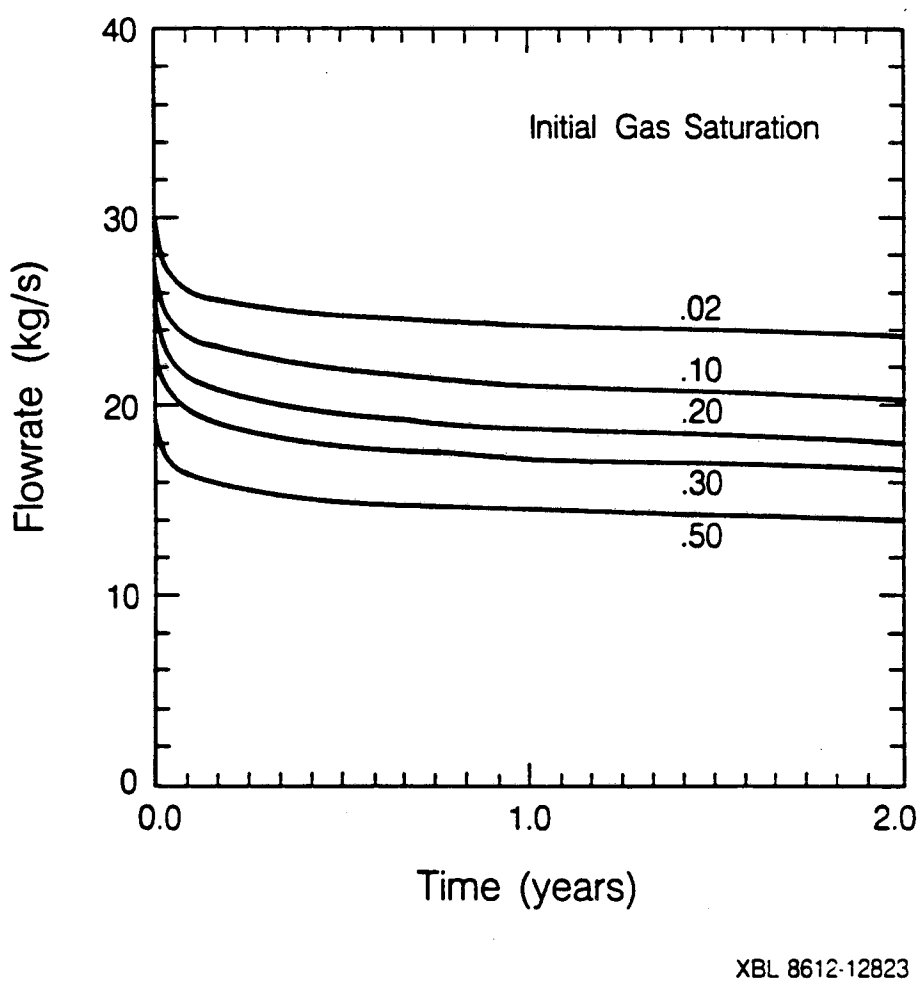

Figure (3-29). Effect of initial gas saturation on mass flowrate transients with 10 bars partial pressure of CO_2 present.

gas saturation, varying by only 1 bar over the two year period for the different cases. Pressure drop due to degassing for high CO_2 mass fractions (high gas saturations) tends to offset the pressure drop due to the larger production rates for the cases with low initial gas saturation.

3.12 Thermal Conductivity

The thermal conductivity of the rock controls how rapidly heat is transferred from the matrix to the fracture fluids. Lippmann et al (1985) showed that the thermal conduction had large effects on the flowing enthalpy when no CO_2 is present as shown in Figure (3-30). We find much less significant effects for the cases with 10 bars initial partial pressure of CO_2 as shown in Figure (3-31). The conductive enhancement of flowing enthalpy amounts to only 50 kJ/kg for a thermal conductivity of 4.4 W/m °C over no conductive enhancement. As noted previously, the presence of CO_2 decreases the amount of boiling in the system as well as the temperature gradients. The lower temperature gradient significantly reduces the rate of conduction from the matrix to the fractures. Therefore, the presence of large concentrations of CO_2 in the system significantly reduces the flowing enthalpy.

After two years of production the partial pressure of CO_2 is 4.5 bars and 5.5 bars for thermal conductivities of 4.4 W/m °C and 0.0 W/m °C, respectively. This considerable difference in the partial pressure of CO_2 results in a substantial difference in gas saturation in the fractures. A lower concentration of CO_2 results in a lower gas saturation. A drop in the gas saturation causes a drop in the gas phase mobilities which lowers the flowing enthalpy.

The partial pressure variation between the two cases is related to the complex thermodynamics of H_2O–CO_2 mixtures which causes fluid to recharge the matrix in order to equilibrate CO_2 partial pressures between fracture and matrix (see Chapter 4). Because the rate at which CO_2 is lost to the matrix is related to the rate of thermal conduction, the partial pressure and therefore the flowing mass fraction of CO_2 vary directly with the thermal conductivity (see Figure (3-32)). However, the total variation

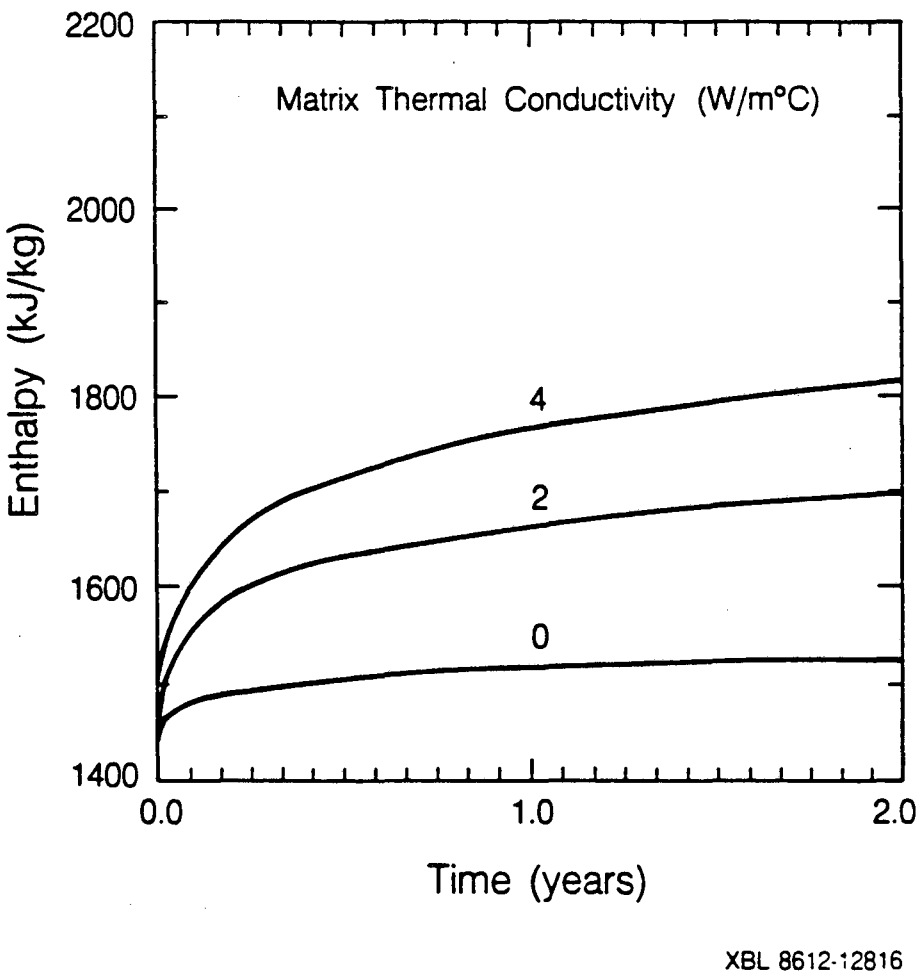

Figure (3-30). Effect of matrix thermal conductivity on flowing enthalpy transients without CO_2 present (Lippmann et al, 1985).

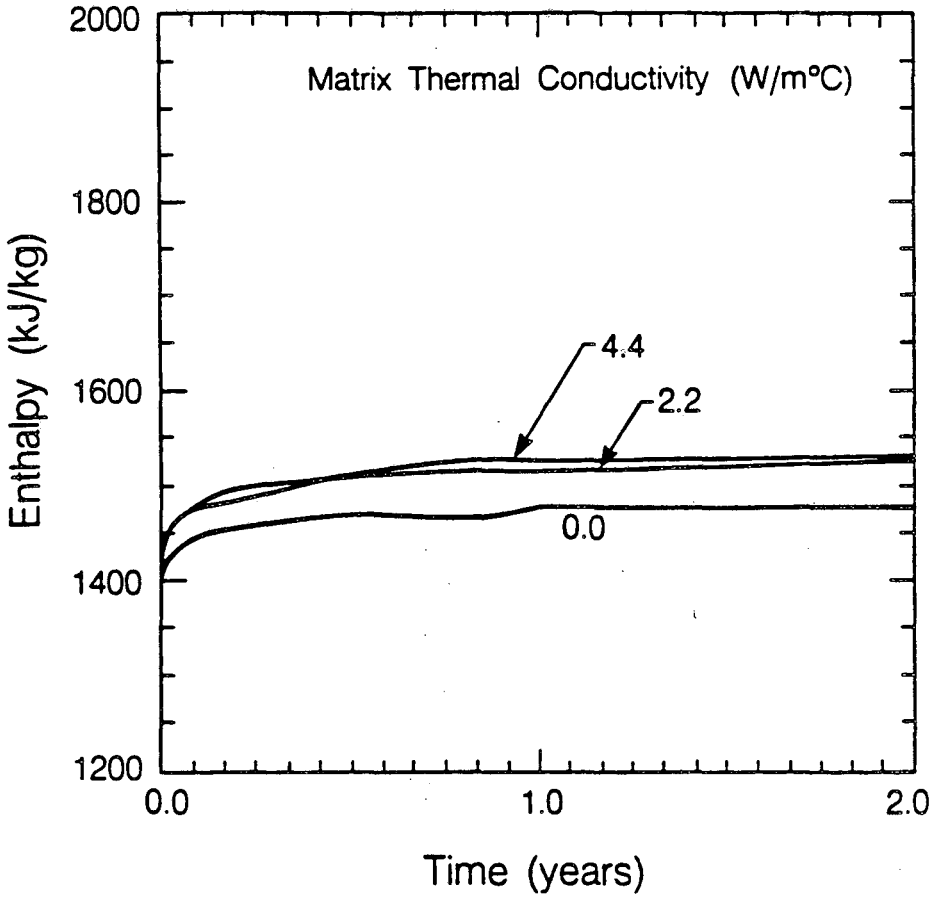

XBL 8612-12812

Figure (3-31). Effect of matrix thermal conductivity on flowing enthalpy trasients with 10 bars initial partial pressure of CO_2 present.

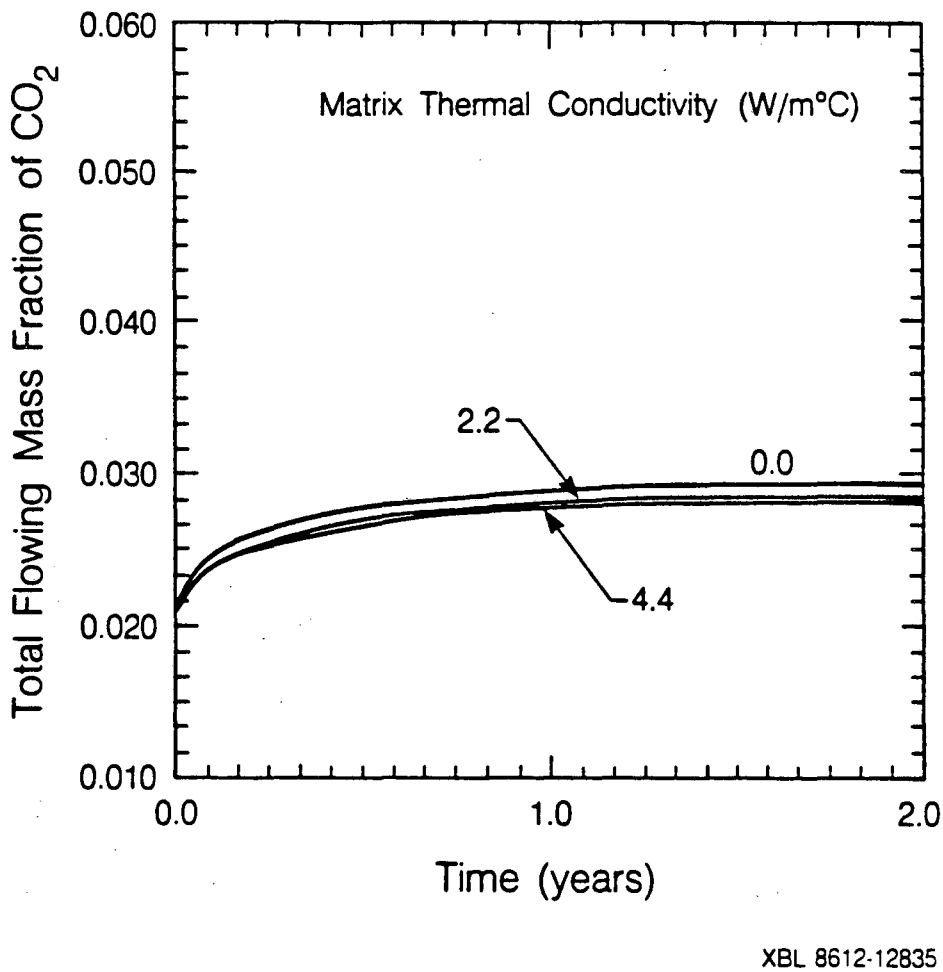

Figure (3-32). Effect of matrix thermal conductivity on transients of total flowing mass fraction of CO_2 with 10 bars initial partial pressure of CO_2 present.

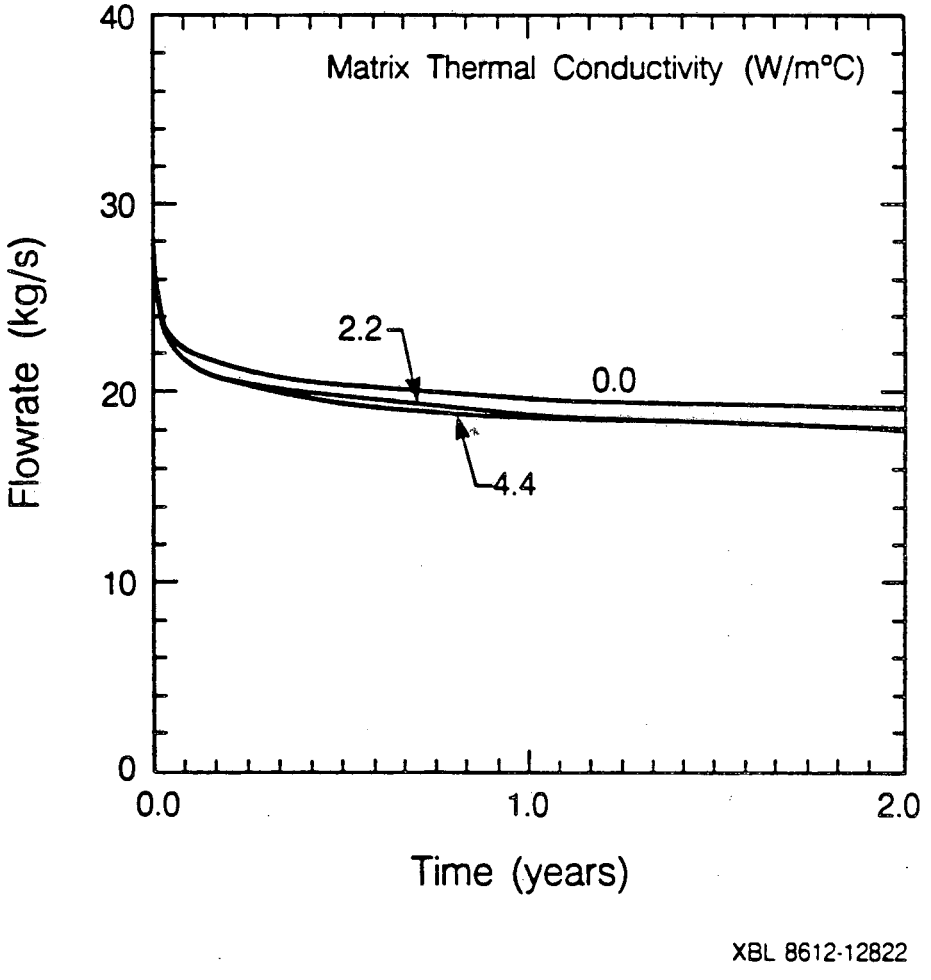

Figure (3-33). Effect of matrix thermal conductivity on mass flowrate transients with 10 bars initial partial pressure of CO_2 present.

in flowing mass fraction of CO_2 after two years is less than 0.2 percent.

Since the mass flowrate is controlled by the gas saturation in the fractures, the flowrate increases slightly with decreasing thermal conductivity (see Figure (3-33)).

3.13 Fracture Spacing

The fracture spacing is defined as the distance between two parallel fracture planes of the three mutually perpendicular fracture sets discussed previously. For a given reservoir volume, the fracture spacing is inversely proportional to the total surface area between the fractures and the matrix. Figure (3-34) shows the flowing enthalpy transients for fracture spacings of 20, 100 and 500 meters. The fracture spacing has significant effects on the rate of rise in flowing enthalpy. The larger the fracture spacing, the slower the rise in flowing enthalpy. The lower surface area between the fractures and the matrix reduces both the conductive and convective enhancement of fracture fluid enthalpy. The reduction in the convective enhancement can be inferred from the pressure transients shown in Figure (3-35). With a large fracture spacing, the pressure near the well drops rapidly because the recharge rate to the fracture is low. However, with 20 meter fracture spacing the pressure at the well drops much slower initially because of the large recharge from the matrix. After 18 months of production the pressure for the 20 meter fracture spacing case has declined to that of the 100 meter case. This results from the depletion of CO_2 in the fractures near the well in the 20 meter case as CO_2 backflows into the matrix. As the amount of CO_2 in the fractures drops, the flowing enthalpy declines because of a drop in the gas phase mobilities which accompanies the loss of CO_2 (see Figure 34). This will also occur for cases with higher fracture spacings, but a longer time is necessary to deplete the larger matrix blocks due to the reduced surface area between the fractures and matrix. Inversely, since the rate of heat transfer is enhanced with lower fracture spacing the pressure will drop more rapidly at late time.

The fracture spacing has significant effects on the rate of rise in the flowing mass fraction of CO_2 (see Figure (3-36)). The time frame is less than that for flowing

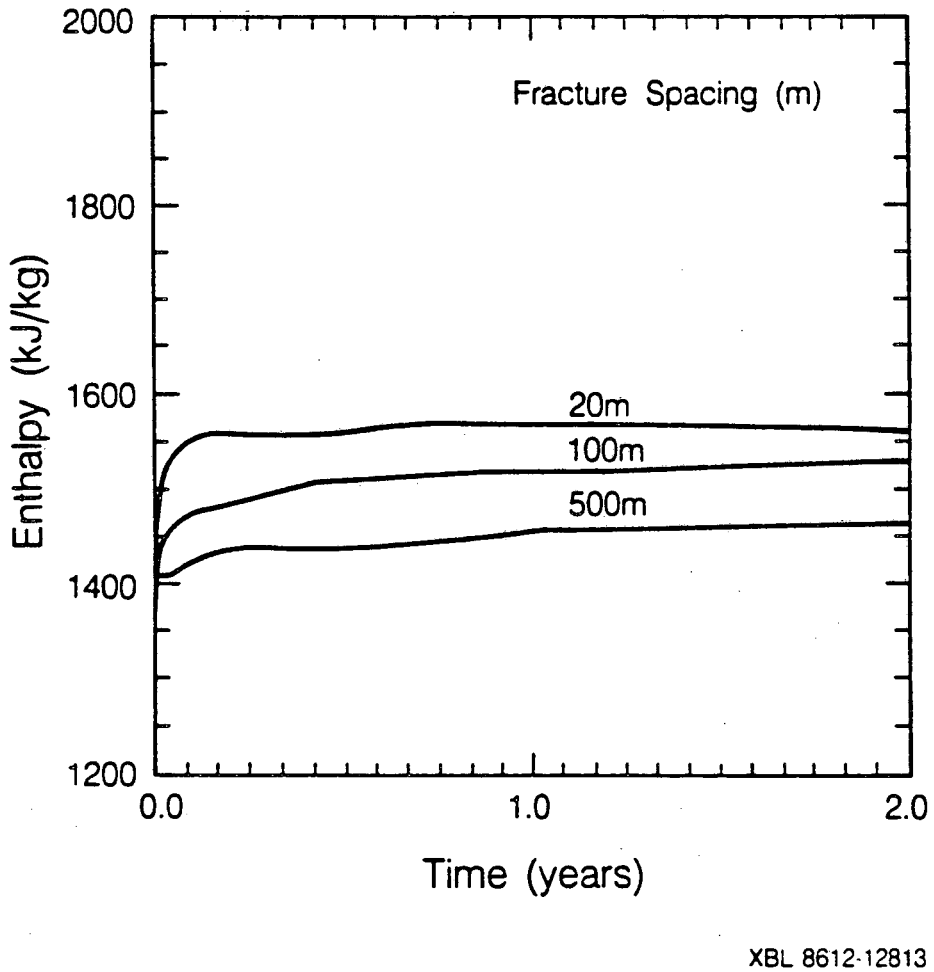

Figure (3-34). Effect of fracture spacing on flowing enthalpy transients with 10 bars initial partial pressure of CO_2 present.

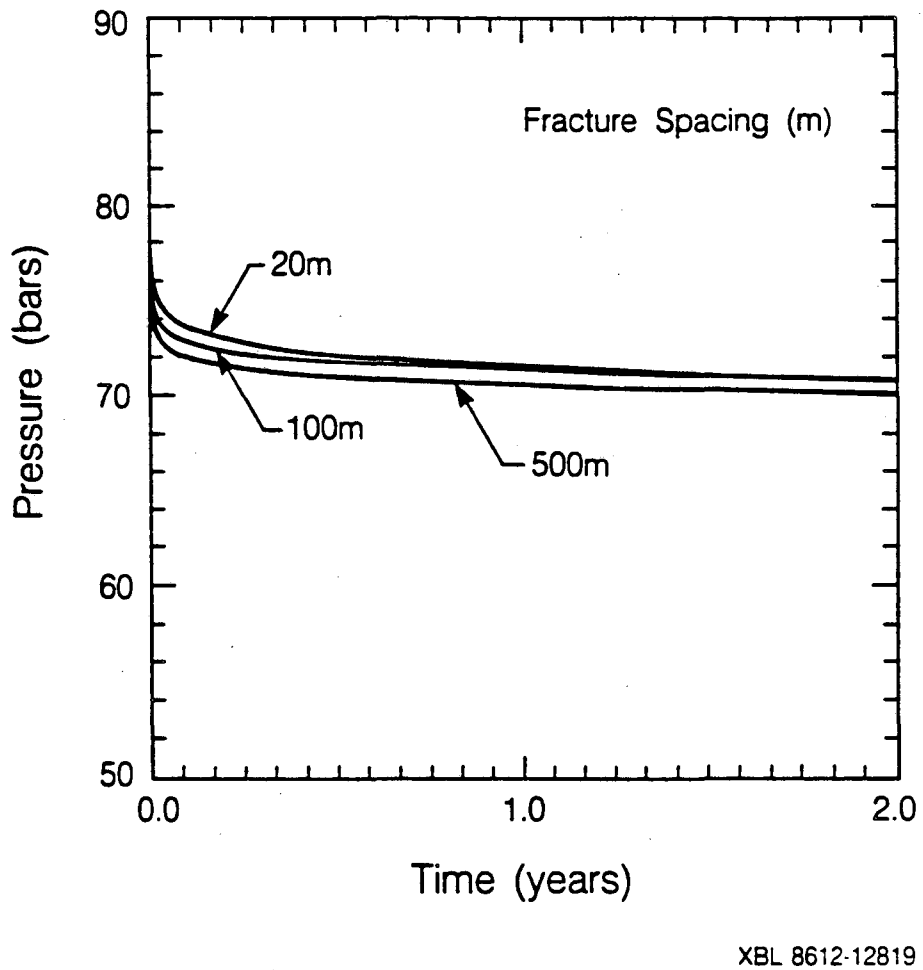

Figure (3-35). Effect of fracture spacing on formation pressure transients with 10 bars initial partial pressure of CO_2 present.

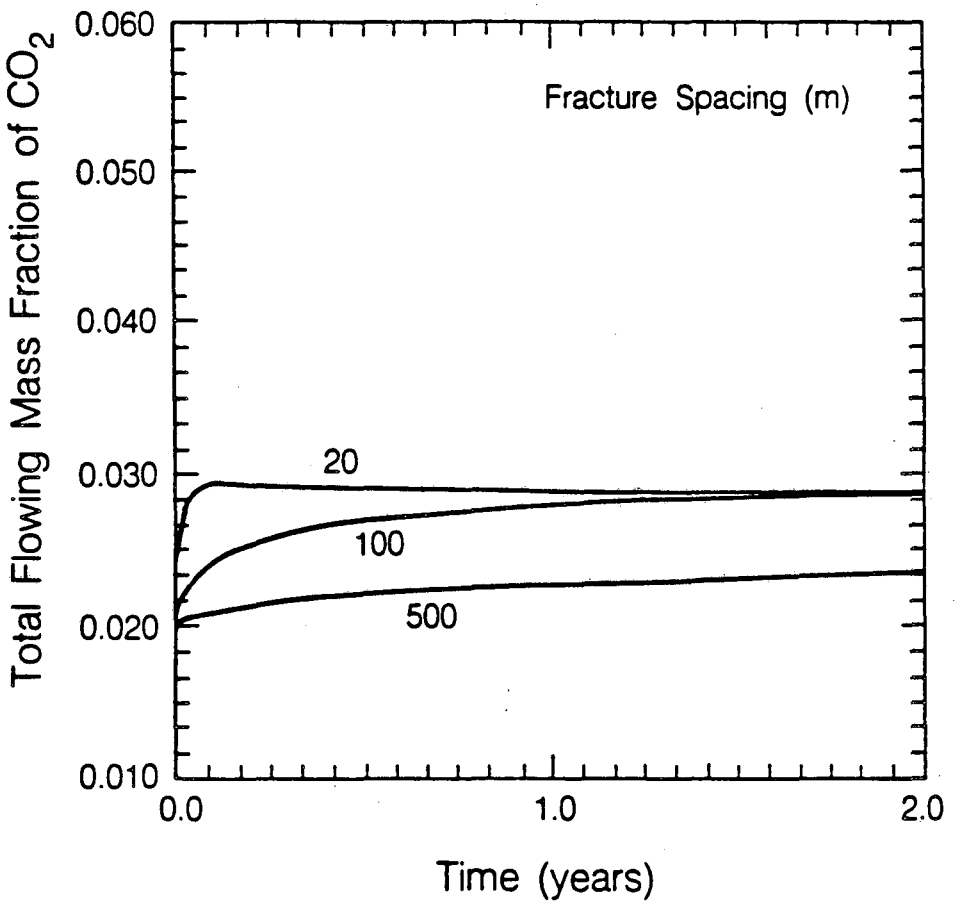

XBL 8612-12838

Figure (3-36). Effect of fracture spacing on transients of total flowing mass fraction of CO_2 with 10 bars initial partial pressure of CO_2 present.

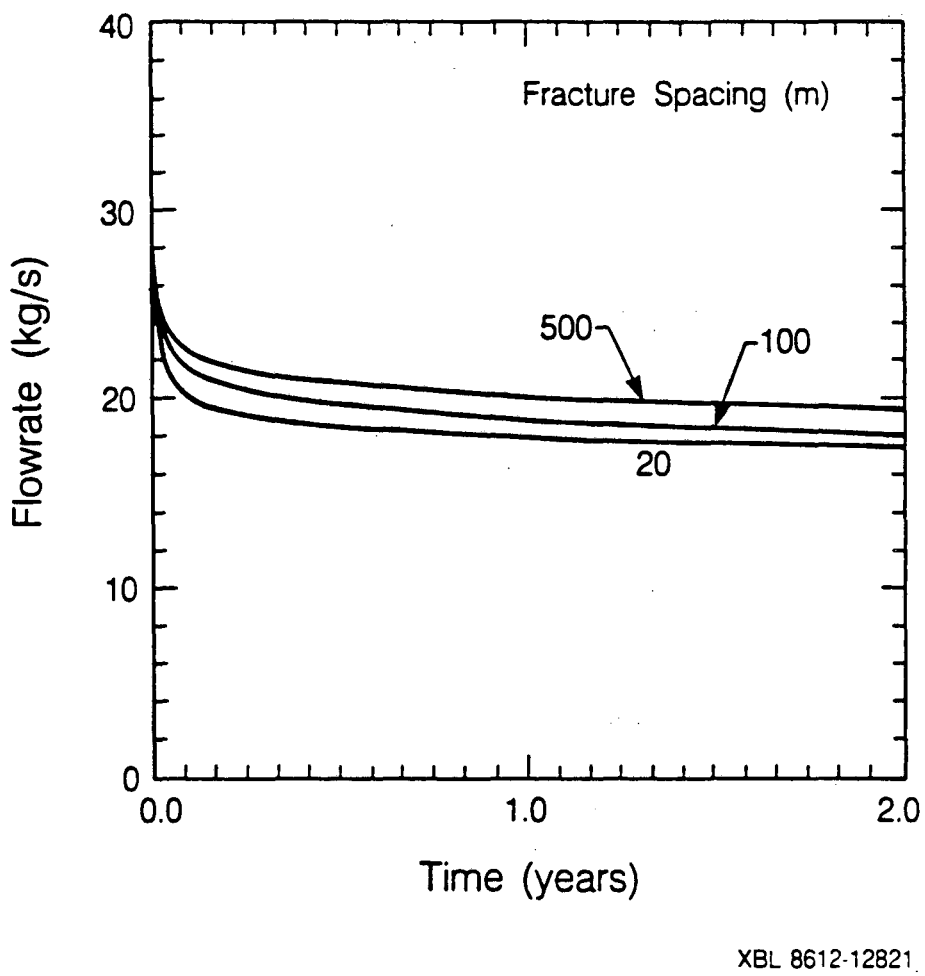

Figure (3-37). Effect of fracture spacing on mass flowrate transients with 10 bars initial partial pressure of CO_2 present.

enthalpy because of the poor solubility of CO_2 in the liquid phase of water. The CO_2 is rapidly lost to the fracture with the vapor phase and is further depleted in the matrix by boiling while the enthalpy requires conduction of heat for stabilization of fracture-matrix interaction. For the 20 meter case, the flowing mass fraction of CO_2 rises rapidly and then begins to decline with time after less than 25 days of production. The decline in the mass fraction is caused by loss of CO_2 to the matrix too near the well where it has been depleted and the total pressure has reached equilibrium (see Chapter 4).

The mass flowrate is moderately effected by fracture spacing. The total variation is slightly more than 2 kg/s for the first 2 years (see Figure (3-37)). This results from the lower liquid phase mobilities with decreasing fracture spacing. A combination of increased boiling and high flowing CO_2 content at early times increase the gas saturation and therefore, the saturation dependant gas relative permeability.

3:14 Relative Permeability Curves

Lippmann et al (1985) showed that the flowing enthalpy is strongly controlled by the saturation dependent fracture relative permeability functions when no gas is present (see Figure (3-38)). The relative permeability functions cause large variation in the total kinematic mobility as shown in Figure (3-3). Because the SGB curves have a much higher gas phase mobility, the results using these curves show 400 kJ/kg enthalpy enhancement in comparison with the results using X-curves. In the presence of CO_2 the effects of the various relative permeability curves are substantially reduced as shown in Figure (3-39). The matrix relative permeability functions have little effect on the flowing enthalpy with gas present. Figure (3-40) shows the variation in flowing enthalpy versus time for the Corey and SGB curves. The case with SGB curves for matrix relative permeabilities has only 50 kJ/kg greater enthalpy after 2 years than for the case with Corey curves. CO_2 degassing drastically reduces the the pressure gradient from the matrix so that the contribution of fluid from the matrix is small. Also, the temperature gradient will be much smaller and, hence, less enthalpy enhancement.

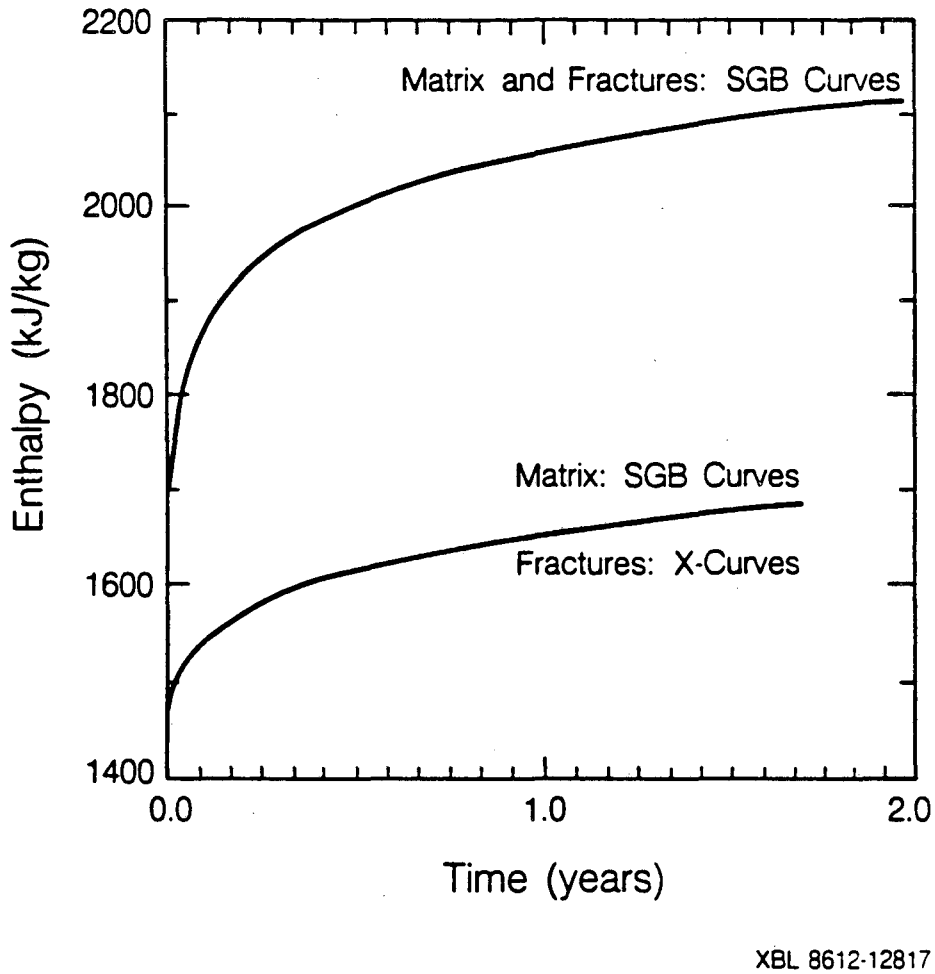

Figure (3-38). Effect of fracture relative permeability curves on flowing enthalpy transients without CO_2 present (Lippmann et al, 1985).

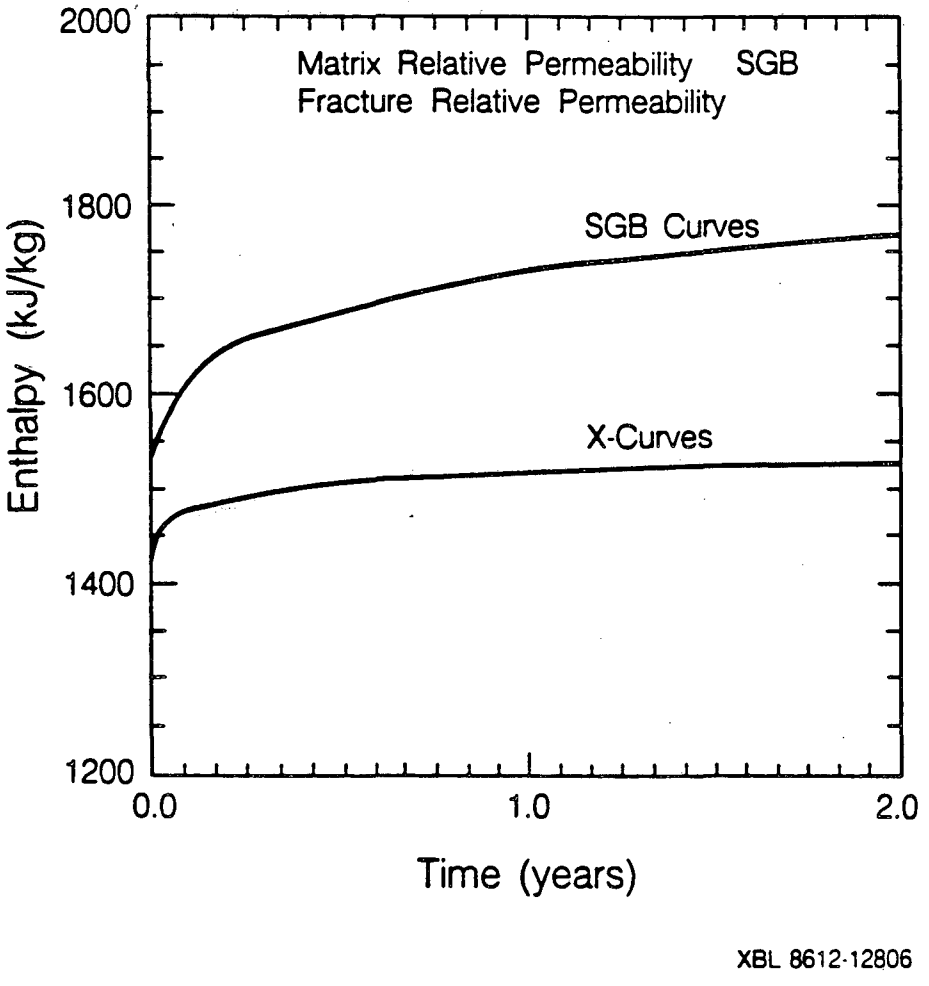

Figure (3-39). Effect of fracture relative permeability curves on flowing enthalpy transients with 10 bars initial partial pressure of CO_2 present.

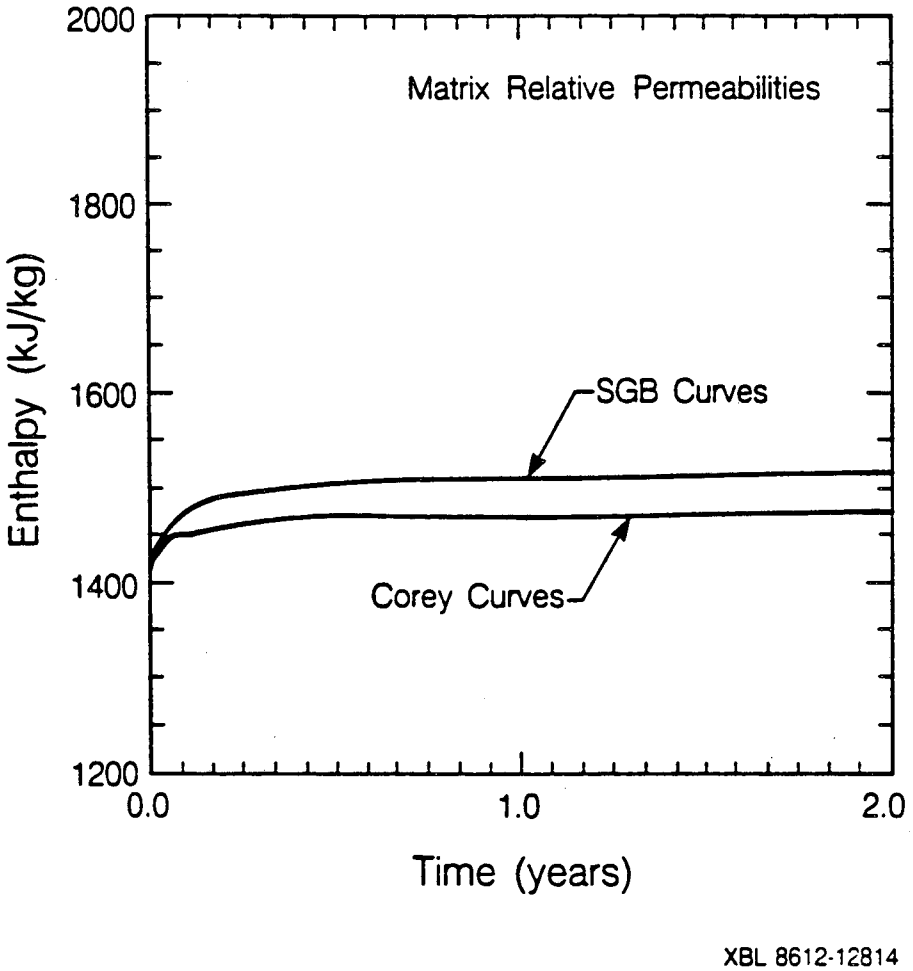

Figure (3-40). Effect of matrix relative permeability curves on flowing enthalpy transients with 10 bars initial partial pressure of CO_2 present.

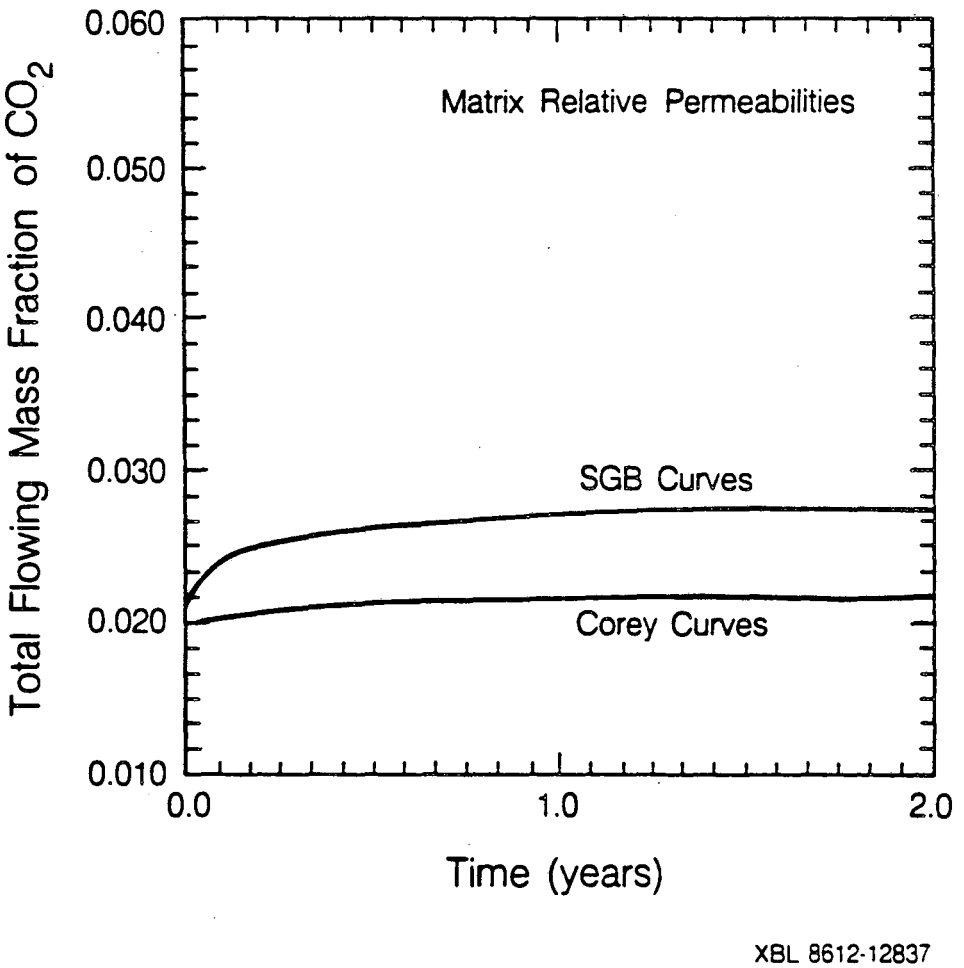

Figure (3-41). Effect of matrix relative permeability curves on transients of flowing mass fraction of CO_2 with 10 bars initial partial pressure of CO_2 present.

Therefore, the higher gas phase mobilities have only a slight effect on the flowing enthalpy. With a lower partial pressure of CO_2, degassing would be less significant. A lower pressure drop due to degassing would result in more boiling and, hence, higher flowing enthalpy.

The flowing mass fraction transients of CO_2 are, however, more strongly affected by the type of matrix relative permeability functions used (see Figure (3-41)). Because of the higher gas phase mobility of the SGB curves, the flowing mass fraction of this case rises 0.6 percent higher after 2 years than that with conventional Corey curves. A higher gas phase mobility allows more CO_2 into the fractures causing a decline in the liquid phase mobility.

3.15 Summary

The presence of CO_2 in a geothermal reservoir has large effects on the flowing enthalpy transients of wells penetrating the reservoir. With CO_2 present, the boiling temperature of water is lower causing an expansion of the two-phase zones within the reservoir. The initial changes in the distribution of the phases can result in large variations in the mobilities of the phases and therefore the flowing enthalpy when compared to that of a reservoir without CO_2 present. Also, the pressure can drop significantly due to degassing of CO_2. The reduction in boiling will result in a lower rate of heat transfer in the reservoir. This causes the important parameters which determine the rise in flowing enthalpy to differ substantially from those without gas present.

Without CO_2 present, the properties that primarily affect the flowing enthalpy are matrix permeability, matrix thermal conductivity, fracture spacing, fracture permeability thickness product, and fracture porosity. With significant amounts of CO_2 present the temperature gradients between the fracture and matrix are reduced with the associated decrease in boiling such that most of these properties have little effect on the flowing enthalpy.

Only the initial gas saturation and the initial partial pressure of CO_2 have large effects on the flowing enthalpy. The initial gas saturation and the initial partial pressure affect the phase distribution within the system, thereby altering phase mobilities. Also, an increase the mass fraction of CO_2, which has a lower heat capacity than steam, will lower the flowing enthalpy. The large effects of the initial partial pressure of CO_2 on the flowing enthalpy suggest that other parameters may be important at lower partial pressures. The fracture spacing has significant effects on the rate of rise in flowing enthalpy. The variation in surface area with fracture spacing affects both conductive and convective heat transfer to the fractures. The flowing mass fraction of CO_2 can be a valuable tool in determining reservoir properties. The flowing mass fraction of CO_2 will vary little in the wellbore unless substantial scaling is occuring and is relatively easy to measure at the surface.

The initial gas saturation, the initial partial pressure of CO_2 and the matrix porosity all have strong effects on the amount of CO_2 in a system and therefore, control the amount of rise in the flowing mass fraction. The matrix permeability and the fracture spacing both have strong effects on the rate of rise in the flowing mass fraction of CO_2. These two parameters control the rate of recharge to the fracture from the matrix.

The flowing mass fraction of CO_2 can be used in conjunction with the flowing enthalpy to determine, qualitatively, the characteristics of a reservoir. The fracture spacing and matrix porosity have strong effects on the rise in the flowing mass fraction of CO_2. However, only the fracture spacing has substantial effects on the rise in the flowing enthalpy. Therefore, if there is a rise in the flowing mass fraction without a similiar response in the flowing enthalpy then it is likely that there is a change in the matrix porosity. Likewise, if there is large rise in both the enthalpy and the flowing mass fraction of CO_2 after sustained production this points to an increase in the gas saturation. However, if the rise occurs upon initial production it can be the result of either an increase in the gas saturation or a large initial CO_2 partial pressure. Another possibility is if the enthalpy rises without a change in the flowing gas saturation then

this represents a change in the permeability of the fractures or matrix. These elimination processes can be very valuable in determining characteristics of the reservoir. They point to the great importance of using all the information that is available in order to characterize a reservoir system.

4.0 Fracture-Matrix Interaction and Fluid Recovery From Gas-Rich Reservoirs.

4.1 Introduction

It has been shown that significant amounts of CO_2 can greatly affect the behavior of a reservoir during exploitation (Grant, 1977; Zyvoloski and O'Sullivan, 1978; Zyvoloski and O'Sullivan, 1980; Atkinson et al, 1980; Pritchett et al, 1981; Barelli et al, 1982; O'Sullivan et al,1985; Pruess et al,1985).

The primary objective of this study is to examine how the presence of CO_2 alters the interaction of fracture and matrix in geothermal systems under exploitation. In addition, the current state of understanding of the kinetics of reactions involving CO_2 will be reviewed. Futhermore, techniques will be examined to improve recovery from geothermal systems by using the effects of CO_2 on flow patterns within the reservoir.

The simulations were conducted using the numerical simulator MULKOM (Pruess, 1982) and an equation of state for H_2O–CO_2 mixtures developed by O'Sullivan et al (1985). The effects of capillarity have been neglected.

4.2 Approach

A simple model which includes a single logarithmically discretized matrix element (100 m^3) with time independent boundary conditions (see Figure (4-1)) was used to investigate fracture-matrix interaction in H_2O–CO_2 systems. Models used in this study are based on the MINC (multiple interacting continua) method (Pruess and Narasimhan, 1980) which is similiar to the double-porosity model of Barenblatt et al (1960) except that the MINC method allows for fully transient heat and mass flow between fracture and matrix (Pruess and Narasimhan, 1980). The fracture element is assumed to be near a producing well so that the thermodynamic state of the fracture fluids remain constant with time. To determine the necessary conditions for the fracture, simulations were carried out using a radially infinite reservoir with a well at the center. The well was produced using a productivity index (see Equation (3-7)) with a

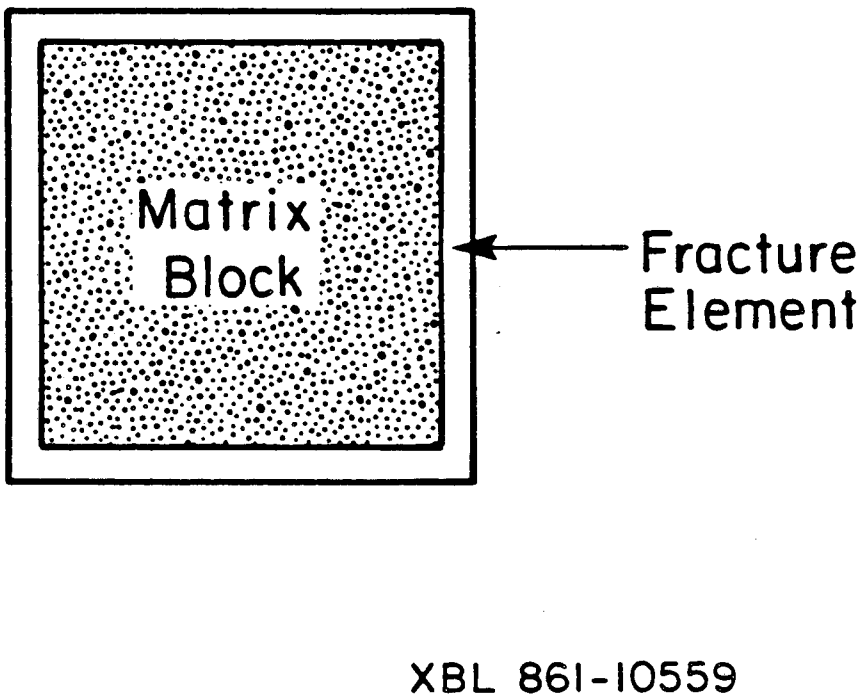

Figure (4-1). Simple model of a matrix block surrounded by a fracture.

constant bottomhole pressure of 40 bars. The rock and fluid properties were the same as those used in the sensitivity studies. The simulations were run until quasi-steady state conditions were achieved (2 years) in the fractures. These conditions were then used as boundary conditions in this study. This approximation neglects the early time effects of transients of pressure and gas saturation in the fracture, however, these effects are not very important in our analysis. The pressure in the fracture was assumed to be 40 or 70 bars, corresponding to a constant bottomhole pressure production and the matrix is initially at 90 bars. Note that for the following cases the total initial pressure is always kept the same so that when different initial partial pressures of CO_2 are used, the initial temperature will be different. Other reservoir parameters can be found in Table (4-1).

Table (4-1). Reservoir Parameters.

Parameter	Radial Value	Block Value
reservoir thickness	1000 m	-----
block size	-----	100 m^3
wellbore radius	0.1 m	-----
bottomhole pressure	40 bars	-----
productivity index	$1.25 \times 10^{-12} m^3$	-----
fracture spacing	100 m	100 m
fracture porosity	1%	-----
matrix porosity	5%	5%
fracture transmissivity	2.0 darcy meters	2.0 darcy meters
matrix permeability	0.01 md	0.01 md
thermal conductivity	2.0 W/m °C	2.0 W/m °C
rock heat capacity	1000 J/kg °C	1000 J/kg °C
rock density	2650 kg/m^3	2650 kg/m^3
fracture relative permeability	X-curves	X-curves
	S_{rl}=.0 S_{rg}=.0	S_{rl}=.0 S_{rg}=.0
matrix relative permeability	SGB curves	SGB curves
	S_{rl}=.05 S_{rg}=.40	S_{rl}=.05 S_{rg}=.40
initial pressure	90 bars	40 or 70 bars fractures
		90 bars matrix
initial gas saturation	20%	2%,10%,20%,30%,50%
initial partial pressure of CO_2	0,10 bars	0.01,1.0,5.0,10.0 bars
intial temperature	≈295 °C	≈295 °C
diffusion coefficient	$1.38 \times 10^{-5} m^2$	$1.38 \times 10^{-5} m^2$
tortuosity	0.25m/m	0.25m/m

4.3 Results

Figure (4-2) illustrates the effects of CO_2 partial pressure on the mass recovery normalized by the fully saturated mass in the matrix. This figure shows an inverse relationship between initial partial pressure of CO_2 and the amount of fluid that can be recovered from the matrix; the higher the initial partial pressure, the lower the recovery from the matrix. This relationship is due to the effects of CO_2 on the boiling curve of water. For a given total pressure, the higher the partial pressure of CO_2, the lower the water vapor pressure and, hence, the lower the saturation temperature. A large pressure drop can occur without a significant amount of boiling in the system thereby reducing the amount of fluids produced from the matrix. This phenomena can result in tens of bars initial pressure drop (Atkinson et al, 1980; O'Sullivan et al, 1985) which will dramatically reduce the amount of recoverable reserves in liquid dominated geothermal systems where there are large amounts of gas present.

Another important phenomena is suggested by the decline in recovery at late time which is due to the complex thermodynamics of H_2O–CO_2 mixtures. In order to achieve complete thermodynamic equilibrium between the fracture fluids and the fluids in the adjacent matrix, there must be equilibrium in the pressure, temperature, and partial pressures of the non-condensible gases which are present (Bodvarsson and Gaulke, 1986). Most geothermal systems are believed to be approximately in thermal and hydrological equilibrium prior to exploitation. During exploitation, the fluid pressure in the fracture near the well will stablize rapidly to the production level, creating a large pressure gradient between the fracture and the matrix. Figure (4-3) schematically shows the results of changes in pressure, temperature, gas saturation, and CO_2 partial pressure with time for a typical matrix block. Two cases are represented in Figure (4-3); the solid line represents the case in which chemical reactions involving CO_2 may be neglected and the dots represent results when chemical buffers are included. The chemical buffers in the latter case are assumed to provide CO_2 to the matrix by rock-fluid reactions at a rate necessary to prevent recharge of CO_2 from the fracture fluids. The dashed lines represents the stablized fracture conditions.

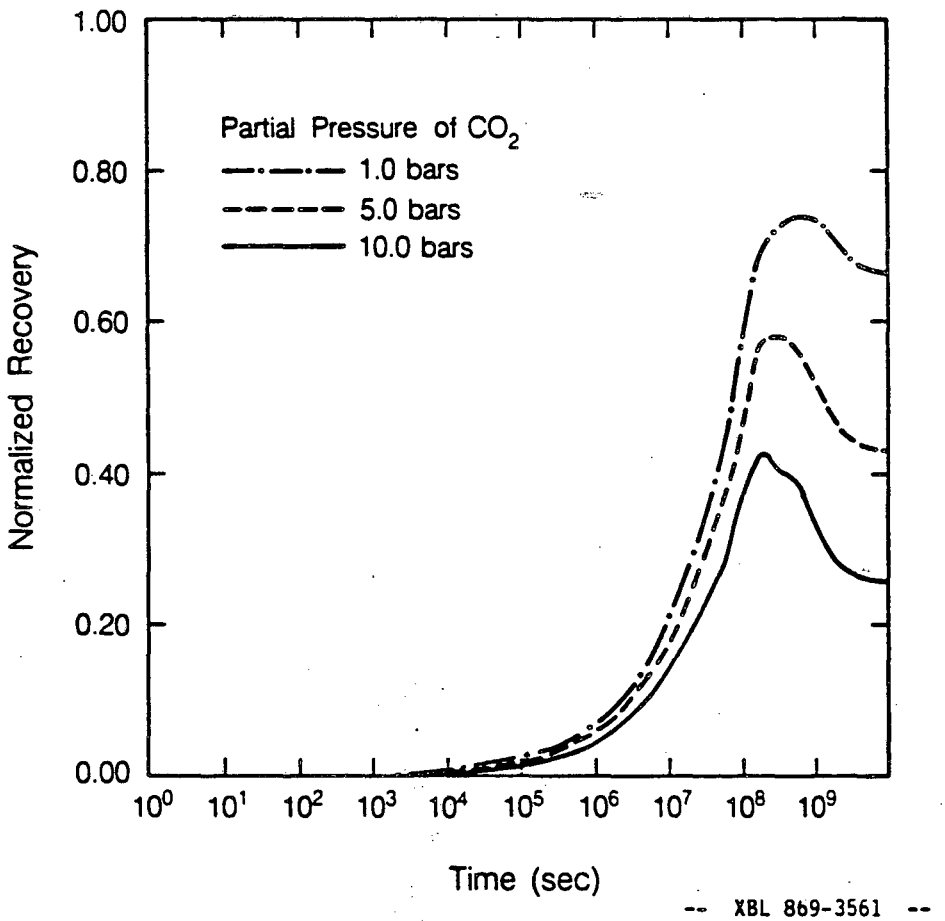

Figure (4-2). Effect of initial partial pressure of CO_2 on recovery transients normalized by the by the initial mass in the matrix.

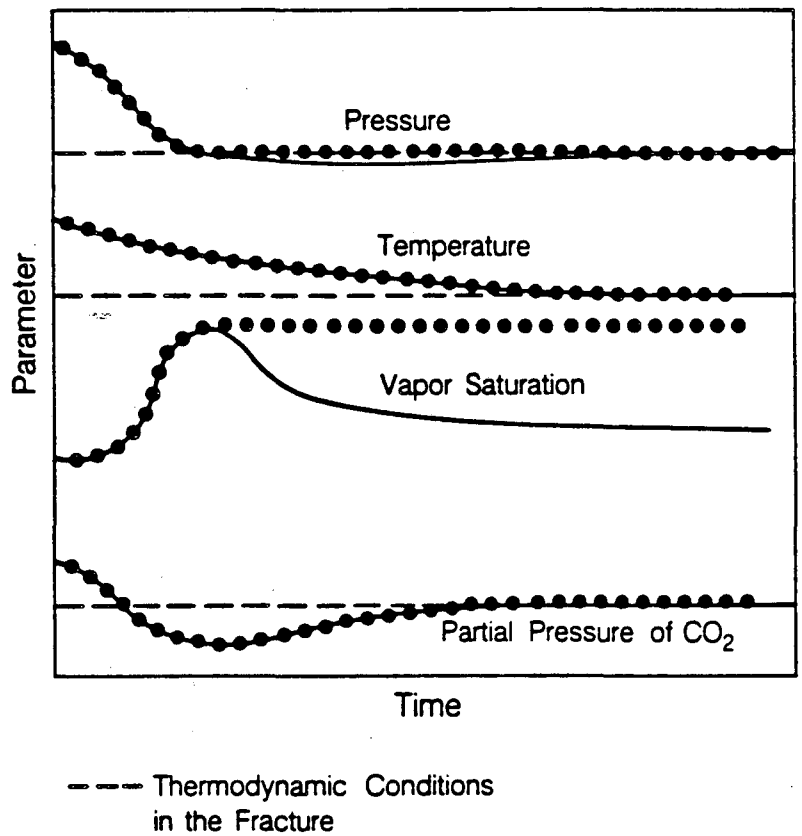

Figure (4-3). Schematic results of changes in pressure, gas saturation, temperature, and CO_2 partial pressure with time for cases with and without chemical buffers in the matrix.

Initially, the large pressure gradient drives fluid to the fracture from the matrix. This results in declining pressures, boiling and an increasing gas saturation in the matrix. CO_2 flows into the fracture with the gas phase and since little CO_2 is produced by boiling due to its low liquid solubility, the partial pressure of CO_2 in the matrix drops drastically. Eventually, the pressure in the matrix becomes the same as that in the fracture but a temperature gradient still exists due to the imbalance in the partial pressures of CO_2. The equilibration of CO_2 partial pressures between the fracture fluids and those in the matrix may be accomplished in two ways, either by chemical reactions in the matrix which produce CO_2 or by flow of gas-rich fluids from the fracture to the matrix (backflow). CO_2 can be produced by rock-fluid reactions in the matrix as the temperature equilibrates due to conduction. If this happens, the saturation will stabilize because the production of CO_2 by reactions will maintain a total pressure in the matrix equal to that of the fracture. However, if the rate of CO_2 production by rock-fluid reactions in the matrix is slow when compared to the rate of heat transfer to the fracture fluid, the temperature drop in the matrix will cause the total pressure in the matrix to dip below the total pressure in the fractures since two-phase conditions prevail in the matrix. The pressure imbalance is due to the excess CO_2 in the fractures which increases the total pressure there without affecting the stable temperature. This in turn will drive gas-rich fluid from the fracture to the matrix until the two continua achieve total equilibrium. Fluid recharge to the matrix from the fractures causes a declining gas saturation there as shown in Figure (4-3).

An analytical expression has been derived for estimating the amount of backflow that will occur in dependence of the gas saturation. The derivation which neglects binary diffusion and chemical buffers, is given in appendix C. The amount of backflow per unit pore volume assuming negligible changes in the fracture gas saturation is

$$\frac{M}{\phi V} = \frac{\rho_{CO_2} S_g + \rho_l X_{cl}(1.-S_g)}{\frac{k_{rl}}{\mu_l}\rho_l \nu_t X_{cl} + \frac{k_{gl}}{\mu_g}\rho_g \nu_t X_{cg}} \tag{4-1}$$

All symbols are defined in the nomenclature. This expression defines the total amount

of fluid per unit pore volume that must be supplied to the matrix in order to equilibrate the partial pressure of the matrix in with that of the fracture. Using the final saturation in the matrix, the numerator gives the total amount of CO_2 required to balance the partial pressure in the matrix with that in the fracture based upon the assumption that the matrix is gas depleted when backflow begins. This approximation appears reasonable, as complete degassing of the matrix block during pressure equilibration occurs in most cases. The final gas saturation of the matrix is what primarily determines how much CO_2 is necessary to equilibrate the fracture and matrix partial pressures given a liquid-vapor distribution determined by Henry's law. The denominator defines the fraction of each phase that is mobile, thereby, designating the relative amounts of each phase flowing into the matrix.

Figure (4-4) shows the normalized recovery from the matrix of our two continua model versus time in dependence of the flowing saturation in the fracture. The matrix has 20% initial saturation and other conditions are as listed before. A decrease in the recovery in the matrix at late time is indicative of backflow of fluid from the fracture to the matrix. The amount of backflow is inversely related to the flowing gas saturation in the fractures; a high gas saturation in the fracture indicates a high gas phase mobility. Therefore, only a small amount of fluid mass is required to equilibrate the CO_2 partial pressures, because of the high CO_2 concentration in the gas phase. However, if the gas saturation is low, liquid mobility is high and a large amount of fluid backflow to the matrix is required to equilibrate the CO_2 partial pressures.

Gas saturation and mass fraction of CO_2 scale linearly for a given partial pressure. This indicates that the amount of backflow that will occur can be estimated by measuring the mass fraction of CO_2 at the surface. Figure (4-5) shows that the amount of backflow per unit pore volume depends on the matrix gas saturation and the flowing mass fraction of CO_2. The data shown in Figure (4-5) were calculated using Corey curves for relative permeabilities. Chemical reactions producing CO_2 were neglected. Numerical simulations were completed in order to verify the results in this figure. The variations between analytical and numerical values at steady state were

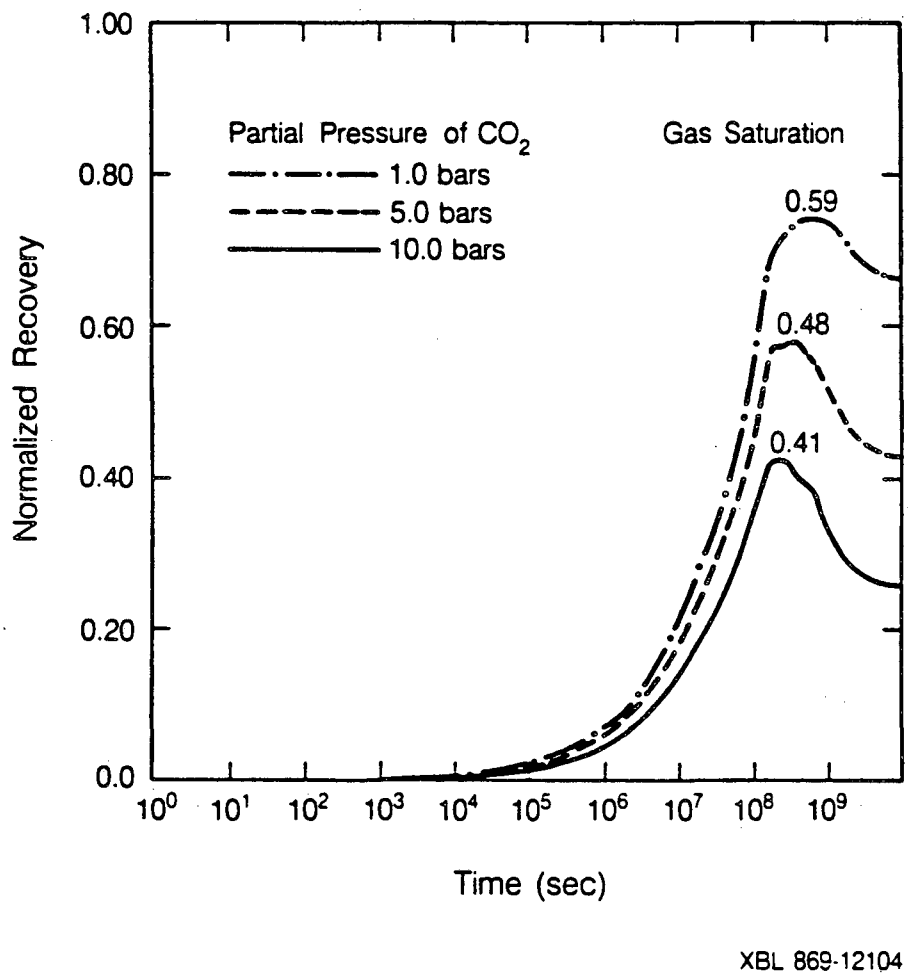

Figure (4-4). Effect of gas saturation in the fracture on backflow of fluid to the matrix.

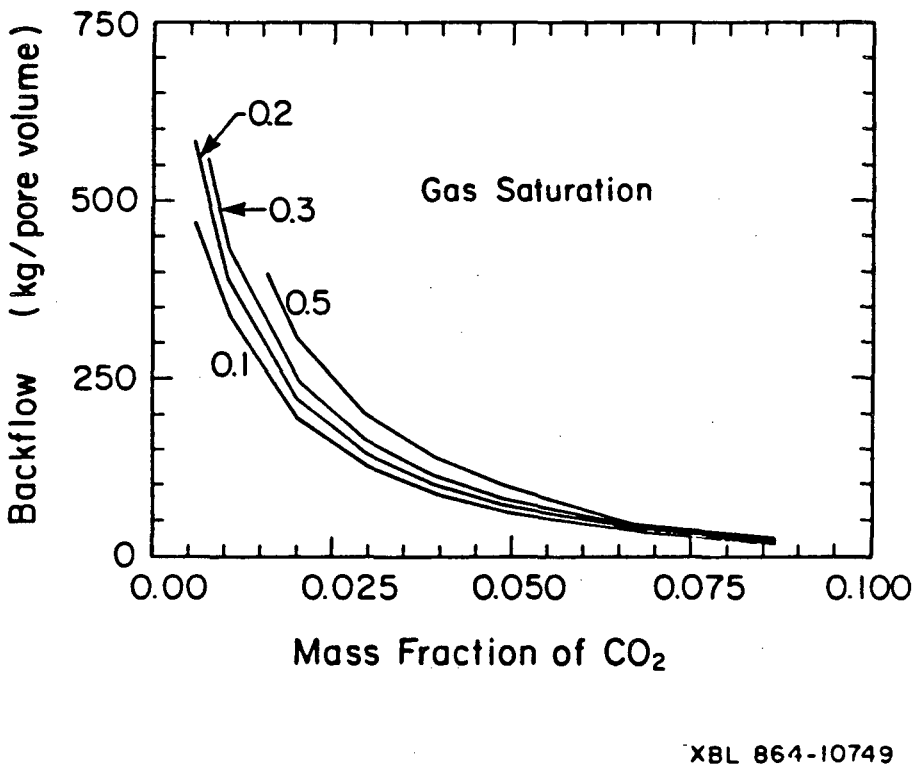

Figure (4-5). Effect of total flowing mass fraction of CO_2 on the amount of backflow per unit pore volume for various final matrix gas saturations.

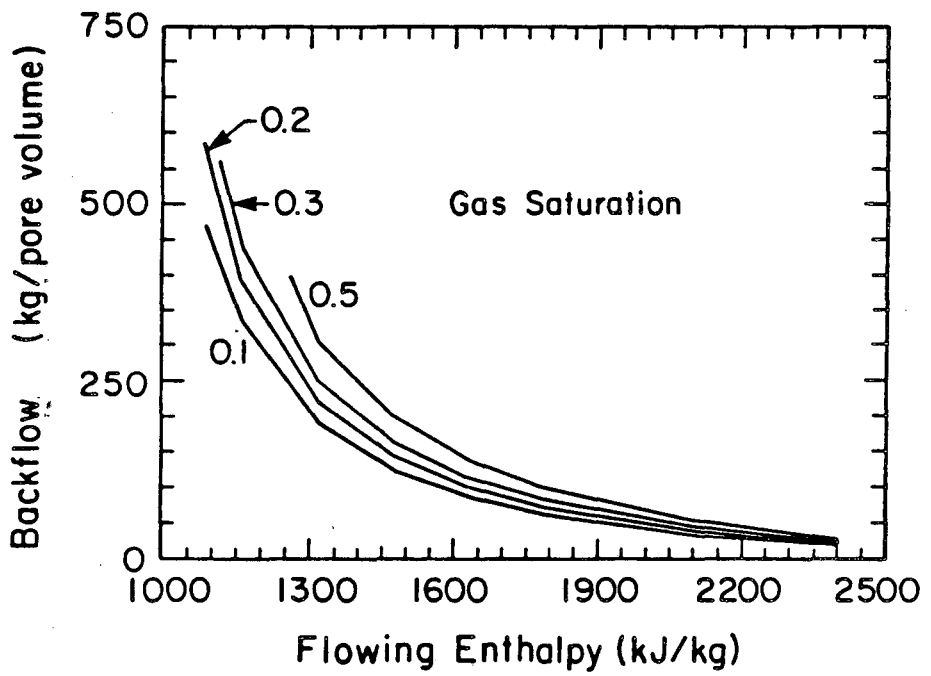

XBL 864-10748

Figure (4-6). Effect of flowing enthalpy on the amount of backflow per unit pore volume for various final matrix gas saturations.

small. The variations are the result of the assumptions that CO_2 was not present in the matrix prior to backflow of fluid from the fractures. If this slight error is removed the analytical and numerical results are identical.

Figure (4-5) also shows that since the amount of backflow is primarily dependant on the flowing mass fraction of CO_2, backflow is very substantial for low enthalpy wells, but is insignificant for wells which produce predominantly steam. This is confirmed in Figure (4-6) which shows that the amount of backflow per unit pore volume is dependent on the flowing enthalpy. There is a sharp increase in the amount of backflow with decreasing flowing enthalpy. It should also be noted that there is little change in the amount of backflow for various initial gas saturations, therefore, the in situ conditions are not very important in predicting the amount of backflow that occurs. It is shown clearly in Figures (4-5) and (4-6) that backflow may be very important for low enthalpy wells for which the amount of backflow can be hundreds of kilograms per cubic meter.

Figure (4-7) shows the normalized recovery versus the initial pressure gradient between the fracture and the matrix for various initial partial pressures of CO_2. Two curves are included for each partial pressure; the upper curve indicates recovery prior to backflow and the lower curve includes the effects of backflow. This figure confirms that the initial partial pressure of CO_2 has large effects on recovery. This figure also shows that the amount of fluid which is required to equilibrate partial pressures between the fracture and the matrix is practically independent of the initial pressure gradient. Since the partial pressure of CO_2 rapidly decreases as CO_2 flows out of the matrix with the gas phase and boiling produces little CO_2, the matrix becomes depleted of CO_2 even for small initial pressure gradients.

Figure (4-8) shows the normalized recovery versus the initial gas saturation for various initial partial pressures. This figure confirms that the recovery is strongly influenced by the initial partial pressure as previously indicated. The dashed line in the figure indicates the normalized mass of fluid per unit pore volume within the system initially. This would be the maximum amount of fluid that can be recovered.

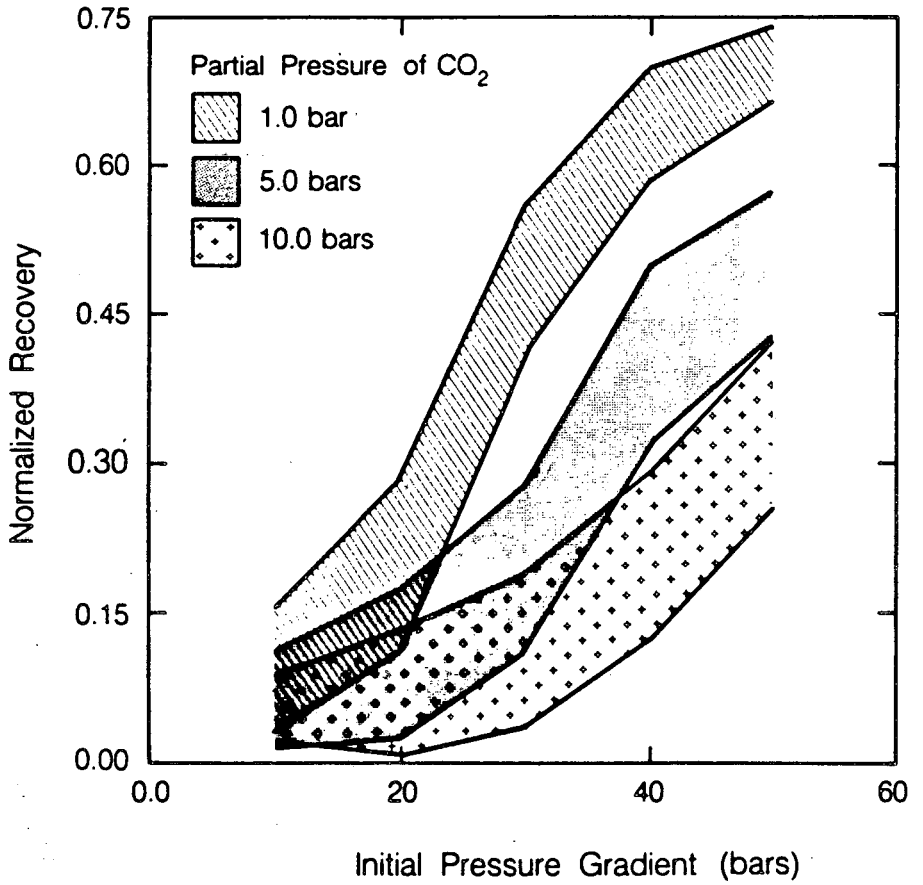

XBL 869-12101

Figure (4-7). Effect of initial pressure gradient on intermittent recovery and recovery after backflow. Recovery is normalized by the mass necessary to fully saturate the matrix for various initial partial pressures of CO_2.

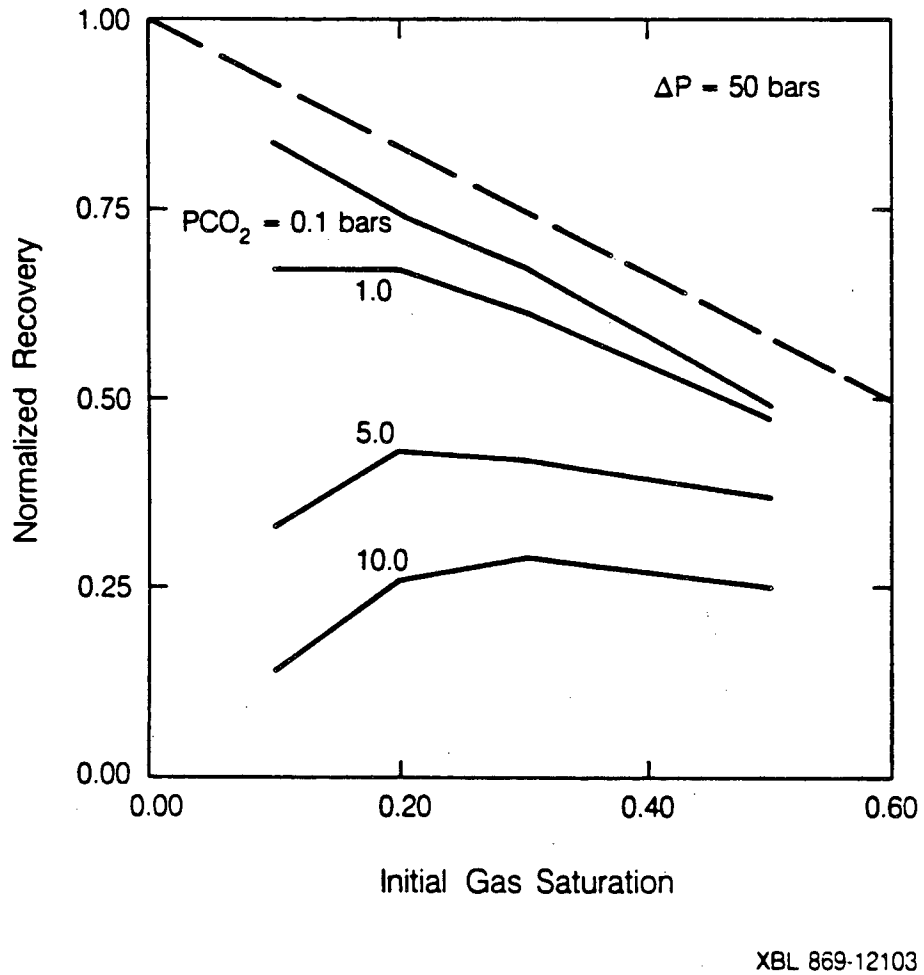

Figure (4-8). Effect of initial gas saturation on recovery normalized by the mass necessary to fully saturate the matrix for various initial partial pressures of CO_2.

Deviation of the curves from the slope of the ideal curve at low initial gas saturations is indicative of backflow to the matrix. At low gas saturation the liquid mobility is high, therefore, the fluids backflowing into the matrix will have a low gas content and, hence, a large amount of backflow will occur before complete thermodynamic equilibrium has been achieved. In addition, since the presence of CO_2 reduces the boiling temperature for water in relation to the partial pressure of CO_2, the amount of boiling will be reduced with increasing partial pressures. Less boiling results in lower flowing gas saturations at higher partial pressures of CO_2 so that backflow will be increased with increasing partial pressures as well as with decreasing gas saturation.

It is of interest to determine which factors control the rate of backflow and over what time period it occurs. This is very important if chemical buffers involving CO_2 are present so that there are ways to compare the kinetic rates of reactions which supply CO_2 with the rate of backflow. The primary factors controlling the rate of backflow are the geochemical, thermal and hydrological parameters of the matrix blocks. As backflow occurs during the time when the temperatures in the fractures and matrix are equilibrating, the thermal parameters, especially the thermal conductivity, are important. The hydrological parameters of the matrix are also important, especially the absolute and relative permeabilities. However, the fracture spacing is probably the single most significant parameter controlling the rate of backflow. The fracture spacing (D) strongly affects both the conductive heat transfer and the rate of fluid flow since the surface area (per unit surface area) between the matrix and the fractures is proportional to D^2. Thus, one would expect that for reservoirs with relatively small average fracture spacing, the time period necessary for backflow to occur would be small.

4.4 Radial Cases

In order to test the backflow theory on a more realistic problem, a numerical model of a well in a fractured reservoir of uniform thickness (1000m) was studied. All reservoir parameters are listed on Table (4-1). The grid was developed using the

MINC method (Pruess and Witherspoon, 1982) for a fractured porous reservoir. A productivity index was used to provide flowrates (30-40kg/s) typical of high temperature geothermal wells. Linear curves without cutoffs were used for the fracture relative permeabilities and Corey curves were assumed for the porous rock matrix. Gravity effects were neglected in these simulations so that the fractures and matrix started with a uniform saturation. In the simulations, binary diffusion was included as outlined by Pruess et al (1985). The diffusivity was calculated using a Bosanquet type formulation (Pollard and Present, 1948) and adjusted for reservoir temperatures and pressures with a method introduced by Perry, (1963). This method assumes that diffusivity is directly related to temperature, however, recent work suggests that temperature effects on gas diffusivity are limited by pore radius within the medium (Tokunaga, 1985) so the actual diffusivity may be lower than that calculated at reservoir temperatures.

Figures (4-9) and (4-10) show the gas saturation transients for CO_2 partial pressures of 0 and 10 bars, respectively. The various curves represent conditions within fracture and matrix elements at different radial distances from the producing well. It is important to note that the matrix curves represent conditions nearest to the fractures; the matrix is discretized into five different elements after the method of Pruess and Narasimhan, (1983). In both cases the gas saturation in the fractures rises monotonically until it reaches quasi-steady state. The stablization time is dependant on many of the reservoir parameters, however, of primary importance are the fracture spacing or surface area between matrix and fracture and the matrix permeability (Lippmann et al, 1985). Basically, the gas saturation in the fractures stabilizes when quasi-steady state fluid and heat flow has been established between the fracture and matrix. The gas saturation in the fracture elements rises significantly higher when noncondensible gas is not present as compared to the case with a 10 bar partial pressure of CO_2.

There is a substantial variation in the gas saturation transients of matrix elements for the two cases. Without CO_2, the gas saturation in the matrix rises drastically due to both boiling and the flow of high enthalpy fluids to the fractures. In

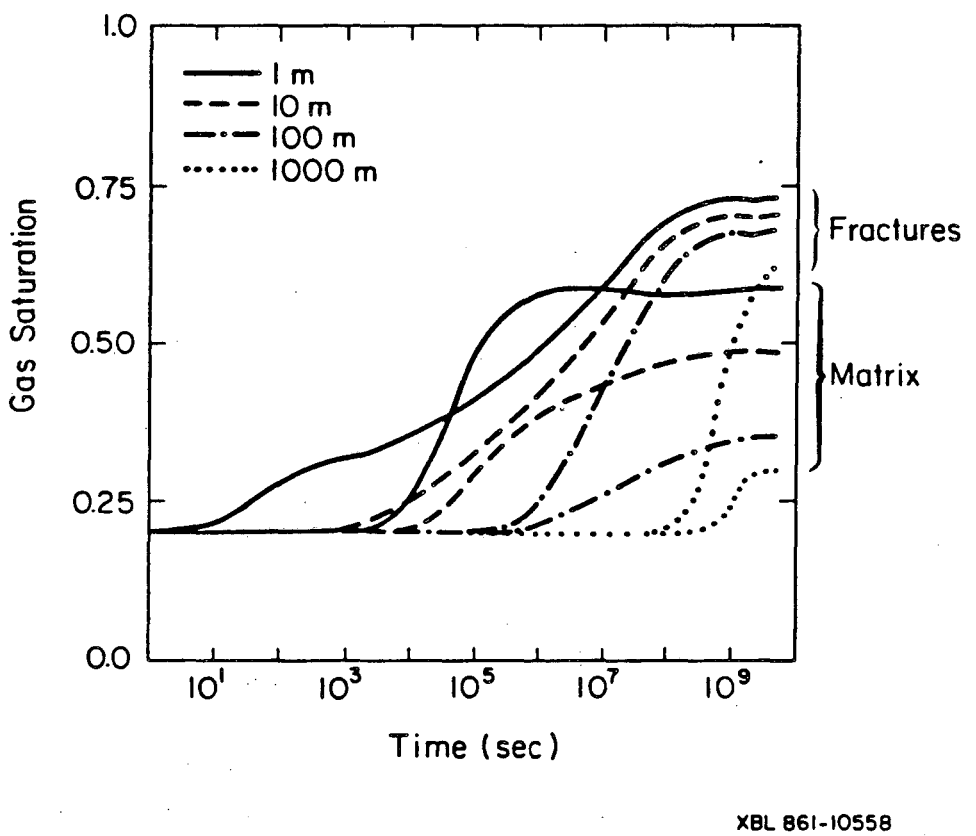

Figure (4-9). Changes in gas saturation with time for various fracture and matrix elements without CO_2 present.

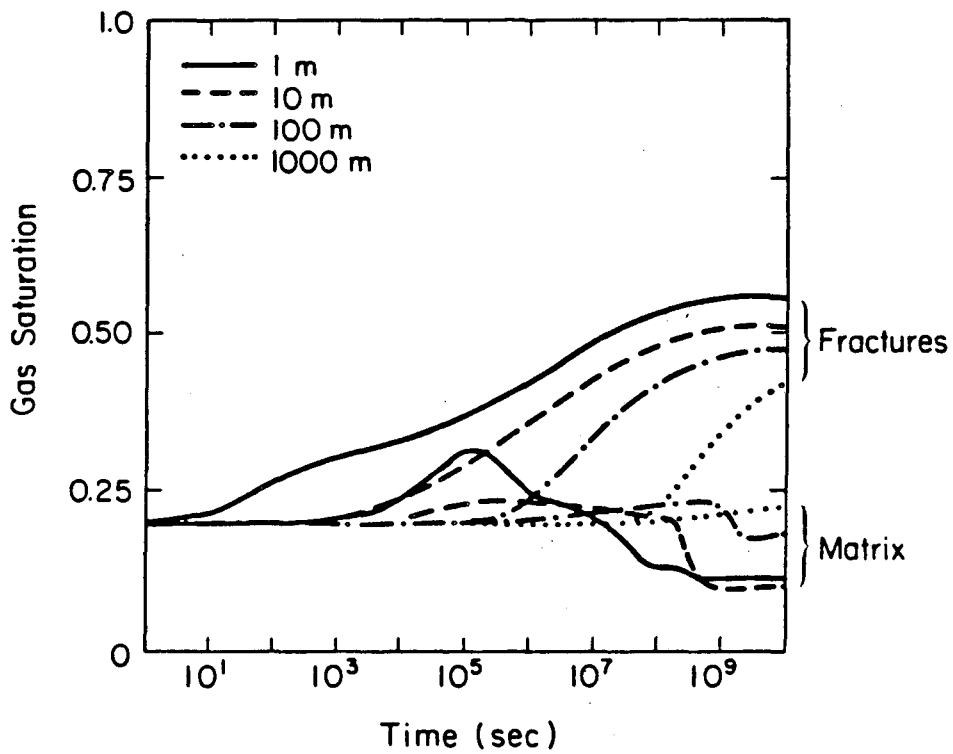

XBL 861-10557

Figure (4-10). Changes in gas saturation with time for various fracture and matrix elements with 10 bars of CO_2 present.

contrast, with CO_2 present there is less boiling and, hence, a smaller rise in gas saturation because degassing causes a substantial pressure drop without boiling. Later, the gas saturation in the matrix declines, which suggests a reversal of flow patterns; gas-rich fluid flows from the fractures to the matrix. In Figure (4-10), the outer most matrix elements have a lower gas saturation after a simulated 30 year production period than they intially contained. As Figures (4-9) and (4-10) only show the gas saturation transients in individual matrix elements, it is of interest to determine the net gas saturation changes intergrated over the entire matrix blocks. Figure (4-11) shows the variations in the average matrix gas saturation with radial distance for the case with 10 bars of CO_2 present. Gas saturation profiles are shown for different times ranging from 1 to 30 years. The figure shows that substantial backflow occurs near the well after 5 years, the time necessary for pressure equilibrium of the large matrix blocks (100 m^3) with the fractures. Figures (4-9) through (4-11) clearly show that the presence of non-condensible gases in a liquid dominated reservoir can substantially reduce the matrix depletion. With CO_2 present however, the total mass flowrate from an infinite reservoir is higher than without CO_2 present (see Figure (4-12)). This results from the effect of CO_2 on the boiling temperature in a reservoir. Since the pressure drops substantially without boiling when CO_2 is present, the flowing saturation is lower and thus the total fluid mobility is higher. Without CO_2, there is more vigorous boiling, higher gas saturation and, hence, a lower overall fluid mobility. Figure (4-13) shows the flowing enthalpy transients feeding the well for the cases with 10 bars and without CO_2. When CO_2 is not present, the enthalpy is much higher. This is due to more vigorous boiling and also the lower enthalpy of CO_2. Futhermore, the rise in enthalpy at late times is greater without CO_2 because of the higher enthalpy fluids recharging from the matrix as a result of more substantial boiling in the matrix.

Figure (4-14) shows the gas saturation transients for the same infinite reservoir with gaseous diffusion included. The diffusion coefficient used was $1.38 \times 10^{-5} m^2/s$ along with a tortuosity of 0.25. Comparison of Figures (4-10) and (4-14) shows that the effects of binary diffusion for the case studied are rather small. With gaseous diffusion included the gas saturation in the fracture elements rises approximately 2-3% higher

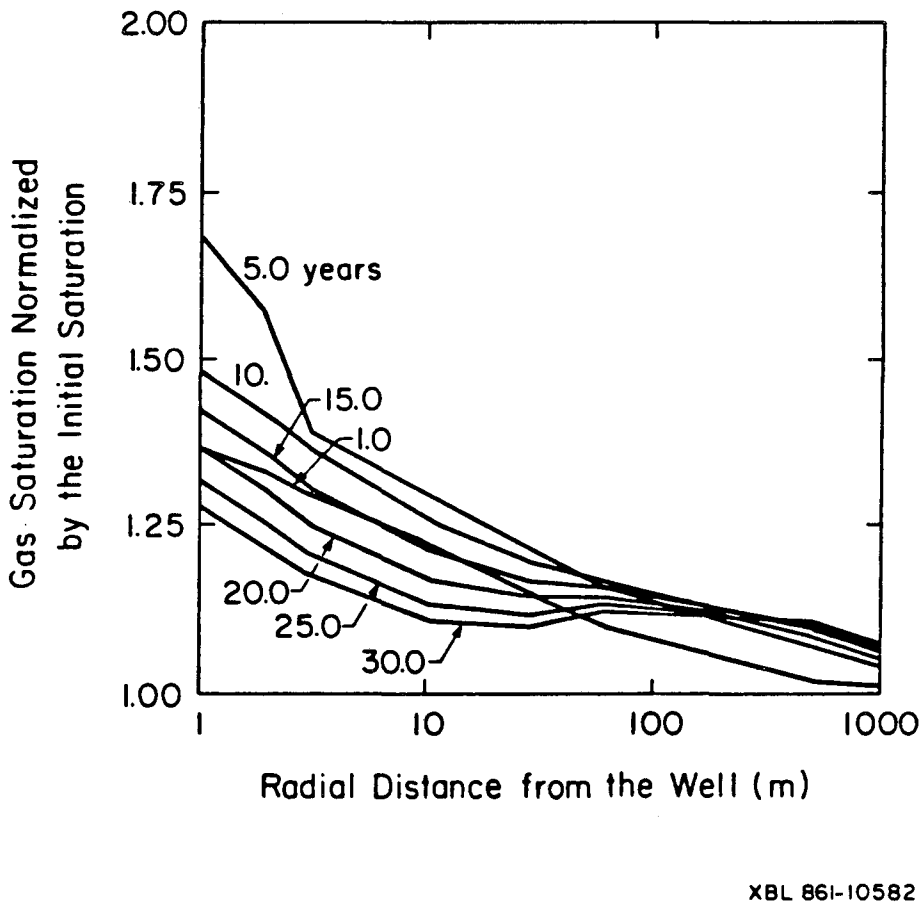

Figure (4-11). Variations in the average matrix gas saturation with radial distance from the well.

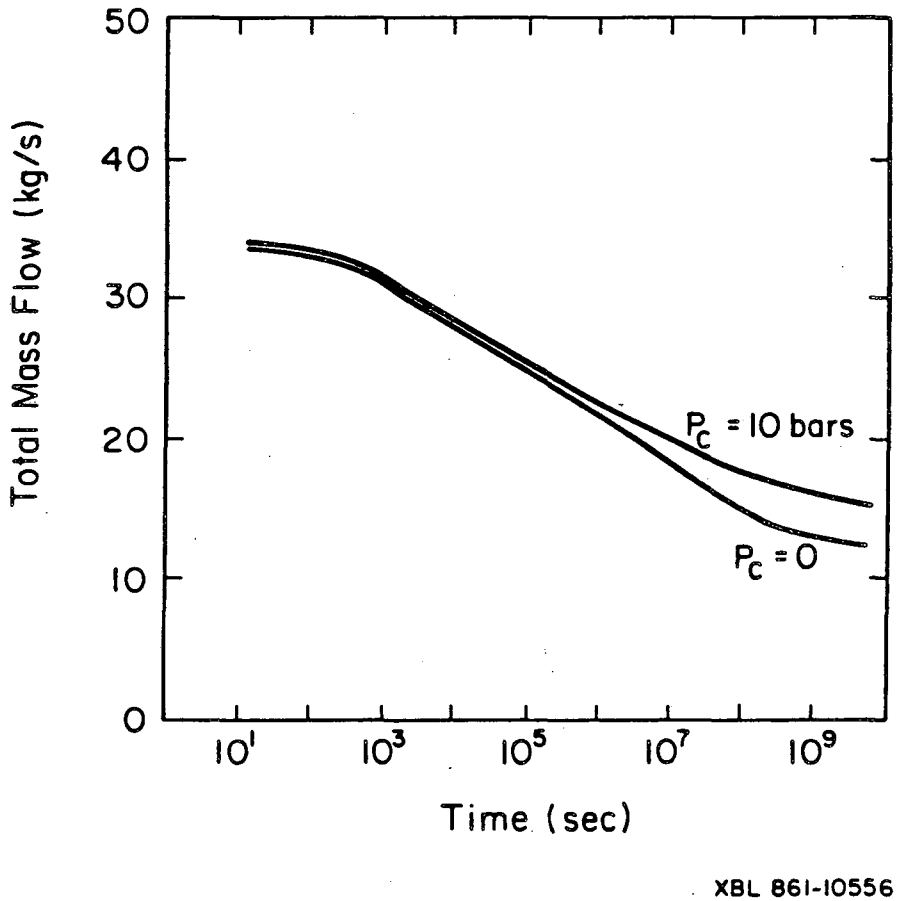

Figure (4-12). Changes in mass flowrate with time for the cases of no CO_2 and 10 bars initial CO_2 partial pressure.

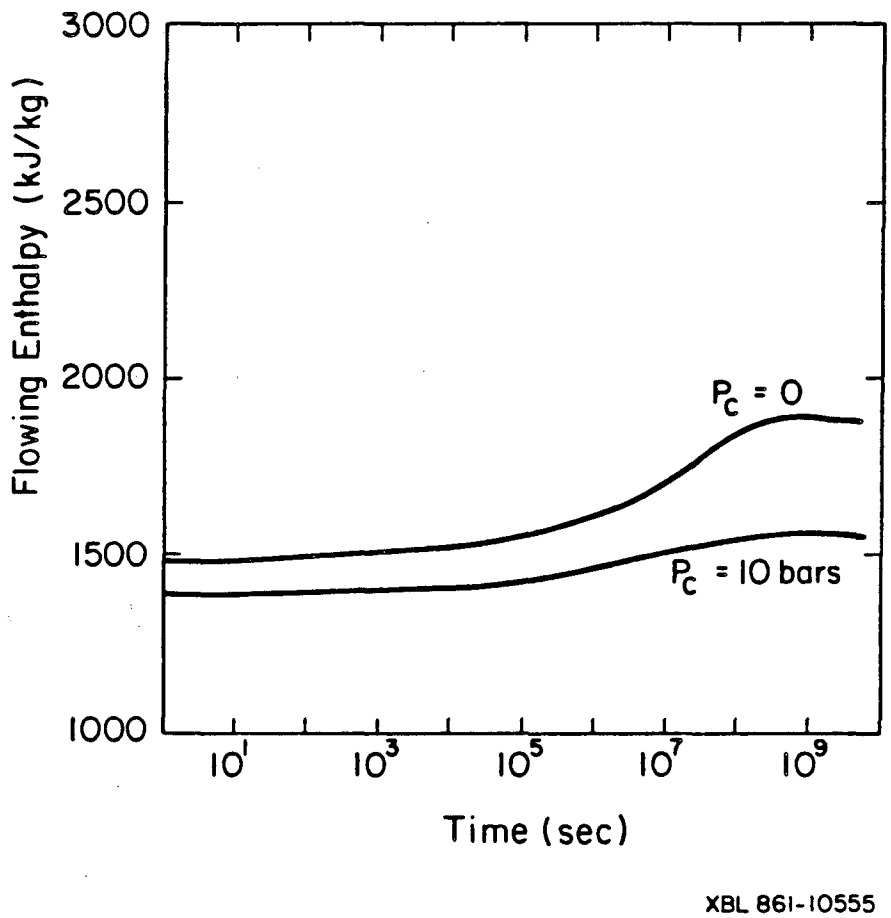

Figure (4-13). Changes in flowing enthalpy with time for the cases of 0 and 10 bars initial CO_2 partial pressure.

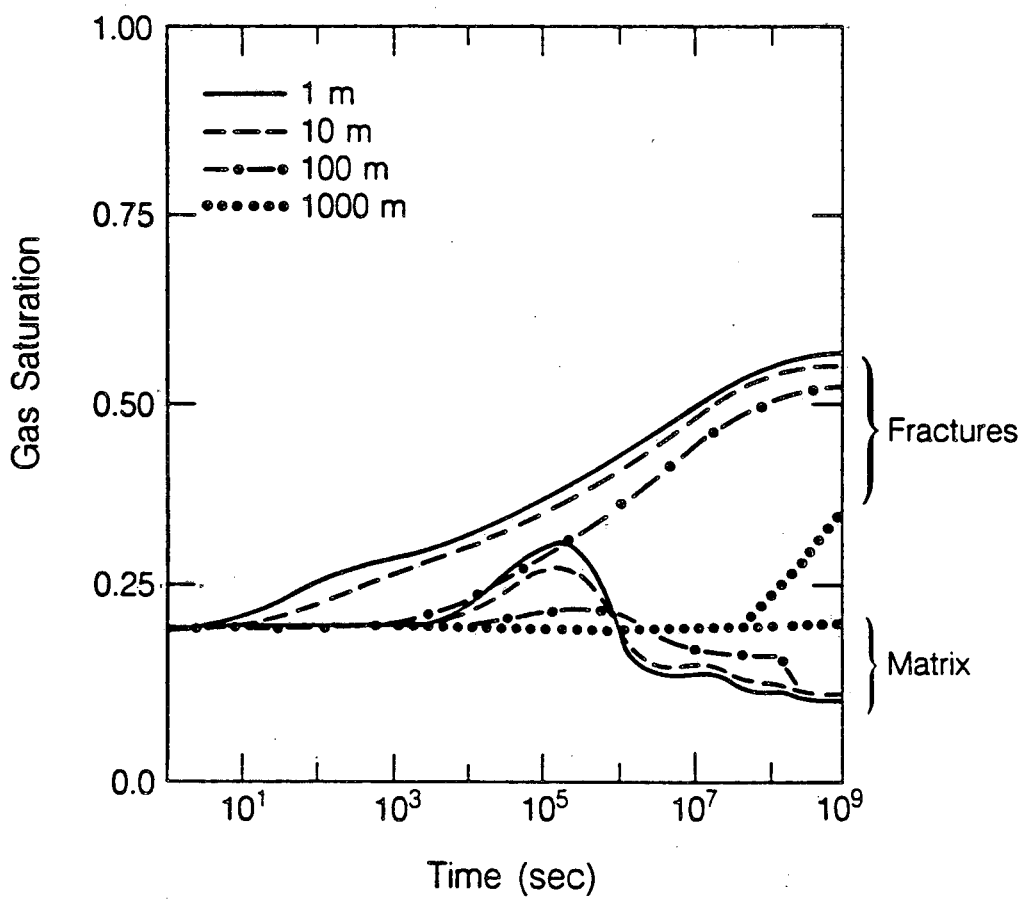

XBL 866-10867

Figure (4-14). Changes in gas saturation with time for various fracture and matrix elements with 10 bars initial partial pressure of CO_2 present and gaseous diffusion included.

after a simulation period of 30 years. Initially the gas saturation rise in the matrix elements is higher, however, the final conditions in the matrix elements are almost identical for the two cases indicating that gaseous diffusion is not an important factor in the problem considered here.

4.5 Chemical Effects and/or Backflow

As mentioned earlier, it is possible that the equilibrium of CO_2 partial pressures in the fractures and the matrix is attained through chemical reactions involving CO_2 rather than by backflow from the fractures into the matrix. Some considerations of chemical buffering of CO_2 and experience from producing geothermal fields are given below. CO_2 is actively introduced to geothermal systems in two general ways; either by volcanism, as in Krafla, Iceland, and/or by rock-fluid reactions involving carbonate rocks such as are found in the Larderello field of Italy. Certainly over geologic time, CO_2 will equilibrate with the local suite of rocks, the equilibrium conditions depending upon the rock composition and the prevailing temperature. This includes dissolution of CO_2 from the fluid as the fluid reacts with minerals such as andesine to form calcite on fracture and pore surfaces (Ellis, 1969). If the partial pressure of CO_2 is known or can be estimated, simple calculations can be carried out using the free energy of formation to determine the equilibrium mineral assembleges in an unexploited reservoir (see Appendix B). The presence of calcite, along with other carbonate minerals, can be expected to buffer changes in the partial pressure of CO_2 within a reservoir by dissolution to produce CO_2 gas. The effectiveness of this buffering is dependent on the amount and distribution of the buffering agent and the kinetics of the rock-fluid reactions. The stability and distribution of the buffering agents are influenced by factors that include temperature, permeability, porosity, rock type, fluid composition, total pressure, and the rate of fluid flow (Brown and Ellis, 1970). Geothermal reservoirs are complex systems where all of these parameters may vary both temporally and spatially. In a producing reservoir where boiling and acceleration in fluid movement are likely to combine with decreasing temperatures, reaction rates can be substantially

reduced, progressively impeding attainment of rock-fluid equilibrium (Giggenbach, 1981). Under these conditions it is difficult to apply static equilibrium tables and obtain any deep insight as to the chemical state within a producing reservoir.

Given the current limitations of theoretical work on the kinetics of CO_2 systems, valuable insight may be obtained from experience with producing reservoirs. Wells in Larderello have produced steam with a similiar concentration of CO_2 for decades (Pruess et al, 1985). Pruess et al (1985) preformed numerical simulations of CO_2 transients and concluded that most of the CO_2 was not contained in the fluids originally in place but was introduced into the system by other sources, probably by chemical buffers. This suggests rather rapid kinetics of CO_2 chemical buffers, at least for the carbonate rocks at Larderello. However, significant transient changes in produced CO_2 content were noted during an injection experiment at Larderello indicating incomplete buffering of CO_2 (Giovannoni et al, 1981).

Another example is Krafla geothermal field in Iceland where there were significant changes in the CO_2 concentration of the produced fluids as shown in Figure (4-15). These changes indicate incomplete buffering of CO_2 (Steingrimsson et al, 1984). Between the years of 1976 and 1978 volcanic activity produced large amounts of CO_2. After the volcanism ceased there was a rapid decline in CO_2 within the reservoir. This was due to either not enough mineral buffering within the system and/or the kinetics were too slow to effectively control CO_2 transients in the producing reservoir. These field examples suggest that the effectiveness of chemical buffering of CO_2 depends on the rock types involved. The backflow phenomena proposed here and in an earlier paper (Bödvarsson and Gaulke, 1985) may only be important for certain reservoirs.

4.6 Injection Effects

It is of interest to investigate how injection of fluids with low gas content will affect the fluid recovery from the matrix. This scenario is modeled in rather a coarse manner by spatial variations in the initial gas concentration. A single well is modeled with gas-rich fluids close to the well. Outside a radial distance of 1 kilometer from the

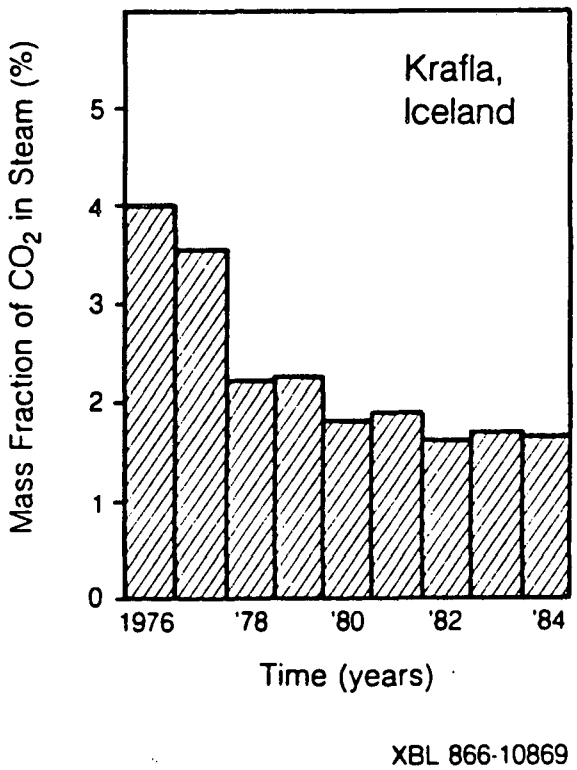

Figure (4-15). Changes in the flowing mass fraction of CO_2 in the steam phase with time for Krafla geothermal field, Iceland (Steingrimsson et al, 1984).

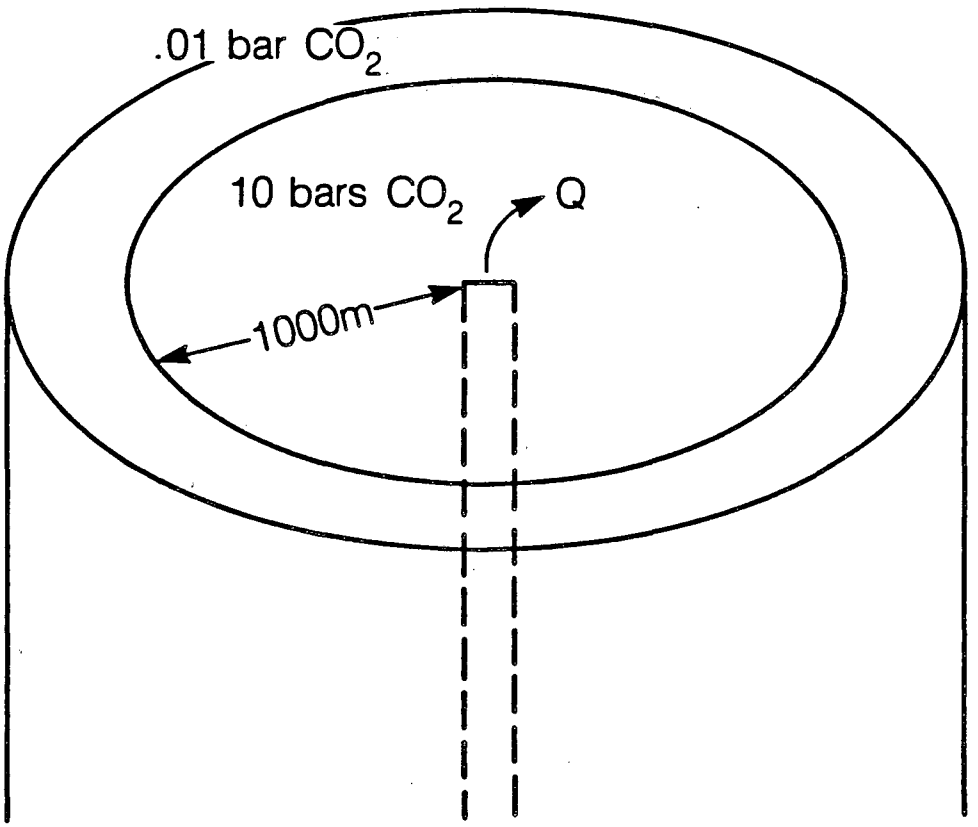

XBL 8612-12792

Figure (4-16). Sketch of CO_2 distribution used to approximate conditions during injection of pure water into a reservoir with 10 bars initial partial pressure of CO_2.

well there are fluids with a low gas concentration (see Figure (4-16)). Other parameters are the same as those discussed in the previous sections. This model neglects the temperature difference due to the varying gas content, however, this approximation is not very important for the aspect of the problem we are interested in.

Figure (4-17) shows the transients in total fluid mass flowrate and CO_2 content at the well. In less than a year there is a pronounced drop in the CO_2 content of the produced fluids accompanied with stablization and then a rise in the total mass production rate. This is caused by the low gas content of the outer regions fluids. The low flowing CO_2 concentration increases total fluid production in two ways, by decreasing the gas saturation in the fractures and by increasing recovery from the matrix. With a lower gas saturation, the liquid phase mobility will be increased. This in turn allows more fluid mass to flow to the well. This is shown clearly when Figures (4-12) and (4-17) are compared. The fluid recovery is much greater as the CO_2 content declines in the reservoir.

Recovery from the matrix will be enhanced by the creation of a CO_2 concentration gradient between the fractures and the matrix. This gradient prevents backflow of fluid to the depleted matrix near the well. Consider again Figure (4-11) where the gas saturation near the well begins dropping significantly 5 to 10 years after production initiates. This is the indentical case as before except for the lower gas content in the outer region. The matrix is much less depleted after 30 years than it was at 5 years for a distance from the well of several hundred meters. With the lower gas content of the outer region, the resaturation of the matrix indicated in Figure (4-11) will not occur or will be drastically reduced depending on the CO_2 depletion of the matrix. The low flowing gas content (partial pressure) in the fractures is nearly equal to that in the CO_2 depleted matrix and, hence, the temperature variations between fracture and matrix fluids associated with partial pressure imbalances is much less. Therefore, the pressure drop related to cooling of the CO_2 depleted matrix is not significant. This is confirmed by the rise in the flowing mass fraction of CO_2 after 7 years of production while the total flowrate is declining. The CO_2-rich fluids flow out of the matrix while

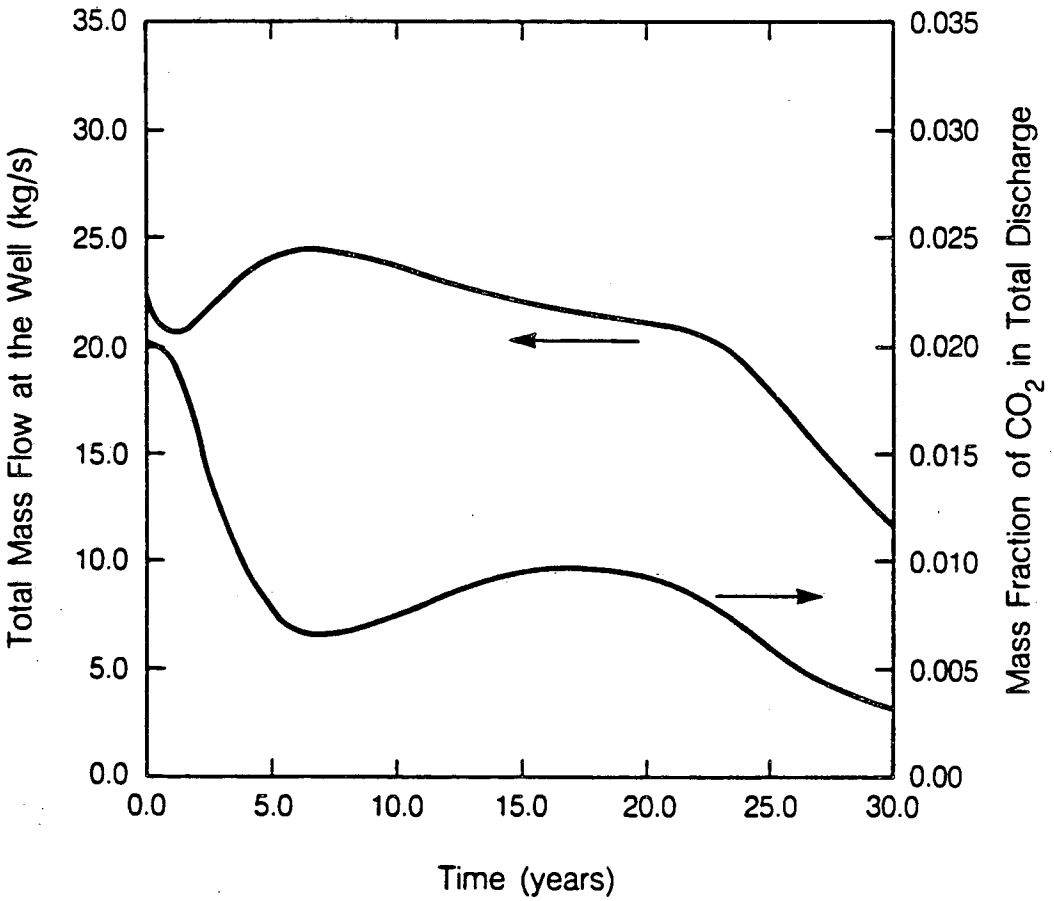

XBL 869-12102

Figure (4-17). Changes in mass flowrate and total mass fraction of CO_2 with time.

no backflow occurs near the well. The amount of additional fluid recovery (ie. matrix depletion) may be estimated by using Figure (4-5) since the decrease in the flowing mass fraction of CO_2 is known. The flowing mass fraction of CO_2 declines from 2 percent to 0.8 percent in the first 5 years of production. This indicates an improvement in recovery per unit pore volume of between 150 and 500 kilograms depending on the final matrix saturation. Thus, injection of gas-free water will drastically reduce potential adverse effects of CO_2 on matrix depletion and energy recovery.

4.7 Summary

Numerical simulation techniques are used to investigate the effects of CO_2 on matrix depletion and fluid recovery from fractured geothermal reservoirs. It is shown that the degassing of liquid dominated geothermal reservoirs due to the effects of CO_2 on the boiling curve of water can substantially reduce fluid recovery from liquid dominated systems. The drop in total pressure of the reservoir, due to degassing of CO_2, results in lower heat and mass recovery.

The backflow of fluid to the matrix, due to the effects of CO_2 on the pressure-temperature relationship of water, is identified. An analytical expression is derived to quantify the total amount of backflow that might occur depending on the final saturation in the matrix while neglecting chemical reactions involving CO_2. It is noted that complete thermodynamic equilibrium, including the partial pressures of CO_2, must be considered to understand fracture-matrix interaction in a producing reservoir. The equilibration of CO_2 partial pressures between the fracture and matrix can occur by "backflow" of gas-rich fluids or chemically by rock-fluid reactions. Much more work is necessary to understand the kinetics of rock-fluid and water-gas reactions within complicated reservoir systems to determine the relative importance of each phenomena. The petrology of the reservoir can have large effects on the buffering of CO_2 partial pressures causing the buffer to be weaker or stronger. A static equilibrium balance equation is inadequate to accurately predict the behavior in a transient reservoir.

In addition, backflow can be very substantial for low enthalpy two-phase systems. It can amount to hundreds of kilograms per unit pore volume. It will not be very significant in vapor dominated systems. Finally, injection of low gas content fluids can increase recovery from a fractured geothermal reservoir. This is achieved by increasing liquid mobilities within the fractures and reduction in the backflow, hence, increasing matrix recovery.

5.0 Field Example - Well BR21, Ohaaki, New Zealand

5.1 Introduction

Most geothermal fields are liquid-dominated with pressure increasing hydrostatically with depth. Some liquid-dominated reservoirs have large two-phase zones which will significantly alter their production behavior. Many investigators have examined two-phase reservoirs at Momotombo (Dykstra and Adams, 1978), Baca (Grant and Garg, 1981; Pritchett et al, 1981), Krafla (Stefansson, 1980; Bodvarsson et al, 1983) Nesjavellir and Namafjall (Steffansson and Steingrimsson, 1980), and Broadlands (Mahon and Finlayson, 1972; Ellis and Mahon, 1977; Grant, 1980; Grant, 1984). These reservoir systems are complex, and the thermodynamic and hydrologic conditions are often not well known. The study of well behavior, including the analysis of changes in thermal, hydrologic, and chemical characteristics, must be incorporated to help understand two-phase systems. In Chapter 3, we examined how enthalpy and CO_2 transients change with rock and fluid parameters for gassy reservoirs. We have shown that insight into the reservoir behavior can be obtained if detailed transient measurements are made for gassy two-phase geothermal systems.

Data are available on well BR21 (Grant and Glover, 1984) to verify the applicability of techniques suggested in Chapter 3. The well was opened to a constant throttle while the transient changes in downhole pressure, discharge enthalpy, and flowing mass fraction of CO_2 were monitored for a two week period. The flowrate during this period was about 25 kg/s. The results are typical of two-phase systems showing a high degree of variability in enthalpy and flowing mass fraction of CO_2 (see Figure (5-1)). In addition, there is an extended transient period before the enthalpy and mass fraction of CO_2 stabilize suggesting a fractured system as opposed to a porous medium (Grant and Glover, 1984).

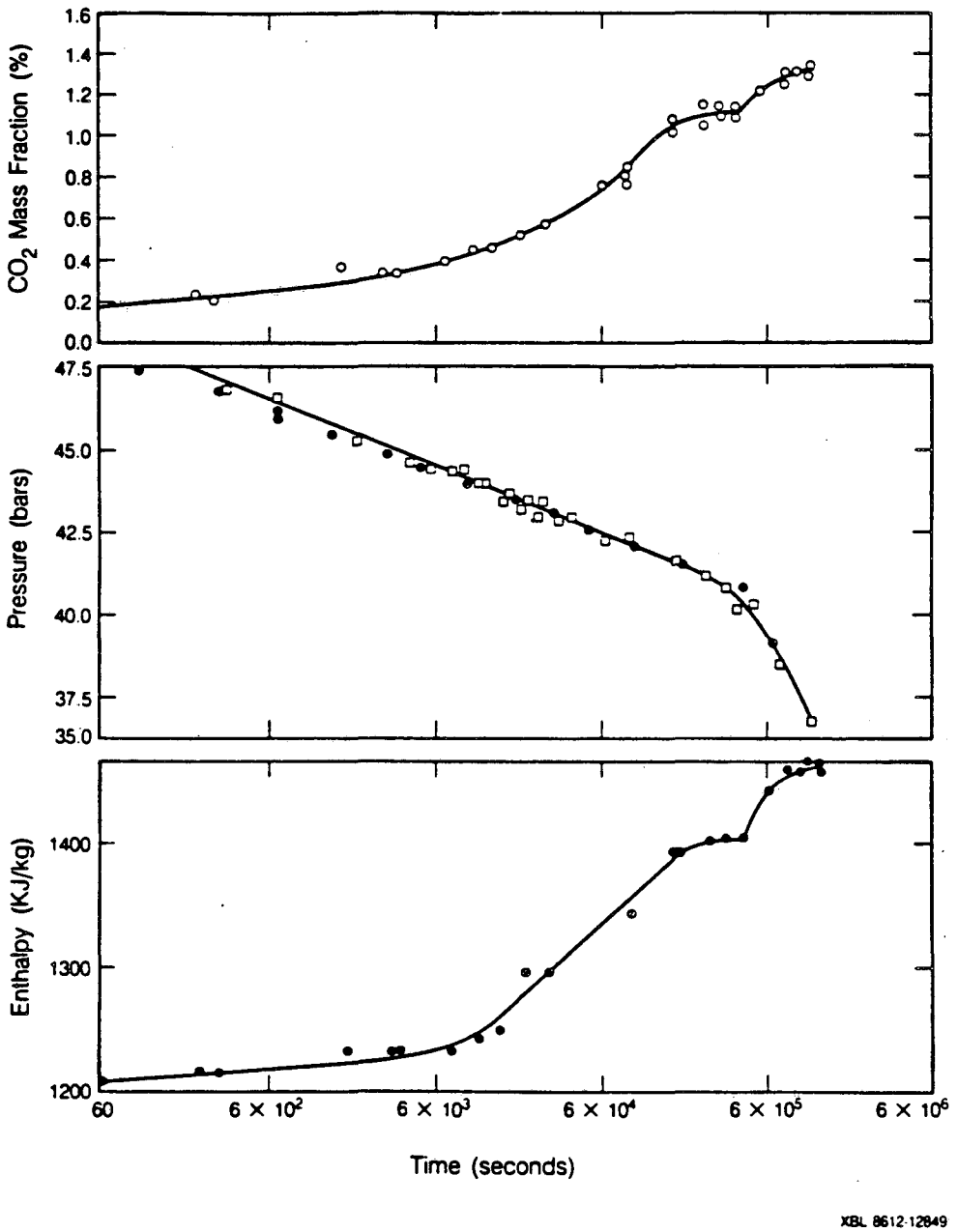

Figure (5-1). Changes in the downhole pressure, flowing mass fraction of CO_2, and flowing enthalpy for well BR21, Broadlands, New Zealand (Grant and Glover, 1984).

In this chapter, results from numerical simulations are shown to aid in the interpretation of the data from well BR21. A match of the pressure, enthalpy, and mass fraction of CO_2 is accomplished to provide insight of the conditions insitu. The use of CO_2 transients is shown to be valuable in the interpretation of reservoir parameters affecting the performance in two-phase wells.

5.2 Reservoir and Well Description

Ohaaki (Broadlands) is the third geothermal field in New Zealand to be substantially developed. Its location on the North Island is shown in Figure (5-2). The area is an active rift zone where extensive geothermal development has occured. To date, over thirty wells have been drilled at the site. Extensive well testing has occured at Broadlands and a large data set exists. The field is a "hot-water" system containing a significant amount of noncondensible gas (carbon dioxide). The exact amount of gas present within the reservoir is still debated although the general concensus is that the reservoir contains between 2 to 4 percent CO_2 by mass (Grant, 1977; Sutton and McNabb, 1977; Grant and Glover, 1984). Total bore discharges show gas fractions of between 0.5 to 10 percent by weight (Grant, 1977).

During the initial discharge period in 1971, the fluid from BR21 contained 4.8 percent gas by mass, however, during a flow test in 1975 the gas content was down to 1.9 percent by mass. The extent of two-phase zones within the field is not known but BR21 is a two-phase well producing fluids with enthalpy in excess of that for a saturated liquid under reservoir conditions. The location of the well within the field is shown in Figure (5-3). The well was drilled to a depth of 1120 meters in 1970 and was cased to 425 meters. There are permeable zones at 500 meters and at 800 to 900 meters, however, the upper zone "dominates" during discharge (Hitchcock, 1971; Grant and Glover, 1984). The lower zone produces fluid with a temperature of 270 °C. The temperature of the upper zone is believed to be 255 °C but upflow from the lower zone disguises the exact temperature. The upper zone has an injectivity of 15 kg/bar-s and a productivity of 1.5 kg/bar-s. The lower zone is not as permeable with corresponding

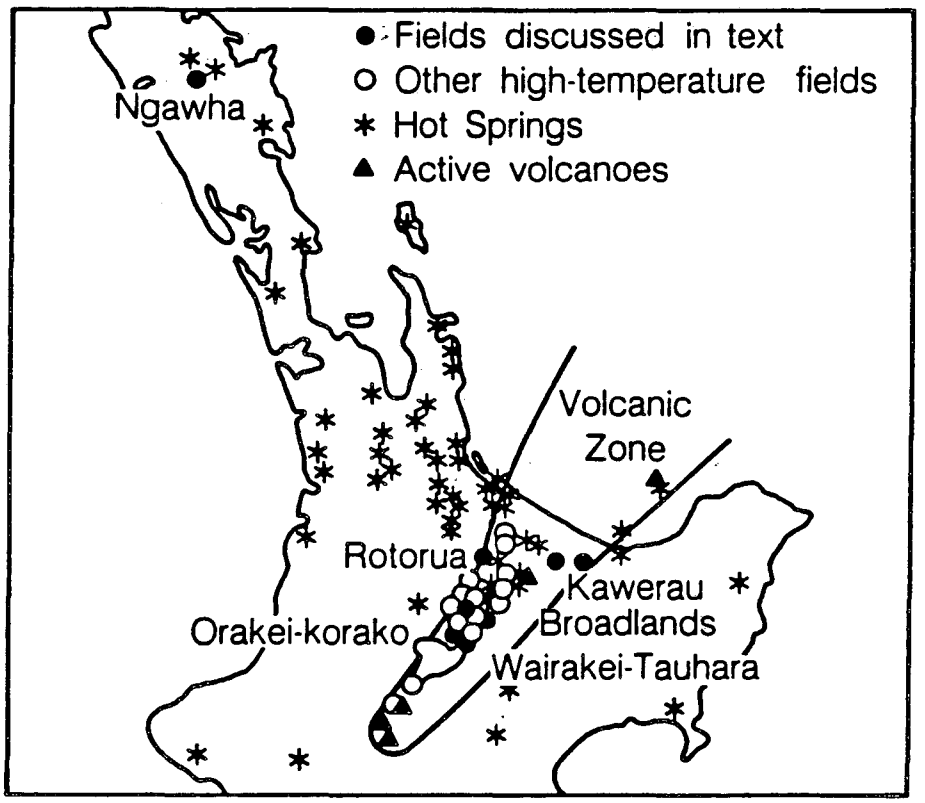

XBL 8612-12793

Figure (5-2). Location map for Broadlands geothermal field on the north island of New Zealand. years.

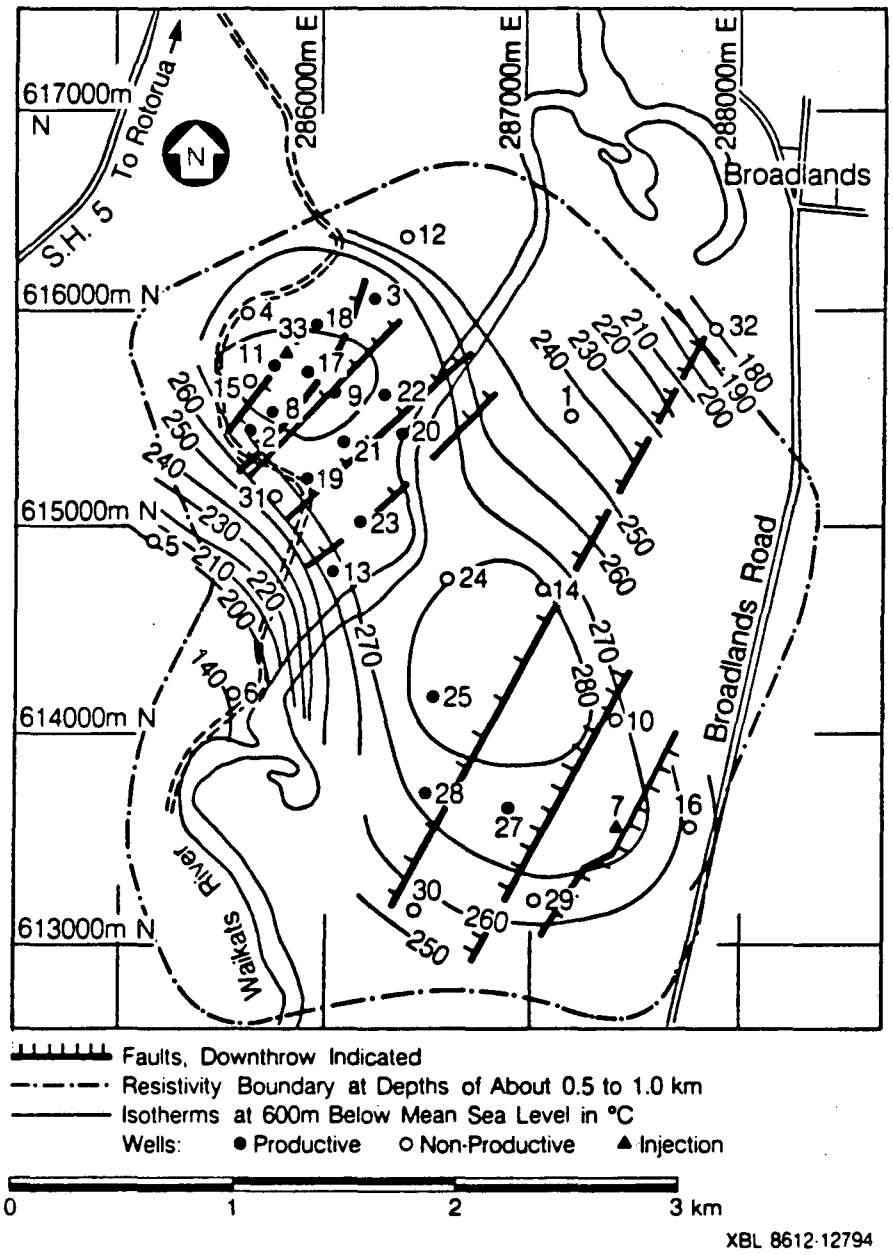

Figure (5-3). Location map of wells including temperature contours in Broadlands geothermal field, New Zealand (Ministry of Works and Development, Wellington).

values of 1.5 kg/bar-s and 0.3 kg/bar-s (Grant and Glover, 1984).

A simiplified cross section for BR21 is shown in Figure (5-4) with the inclusion of the major feedzone (Ministry of Works and Development, 1977). It should be noted that the feedzone is located close to a fault but the fault is not thought to be the primary source of fluid. The major feedzone occurs in the Waiora Formation. This unit is a pumacious lapilli tuff which is locally water-laid and with a low quartz content (Ministry of Works and Development, 1977). Overlying the Waiora Formation is the Ohaki Rhylite. The Ohaki Rhyolite is dense and largely impermeable. The unit directly below the Waiora Formation is the Broadlands Dacite. It is a very dense plagioclase dacite and has low permeability. The lower feedzone is located in the Rautawiri Breccia, a lithic tuff. The permeability in this unit is thought to be largely along the contacts. It is separated from the Waiora Formation by the Broadlands Dacite above. The unit below the Rautawiri Formation is the Rangitaiki Ignimbrite, a quartz-plagioclase welded vitric tuff, which has low permeability.

5:3 The Well Data

Grant and Glover (1984) carried out an extensive analysis of BR21 using analytical techniques developed by Grant (1979). They noted that the enthalpy took weeks to become stable and that the pressure transients indicated a transient period of only minutes or even seconds. Given reasonable parameters for Ohaaki, they determined that the transient period for the enthalpy should be on the order of minutes for a porous medium. From this Grant and Glover concluded that a fractured medium was required to match the enthalpy transients. Impermeable matrix blocks were used to match the short period required for the pressure transients to gain stability. The time necessary for stability of the enthalpy transients was then assumed to be equal to time required for thermal equilibrium between the fluid and the impermeable matrix blocks. They calculated a "relaxation time" for conductive equilibrium between the impermeable matrix block and the discharging fluid. The matrix blocks were then estimated to be 1 to 2 m^3 given a relaxation time of between 400 and 1000 hours. Analysis of the

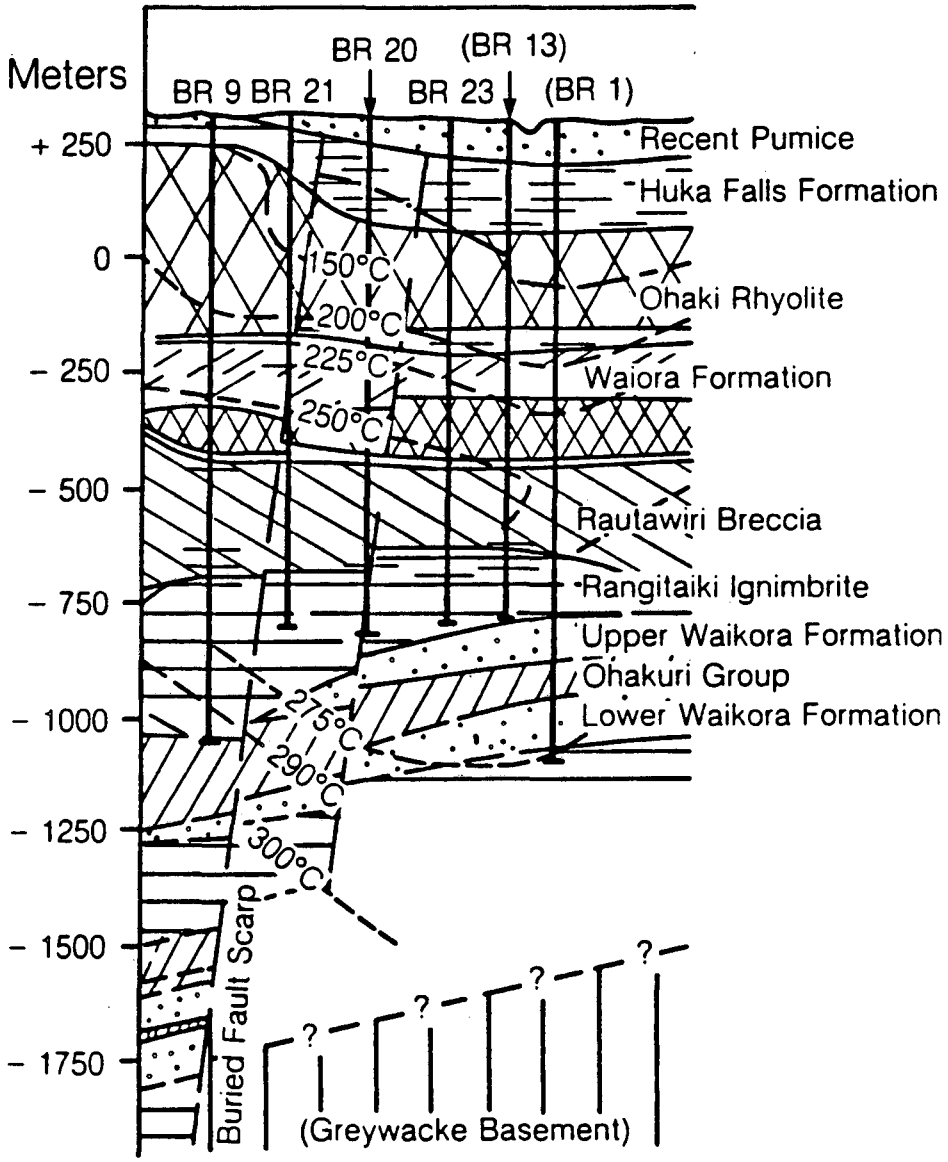

Figure (5-4). Cross section showing the geology surrounding well BR21, Broadlands geothermal field, New Zealand (Ministry of Works and Development, Wellington).

chemical transients was determined to be too complex to approach in this study (Grant and Glover, 1984). These transients can be valuable using numerical methods to provide further insight.

Using the simulator MULKOM (Pruess, 1982) with an equation of state for H_2O–CO_2 mixtures developed by O'Sullivan et al (1983), studies were undertaken to determine the characteristics of the reservoir near well BR21. The upper feedzone was assumed to provide all of the fluid for production and, hence, a single layer radially infinite model was used. The mesh consisted of logarithmically discretised elements with five elements per cycle extending to a radial distance sufficient to prevent boundary effects. The MINC method (Pruess and Narasimhan, 1982) was used to approximate the fractured nature of the reservoir with the matrix being discretised into five nested elements. The effective thickness of the reservoir was assumed to be 100 meters by inspection of the cross section shown in Figure (5-4). The reservoir had initially 50 bars total pressure at the primary feed point and the well was produced at a constant rate of 25 kg/s. The relative permeability functions used in this simulation are linear curves. The fracture curves are without cutoffs and the matrix curves provide for a residual liquid saturation of 40 percent and a 5 percent residual gas saturation. Other rock and fluid parameters can be found in Table (5-1).

The match with the pressure, enthalpy, and mass fraction of CO_2 transient data from BR21 is shown in Figure (5-5). The actual data is shown with a dashed line and the match is indicated with a solid line. A composite reservoir is necessary to match the data. The early transients are dominated by conditions in the fracture. The rapid decline in pressure without a concurrent rise in enthalpy (see Figure (5-5)) indicates that the fracture storage is small and that the fracture is fairly permeable. The small storage in the fracture (fracture porosity of 0.5%) causes the pressure to drop rapidly while the permeability of 0.1 Darcy near the well prevents a rapid rise in the flowing enthalpy. The small storage requirement confirms the choice of a reservoir thickness of 100 meters. If thickness were greater an unrealistic fracture porosity would be necessary to match the pressure decline. Ten meters from the well the permeability is dropped to 0.09 Darcy in order to match the steeper decline in the pressure after 4000

seconds.

Table (5-1). Reservoir Parameters.

Parameter	Reservoir Value(s)
reservoir thickness	100 m
wellbore radius	0.12 m
flowrate	25 kg/s
fracture spacing	30 m
fracture porosity	0.1%
matrix porosity	18%
fracture transmissivity	1.0 dm from well to 10 m
	0.9 dm from 10 to 125 m
	0.1 dm beyond 125 m
matrix permeability	0.3 md
thermal conductivity	2.2 W/m °C
rock heat capacity	1000 J/kg °C
rock density	2650 kg/m^3
fracture relative permeability	X-curves
	S_{rl}=.0 S_{rg}=.0
matrix relative permeability	X-curves
	S_{rl}=.05 S_{rg}=.40
initial pressure	50 bars
initial gas saturation	6% in fracture to 70 m
	15% in fracture beyond 70 m
	33% in matrix
initial partial pressure of CO_2	2.0 bars
intial temperature	≈260 °C
diffusion coefficient	1.38x10^{-5}m^2
tortuosity	0.25m/m

The initial gas saturation computed in fractures near the well is 6 percent so that the initial flowing enthalpy is 1184 kJ/kg and the initial flowing mass fraction of CO_2 is 0.28 (see Figure (5-5)). If the gas saturation is higher the pressure will drop more rapidly to provide for the constant rate production. If the gas saturation is lower the pressure will drop too slowly and the enthalpy will be too low. The partial pressure of CO_2 corresponding to the flowing mass fraction of 0.28 is 2 bars.

With the initial conditions met we will consider the rise in both enthalpy and flowing mass fraction of CO_2. An increase of the gas saturation is required in order to

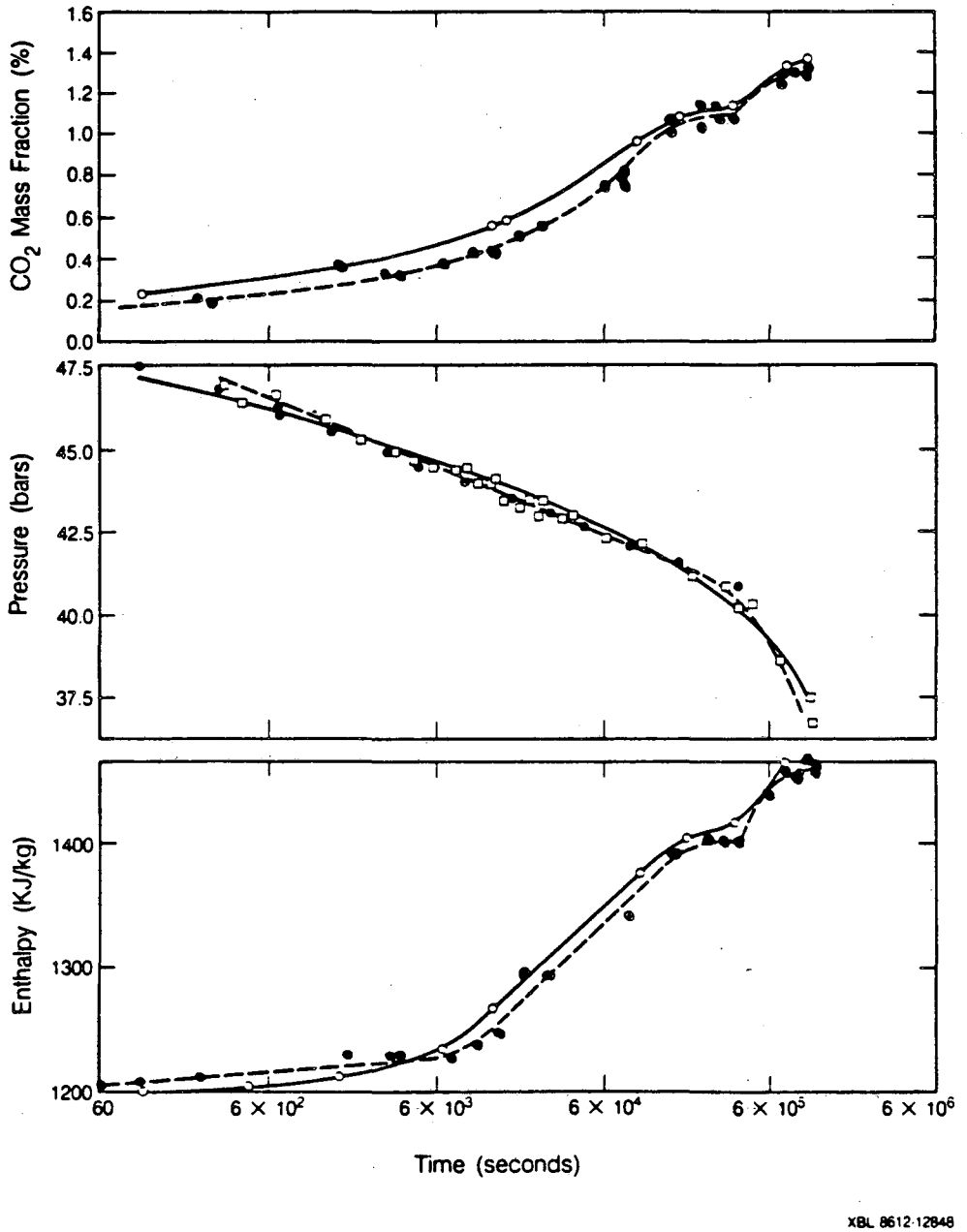

Figure (5-5). Comparison of best fit model to measured results of changes in downhole pressure, flowing mass fraction of CO_2, and flowing enthalpy with time.

match the sustained rise in the flowing mass fraction of CO_2 (see Figure (5-5)). The initial stablilized value of both the enthalpy and the flowing mass fraction of CO_2 help to determine three other parameters. The enthalpy of approximately 1400 kJ/kg is representative of the equilibrium flow between the fracture and the matrix. Therefore, this value dictates the required gas saturation in the matrix. The matrix gas saturation was determined to be 33 percent. In Chapter 3 the matrix porosity was shown to have strong effects on the rise in the flowing mass fraction of CO_2 without significantly affecting the enthalpy. Using a matrix porosity of 18 percent provided sufficient CO_2 to cause the increase to 1.1 percent by mass. The matrix porosity would seem rather high except that the rock is pumaceous suggesting a large void volume.

The time necessary for the rise in both the enthalpy and the flowing mass fraction of CO_2 is controlled primarily by two parameters. The fracture spacing is proportional to the surface area between the fractures and the matrix and, hence, will control the rate at which equilibrium flow of heat and mass is established between the fracture and matrix. In addition, the matrix permeability will also control the amount of fluids recharging the fractures from the matrix. Using a simple trial and error method it is easily established that the best fracture spacing for the time of rise is about 30 meters. The matrix permeability which provides fluid at a rate necessary to enhance the enthalpy and flowing mass fraction of CO_2 is 0.3 millidarcy. If the permeability were lower the rise in enthalpy would be too high and the rise in flowing CO_2 content would be too slow.

The final consideration here is the moderate rise in the both the flowing enthalpy and the flowing mass fraction of CO_2 accompaning a steep drop in the pressure at late times (about five days). If only the enthalpy and the pressure are considered, their changes would be representative of boundary effects. However, since the flowing mass fraction of CO_2 also rises boundary effects are not sufficient by themselves to provide the the changes. Therefore, a combination of changes in the gas saturation and fracture permeability are required in order to accurately match these data. The pressure pulse travels along the fracture more rapidly than the fluid. This indicates that

moderate changes in gas saturation are needed closer to the well than a decrease in fracture permeability in order to match transient conditions. Thus the gas saturation in the fracture is increased to 15 percent from 6 percent at 70 meters while the fracture permeability change from 0.09 Darcy to 0.01 Darcy is at 125 meters. This allows the effects to propagate along the fractures and arrive at the well at approximately the same time. A composite diagram of the model is shown in Figure (5-6).

5.4 Summary

A model of well BR21 (see Figure (5-6)) has been developed that matches the pressure, enthalpy, and flowing mass fraction of CO_2 from the well adequately (see Figure (5-5)). The gas saturation in the fracture near the well could be expected to be rather low considering that the well was produced previously. The gas saturation was 6 percent near the well increasing to 15 percent at 70 meters from the well. Condensation around the wellbore would reduce the gas saturation after production. This would also explain the relative high matrix gas saturation of 33 percent near the well since production will deplete the matrix. The fracture permeability varying from 0.1 down to 0.01 Darcy away from the well was used. The matrix permeability was 0.3 millidarcy. The reservoir thickness of 100 meters combined with 0.5 percent fracture porosity were used to match the small storage requirements indicated by the rapid pressure decline. The matrix porosity of 18 percent helped provide a sufficient rise in the flowing mass fraction of CO_2. The CO_2 partial pressure of 2.0 bars is reasonable. These results show the importance of including CO_2 transient measurements in field data.

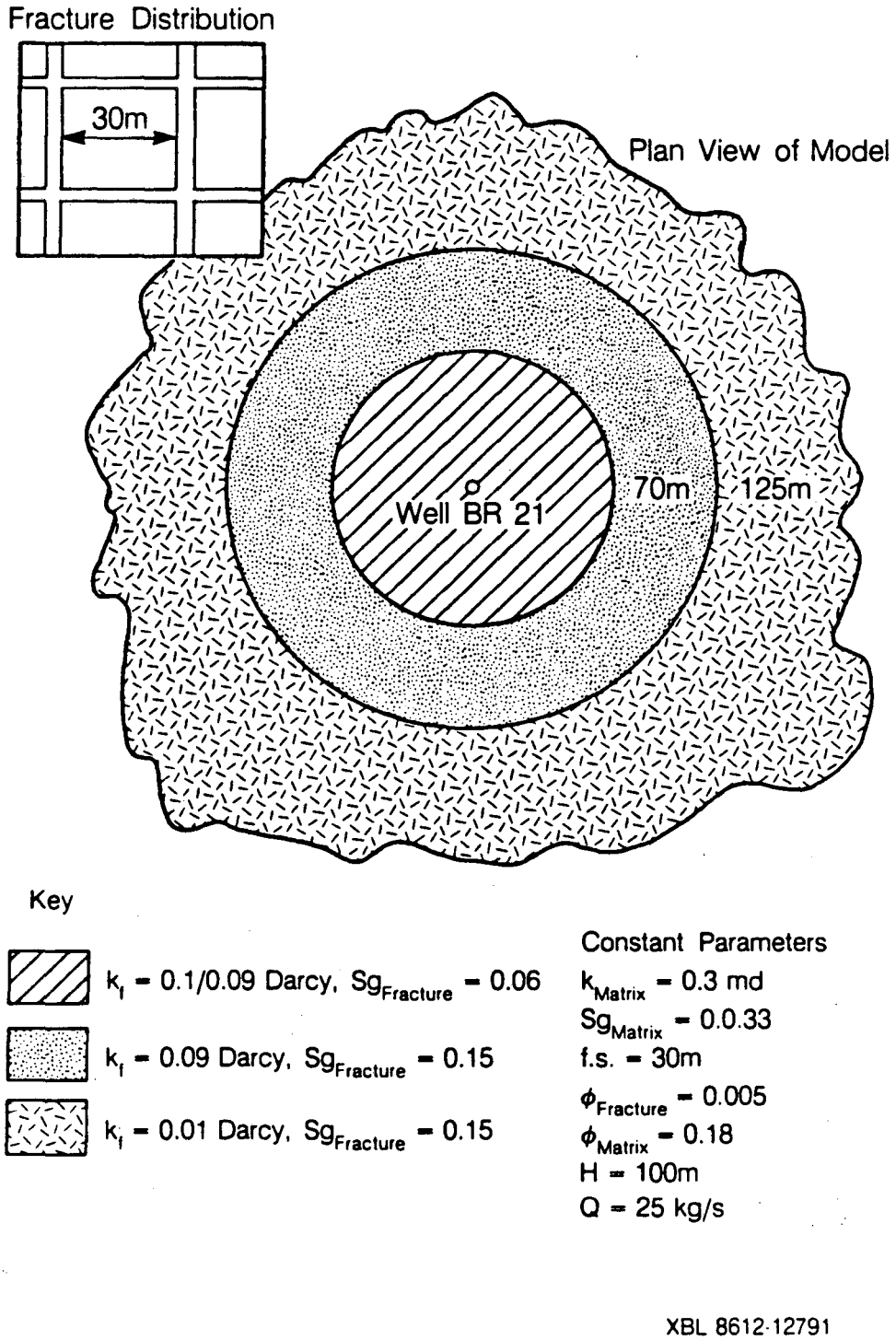

Figure (5-6). Diagram of best fit model including important reservoir and fluid parameters.

6. Conclusion

The purpose of this study was to examine the effect of significant amounts of noncondensible gas on the behavior of fractured two-phase geothermal reservoirs. The amount of noncondensible gas in geothermal systems was surveyed and found to be significant and widespread. The current level of understanding of the effect of noncondensible gas on geothermal systems was reviewed. Information on the behavior of fractured gassy reservoirs under exploitation is limited, however, enthalpy and pressure transients had been examined in terms of controlling parameters for two-phase systems. Since the flowing mass fraction of CO_2 is closely related to the enthalpy in gassy reservoirs, a review of enthalpy transients was made. This work incorporates noncondensible gas (CO_2) into modeling of fractured two-phase reservoirs to examine the transient behavior of these systems. A clear understanding of the effects of noncondensible gases in two-phase systems would improve the evaluation of well transients and, hence, the assessment of the economic feasibility of high temperature geothermal systems.

A complete understanding of flow in two-phase systems is essential to assess the effects of noncondensible gases in geothermal systems. A review was made outlining the importance of phase mobilities and relative permeabilities in controlling transients for these systems.

Upon review of fractured systems, it was determined that the important hydrologic and fluid parameters affecting the transient behavior of these systems are the matrix permeability, fracture permeability-thickness product, matrix and fracture relative permeability functions, initial gas saturation and partial pressure of CO_2, fracture and matrix porosity, and fracture spacing. A sensitivity study was performed to define the important controlling parameters for both enthalpy and CO_2 transients in gassy geothermal systems. Using a base case the effects of changes in various hydrologic and fluid parameters were studied. Figures showing enthalpy transients without CO_2 were included to highlight the significant effects of noncondensible gases on reservoir

behavior.

Evaluating the results of the sensitivity study shows that a high concentration of gas in geothermal systems has large effects on the transient behavior of the reservoir. The presence of CO_2 in a reservoir significantly reduces the variability in enthalpy transients. The sensitivity on wellhead measurements of flowing enthalpy for actual geothermal systems is almost 100 kJ/kg. This indicates that most reservoir parameters can not be determined using enthalpy transients when high noncondensible gas concentrations are present (10 bars). However, if the concentration of CO_2 is lower, the effects of the hydrologic parameters may be grouped according to their effects on the enthalpy to obtain information about reservoir conditions. Parameters such as fracture spacing, fracture and matrix permeability, and thermal conductivity are shown to affect the rate of rise in enthalpy. The initial gas saturation, initial partial pressure of CO_2, and the permeabilities, both fracture and matrix, are shown to affect the total rise in flowing enthalpy. With a high concentration of CO_2 the initial gas saturation and the initial partial pressure of CO_2 are the only significant parameters affecting the flowing enthalpy.

The noncondensible gas transients are far more valuable than the enthalpy transients for reservoir evaluation when high gas concentrations are present. The concentration of CO_2 will not change substantially in the wellbore unless scaling is occuring. This allows accurate measurement of the gas content. The flowing mass fraction of CO_2 varies significantly with several reservoir parameters. It was shown that the initial partial pressure of CO_2, the initial gas saturation, and the matrix porosity have strong affects on the total rise in flowing mass fraction of CO_2. These three factors control the amount of CO_2 in the system. The matrix permeability and the fracture spacing are shown to have significant affects on the rate of rise in the flowing mass fraction of flowing mass fraction of CO_2. These parameters control the interaction between the matrix and fractures.

It was determined that enthalpy transients when used in conjunction with CO_2 transients can be used to provide information that could not be determined otherwise.

The matrix porosity was shown to have large effects on the flowing mass fraction of CO_2 while it had little effect on the enthalpy. The initial partial pressure will drastically reduce the rise in enthalpy and increase the flowing mass fraction of CO_2 in contrast to an increase in the gas saturation which also increases the flowing mass fraction of CO_2 but causes a large increase in the enthalpy. Similiarly, fracture spacing and matrix porosity have strong effects on the rise in the flowing mass fraction of CO_2. However, only the fracture spacing has substantial effects on the rise in the flowing enthalpy. Therefore, if there is a rise in the flowing mass fraction of CO_2 without a similiar response in the flowing enthalpy, it is likely that it is caused by variations in the matrix porosity. It is concluded that the most accurate assessment of a gassy two-phase reservoir requires careful monitoring of both the enthalpy and the the flowing mass fraction of CO_2.

A simple model of a single matrix block was used to examine the ultimate recovery of a reservoir with varying initial partial pressures. It was shown that the higher the initial partial pressure the lower the recovery from geothermal systems. Due to the lower vapor pressure of water in these systems less boiling will occur reducing the recovery from a system. The backflow of fluid to the matrix, due to the effects of CO_2 on the pressure-temperature relationship of water, is identified. It is noted that thermodynamic equilibrium, including the partial pressures of CO_2, must be considered to understand fracture-matrix interaction in a producing reservoir. The equilibration of CO_2 partial pressures between the fracture and matrix can occur by "backflow" of gas-rich fluids or chemically by rock-fluid reactions. An analytical expression is derived to quantify the total amount of backflow that might occur depending on the final saturation in the matrix while neglecting chemical reactions involving CO_2. This expression was used to develop curves to estimate fluid loss to the matrix due to backflow. Much more work is necessary to understand the kinetics of rock-fluid and water-gas reactions within complicated reservoir systems to determine the relative importance of each phenomena. The petrology of the reservoir can have large effects on the buffering of CO_2 partial pressures causing the buffer to be weaker or stronger. A static equilibrium balance equation is inadequate to accurately predict the behavior

in a transient reservoir.

In addition, backflow can be very substantial for low enthalpy two-phase systems. It was shown that backflow may amount to hundreds of kilograms per unit pore volume. However, backflow will not be very significant in vapor dominated systems where liquid phase mobility is small. It is identified that fluid injection of low gas content fluids can increase recovery from a fractured geothermal reservoir. This is done by increasing liquid mobilities within the fractures and, due to the complex thermodynamics of H_2O–CO_2 systems, increasing matrix recovery.

Finally, the background obtained from the literature review, the review of two-phase flow principles, and the sensitivity studies of enthalpy and flowing mass fraction of CO_2 transients was applied to analyse the transients from well BR21 in Broadlands geothermal field of New Zealand. The pressure, enthalpy, and flowing mass fraction of CO_2 were matched for this reservoir. It was shown that much information can be gained by analyzing CO_2 transients in addition to pressure and enthalpy transients. The model developed for this well is consistant with the geology of the area and the hydrology around the well. The fracture permeability was determined to decrease with distance from the well, 0.1 Darcy initially and decreasing to 0.01 Darcy as shown in Figure (5-6). The matrix permeability of 0.3 millidarcy and a 30 meter fracture spacing produced sufficient lag in the time of rise for enthalpy and flowing mass fraction of CO_2. The fracture porosity of 0.5 percent and effective reservoir thickness of 100 meters is consistent with both the geology and the steep pressure decline (small storage). The high matrix porosity of 18 percent is compatible with a pumaceous formation and contributes to the increase in the flowing CO_2 mass fraction. The results of this study can be used as a starting point for a wider study of this field. The use of all the available information in modeling of geothermal fields will lead to more a accurate reservoir evaluation.

References

Andrews, J. N.;"Dissolved Radioelements and Inert Gases in Geothermal Investigatios." Geothermics, Vol. 12, pp. 67-82, 1983.

Ar, G.;"Denizli-Kizildere Geothermal Power Plant, Turkey." Geothermics, Vol. 14, No. 2/3, pp. 429-433, 1985.

Arnorsson, S. and Gunnlaugsson, E.;"Gas Chemistry in Geothermal Systems." Proc. Ninth Workshop Geothermal Res. Engineering, Stanford University, Stanford California, pp. 231-237, 1983.

Atkinson, P., Celati, R., Corsi, R., Kucuk, F., and Ramey Jr., H. J.; Vol. 7, pp. 185-208, 1978.

Atkinson, P., Celati, R., Corsi, R., and Kucuk, F.;"Behavior of the Bagnore Steam/CO_2 Geothermal Reservoir, Italy," Society of Petroleum Engineers Journal, Vol. 20, No. 4, pp. 228-238, 1980.

Barbier, E.;"Geothermal Energy in the Context of Energy in General and Electric Power Supply, National and International Aspects." Geothermics, Vol. 14, no. 2/3, pp. 131-141, 1985.

Barelli, A., Celati, R., and Manetti, G.;"Gas-Water Interface Rise During Early Exploitation Tests in Alfina Geothermal Field (Northern Latium, Italy)" Geothermics, Vol. 6, pp. 199-208, 1978.

Bjornsson, G. and Bodvarsson, G. S.;"A Limited Survey of Geothermal Reservoirs Properties," Geothermal Resources Council Meeting, Palm Springs, Ca., 1986.

Bodvarsson, G.;"On the Temperature of Water Flowing through Fractures," Journal of Geophysical Research, Vol. 74, No. 8, April 15, 1969.

Bodvarsson, G. S., O'Sullivan, M. J., and Tsang, C. F.;"The Sensitivity of Geothermal Reservoir Behavior to Relative Permeability Parameters," Proceedings, Sixth Workshop on Geothermal Reservoir Engineering, Stanford, Ca., pp. 224-237, 1980.

Bodvarsson, G. S.;"Numerical Studies of Enthalpy and CO_2 Transients in Two-Phase Wells," Geothermal Res. Council, Transactions, Vol. 8, pp. 289-294, 1984.

Bodvarsson, G. S. and Witherspoon, P. A.;"Flow Rate Decline of Steam Wells in Fractured Geothermal Reservoirs," Proceedings, Tenth Workshop on Geothermal Reservoir Engineering, January 22-24, 1986.

Brown, P. R. L. and Ellis, A. J.;" The Ohaki-Broadlands Hydrothermal Area, New Zealand: Mineralogy and Related Geochemistry." American Journal of Science, Vol. 269, pp. 97-131, Summer, 1970.

Carelli, R. and Guglielminetti, M.;"Multiple Reservoirs in the Mofete Field, Naples, Italy." Proc., Ninth Workshop Geothermal Reservoir Engineering, Stanford University, Stanford, California, 1983.

Cavarretta, G., Gianelli, G., and Puxeddu, M.;"Formation of Authigenic Minerals and Their Use as Indicators of the Physicochemical Parameters of the Fluid in the Larderello-Travale Geothermal Field." Bull. Soc. Econ. Geol., Vol. 77, No. 5, pp. 1071-1084, 1982.

Cionni, R., Corazza, E., and D'Amore, F.;"Radon in Fumarolic Gases From Vulcano Island." Geothermics, Vol. 13, No. 4, pp. 385-388, 1984.

D'Amore, F. and Nuti, S.;"Notes on the Chemistry of Geothermal Gases." Geothermics, Vol. 6, pp. 39-45, 1977.

D'Amore, F. and Panichi, C.;"Evaluation of Deep Temperatures of Hydrothermal Systems by a New Gas Geothermometer." Geochim. Cosmochim. Acta, Vol. 44, pp. 549-556, 1980.

D'Amore, F. and Truesdell, A.;"Helium in the Larderello Geothermal Fluid." Geothermics, Vol. 13, No. 3, pp. 227-239, 1984.

D'Amore, F. and Truesdell, A. H.;"Calculation of Geothermal Reservoir Temperatures and Steam Fractions from Gas Compositions." Geothermal Res. Council Trans., Vol. 9, pp. 305-310, 1985.

DiPippo, R.; Geothermal Energy as a Source of Electricity, 1979.

Donovan, P. R.;"The status of high enthalpy geothermal exploration in the developing countries." United Nations Report, EP/sem.9/R.84, 1984.

Ellis, A. J.;"Chemical equilibrium in Magmatic Gases." American Journal of Science, Vol. 255, pp. 416-431, 1957.

Ellis, A. J.;"The Solubility of Carbon Dioxide in Water at High Temperatures," American Journal of Science, Vol. 257, pp. 217-234, 1959.

Ellis, A. J. and Golding, R. M.;"The Solubility of Carbon Dioxide Above 100_{eC} in Water and Sodium Chloride Solutions," American Journal of Science, Vol. 261, pp. 47-60, 1963.

Ellis, A. J.;"Chemistry of Some Explored Geothermal Systems." in Geochemistry of Hydrothermal Ore Deposits, pp. 465-511, Holt, Rheinhart, and Winston, New York, 1967.

Giggenbach, W. F.;"Geothermal Gas Equilibria." Geochim. Cosmochim. Acta, Vol. 44, pp. 2021-2032, 1980.

Goyal, K. P., Benoit, W. R., Maas, J. P., and Rosser, J. R.;"Desert Peak: A Geothermal Field in Churchill County, Nevada." Proc., Ninth Workshop on Geothermal Reservoir Engineering, Stanford University, Stanford, California, 1983.

Grant, M. A.;"Broadlands--a Gas-Dominated Geothermal Field," Geothermics, Vol. 6, pp. 9-29, 1977a.

Grant, M. A.;"Permeability Reduction Factors at Wairakei," presented AIChE-ASME Heat Transfer Conference, Salt Lake City, Utah, Aug. 15-17, 1977b.

Grant, M. A.;"Quasi-Analytic Solutions for Two-Phase Flow Near a Discharging Well," Tech. Rep. 86, Appl. Math Div., Dept. of Sci. and Ind. Res., Wellington, New Zealand, 1979.

Grant, M. A. and Sorey, M. L.;"The Compressibility and Hydraulic Diffusivity of a Water-Steam Flow," Water Resources Research, Vol. 15, No. 3, June, 1979.

Grant, M. A.;"Enthalpy and Chemical Transients in Two-Phase Flow in Homogeneous and Fractured Reservoirs," Applied Mathematics Division, Report No. 104, New Zealand Dept. of Sci. and Ind. Res., 1982a.

Grant, M. A.; New Zealand Workshop on Geothermal Engineering, pp. 174, 1982b.

Grant, M. A.;"Enthalpy and Chemical Transients in BR21," App. Math. Div., Rep. NO. 109, New Zealand Dept. of Sci. and Ind. Res., 1983.

Grant, M. and Glover, R.;"Two-Phase Heat and Mass Transfer Experiment at Well BR21 Broadlands," Geothermics, Vol. 13, No. 3, pp. 193-213, 1984.

Hebien, J. J.;"Discussions on a Type of Reservoir Cell Boundary in the Geysers Steam Field." Proc., Tenth Workshop Geothermal Reservoir Engineering, Stanford University, Stanford, California, January 22-24, 1985.

Horne, R. N. and Ramey, Jr., H. J.;" Steam/Water Relative Permeabilities From Production Data," Geothermal Resources Council, Transactions, Vol. 2, July 1978.

Hulston, J. R. and McCabe, W. J.;"Mass Spectrometer Measurements in the Thermal Areas of New Zealand, Part 1, Carbon Dioxide and Residual Gas Analysis." Geochim. Cosm. Acta, Vol. 26, pp. 383-387, 1962.

Kasameyer, P. W. and Schroeder, R. C.;"Applications of Thermal Depletion to Geothermal Reservoirs with Fracture and Pore Permeability." Proc., Second Workshop Geothermal Reservoir Engineering, Stanford University, Stanford, California, 1976.

Kestin, J., DiPippo, R., Khalifa, E., Ryley, D. J., editors;"Sourcebook on the Production of Electricity from Geothermal Energy," United States Dept. of Energy, DOE/RA/28320-2, August, 1980.

Klein, C. W., McNitt, J. R., Sanyal, S. K., Che, M., Tolentino, B. S., Alcaraz, A., and Datuin, R.;"Geochemistry of the Palimpinon Geothermal Field, Southern Negros, Phillipines." Geothermal Resources Council, Tranactions, Vol. 6, October, 1982.

Kruger, P., Semprini, L., Verma, S., Barragan, R., Molinar, R., Aragon, A., Ortiz, J., and Miranda, C.;"Intial Chemical and Reservoir Conditions at Los Azufres Wellhead Power Plant Startup." Proc., Tenth Workshop on Reservoir Engineering, Stanford University, Stanford, California, January 22-24, 1985.

Lippman, M. J., Bodvarsson, G. S. and Gaulke, S. W.;"Enthalpy Transients in Fractured Two-Phase Geothermal Reservoirs." Geothermal Resources Council, Transactions, Vol. 9, July, 1985.

Mahon, W. A. and Finlayson, J. B.;"The Chemistry of the Broadlands Area, New Zealand." American Journal of Science, Vol. 272, pp. 48-68, 1972.

Marini, L., Chiodini, G., and Cioni, R.;"New Geothermometers For Carbonate-Evaporite Geothermal Reservoirs." Geothermics, Vol. 15, pp. 77-86, 1986.

Mazor, E., Fouillac, C., and Michard, G.;"Noble Gases in Some Mineral and Warm Waters in Massif Central, France." Geothermics, Vol. 11, pp. 81-92, 1982.

Mazor, E., and Truesdell, A. H.;"Dynamics of a Geothermal Field Traced By Noble Gases: Cerro Prieto, Mexico." Geothermics, Vol. 13, pp. 91-102, 1984.

Moench, A. F.;"The effect of Thermal Conduction Upon Pressure Drawdown and Buildup in Fissured, Vapor-Dominated Geothermal Reservoirs," Proc. Fifth Workshop on Geothermal Reservoir Engineering, Stanford U., Stanford, Ca., 1978.

Nehring, N. L. and D'Amore, F.;"Gas Chemistry and Thermometry of the Cerro Prieto, Mexico, Geothermal Field." Geothermics, Vol. 1/2, pp. 75-89, 1984.

Nockolds, S. R. and Allen, R.;"The Composition of Some Common Igneous Rocks." Geol. Soc. Amer. Bull., Vol. 65, pp. 1007-1032, 1954.

Nuti, S., Noto, P. and Ferrara, G. C.;"The System H_2O-CO_2-CH_4-H_2 at Travale, Italy: Tentative Interpretation." Geothermics, Vol. 9, pp. 287-295, 1980.

Nuti, S.;"Elementary and Isotopic Compositions of Noble Gases in Geothermal Fluids of Tuscany, Italy." Geothermics, Vol. 13, No. 3, pp. 215-226, 1984.

O'Sullivan, M. J.;"A Similarity Method for Geothermal Well Test Analysis," Water Resources Research, Vol. 17, No. 2, pp. 390-398, 1981.

O'Sullivan, M. J., Bodvarsson, G. S., Pruess, K., and Blackeley, M. R.; of Petroleum Engineers, No. 12102, Presented October 5-8, 1985.

Pritchett, J. W., Rice, M. H., and Riney, T. D.;"Equation-of-State Water-Carbon Dioxide Mixtures: Implications for Baca Reservoir," DOE/ET/27163-8, 1981.

Pruess, K.;"Heat Transfer in Fractured Geothermal Reservoirs With Boiling," Water Resources Research, Vol. 19, No. 1, pp. 201-208, Feb., 1983.

Pruess, K., Celati, R., Calore, C., and D'Amore, F.;"CO_2 Trends in the Depletion of the Larderello Vapor-Dominated Reservoir." Proc., Tenth Workshop on Geothermal Reservoir Engineering, January 22-24, 1985.

Pruess, K. and Narasimhan, T. N.;"On Fluid Reserves and the Production of Superheated Steam from Fractured, Vapor-Dominated Geothermal Reservoirs," Journal of Geophysical Research, Vol. 87, No. B11, pp. 9329-9339, 1982.

Riney, T. D. and Garg, S. K.;"Evaluation of Injection Test Data From a Baca Well." Proc., Eighth Workshop Geothermal Reservoir Engineering, Stanford University, Stanford, California, December, 1982.

Semprini, L. and Kruger, P.;"Relationship of Radon Concentration to Spatial and Temporal Variations of Reservoir Thermodynamic Conditions in the Cerro Prieto Geothermal Field." Geothermics, Vol. 13, No. 1/2, pp. 103-115, 1984.

Sorey, M. L., Grant, M. A., and Bradford, E.;"Nonlinear Effects in Two-Phase Flow to Wells in Geothermal Reservoirs," Water Resources Research, Vol. 16, No. 4, pp. 767-777, August, 1980.

Stefansson, V.;"The Nesjavellir High Temperature Geothermal Field in Iceland," Tenth Workshop Geothermal Reservoir Engineering, Stanford U., Stanford, Ca., 1985.

Stefansson, V. and Steingrimsson, B.;"Production Characteristics of Wells Tapping Two-Phase Reservoirs at Krafla and Namafjall," Sixth Workshop on Geothermal Reservoir Engineering, Stanford U., Stanford, Ca., 1980.

Steingrimsson, B., Gudmundsson, A., Gudmundsson, G., and Armannsson, H.; September, 1984.

Straus, J. M. and Schubert, G.;"Effects of CO_2 on the Buoyancy of Geothermal Fluids," Geophysical Res. Letters, Vol. 6, No. 1, pp. 5-8, 1979.

Sutton, F. M.;"Pressure-Temperature Curves for a Two-Phase Mixture of Water and Carbon Dioxide." New Zealand Journal of Science, Vol. 19, pp. 297-301, 1976.

Sutton, F. M. and McNabb, A.;"Boiling Curves at Broadlands Geothermal Field, New Zealand." New Zealand Journal of Science, Vol. 20. pp. 333-337, 1977.

Takenouchi, S. and Kennedy, G. C.;"The Binary System H_2O–CO_2 at High Temperatures and Pressures," American Journal of Science, Vol. 262, pp. 1055-1074, 1964.

Tan, E.;"Reservoir Characteristics of the Kizildere Geothermal Field." Geothermics, Vol. 14, No. 2/3, pp. 419-428, 1985.

Udell, K.;Verbal communication December 15, 1986.

Zyvoloski, G. and O'Sullivan, M.;"Simulation of the Broadlands Geothermal Field, New Zealand," Proc. Fourth Workshop on Geothermal Reservoir Engineering, Stanford U., Stanford, Ca., 1978b.

Zyvoloski, G. and O'Sullivan, M.;"A Simple Model of Broadlands Geothermal Reservoir," New Zealand Journal of Science, Vol. 21, 505-510, 1978a.

Zyvoloski, G. and O' Sullivan, M.;"Simulation of a Gas-Dominated, Two-Phase Geothermal Reservoir," Society of Petroleum Engineers Journal, pp. 52-58, 1980.

Appendix A: Sources of Commonly Found Gases in Geothermal Reservoirs

Typically, reservoir fluids have a significant amount of gas which can be helpful in inferring conditions within the reservoir. The most abundant gas is carbon dioxide which in general, accounts for more than 90 percent of the gases present (Kestin et al, 1980) with hydrogen sulfide also being significant. Other gases present include nitrogen, methane, ethane, argon ammonia, hydrogen, radon, helium, krypton, and xenon (Kestin et al, 1980; D'Amore and Truesdell, 1984; Semprini and Kruger, 1984; Nuti, 1984).

Geology is important in determining the gas constituents within a reservoir. Gases may be derived from a variety of sources including volcanism, rock-fluid reactions, decay of organic compounds, and radioactive decay. If the source is known, gas may be used to determine flow patterns in the reservoir. Carbon dioxide, by far the most abundant gas, is derived both from volcanism and from rock-fluid reactions involving carbonate rocks. Carbon dioxide from volcanism, a primary source, was noted by Steingrimsson et al (1984) during an eruptive period at Krafla field in Iceland. Pruess et al (1985) suggested that carbonate rocks buffer carbon dioxide fugacities, a secondary source, at Larderello field in Italy. The following equilibrium reactions for controlling carbon dioxide were suggested by Cavarretta et al (1982) for the largely carbonate Larderello-Travale reservoir:

$$\text{3 K-bearing mica} + \text{4 calcite} + \text{6 quartz} ===$$
$$\text{2 clinozoisite} + \text{4 K-feldspar} + 4CO_2 + 4H_2O \qquad \text{(A-1)}$$

$$\text{2 clinozoisite} + \text{3 quartz} + \text{2 calcite} === \text{3 prehnite} + 2CO_2 \qquad \text{(A-2)}$$

The reservoirs of both Bagnore and Larderello fields in Italy contain a large volume of carbonate rock which can react with reservoir fluids as indicated above to produce carbon dioxide. Both fields have stable flowing carbon dioxide concentrations well above other systems where widespread carbonates are not present. In volcanic terrains, carbon dioxide is derived from degassing of magma at depth (Arnorsson and Barnes, 1983) and is a minor constituent of nepheline syenites (Nockolds and Allen, 1954) which can

be released during hydrothermal alteration. At temperatures >250 °C, Arnorsson and Barnes (1983) suggest carbon dioxide levels are controlled by the assemblage epidote-prehnite-calcite-quartz for volcanic rock reservoirs of basic to acidic composition. It has not been established which minerals control carbon dioxide fugacities at <250 °C or what rate the above reactions will occur.

Hydrogen sulfide is derived from volcanism (Ellis, 1967) and rock-fluid reactions with iron oxides and silicates (Nehring and D'Åmore, 1984). At Cerro Prieto, S-fugacities along with geology suggest that the presence of pyrite and epidote control hydrogen sulfide concentrations in the reservoir (Nehring and D'Amore, 1984). At the Geysers in California, widespread reaction of realgar and/or other epithermal sulfides with reservoir fluids is thought to control hydrogen sulfide fugacities (Hebien, 1985). Arnorsson and Barnes (1983) suggest that the mineral assemblage pyrrhotite-epidote-magnetite buffer hydrogen sulfide in the presence of liquid with <500 ppm chloride and pyrite-epidote-prehnite-magnetite or chlorite buffer hydrogen sulfide with >500 ppm chloride present.

Methane, ethane, ammonia and nitrogen in hydrothermal systems are believed to be derived from the decay of organic compounds containing carbon and nitrogen in local sedientary rocks (Hulston and McCabe, 1962; Ellis, 1967; D'Amore and Nuti, 1977; D'Amore and Truesdell, 1984). The reservoirs with sedimentary rocks such as Larderello and Cerro Prieto contain substantial amounts of nitrogen, methane, and ammonia due to the presence of organic material while reservoirs in volcanic terrains are much less likely to have organic material and therefore methane, nitrogen and ammonia. Ohaki-Broadlands reservoir has partial pressures of nitrogen, methane and ammonia that are five to ten times higher than those at Wairakei. This is thought to originate from the greater volume of sedimentary rock at Ohaki-Broadlands (Mahon and Finlayson, 1972).

Helium, radon and other noble gases are derived from the radioactive decay of Th and U-rich rocks (Cionni et al, 1984; Semprini and Kruger, 1984; D'Amore and Truesdell, 1984) although helium and other noble gases can be derived from the atmosphere

by shallow recharge (D'Amore and Truesdell; 1984).

Appendix B: Determination of Controlling Mineral Assembleges

To determine the mineral assembleges that control the noncondensible gas content in a geothermal system under equilibrium conditions, the free energy of formation can be calculated for the reaction from the measured partial pressure. The partial pressure is

$$P_{gas} = \frac{f}{\gamma} \tag{B-1}$$

where f is the fugacity and γ is the activity coefficient. However, if the gas is assumed to behave ideally under reservoir conditions then

$$a_{gas} = P_{gas} \tag{B-2}$$

where a_{gas} is the activity of the gas and P_{gas} is the partial pressure of that gas. This assumption is quite good for conditions typical in high temperature geothermal systems where the elevation in temperature compensates for the high pressure. The activities for liquids and solids under isothermal conditions are

$$\ln a = \frac{1}{RT} \int_{1atm}^{P} V \, dP \tag{B-3}$$

where a is the activity of the solid or liquid, R is the universal gas, T is the temperature in degrees Kelvin, V is the volume, and P is the pressure of interest. Under moderate pressure changes the volume V is essentially constant and much less than RT so that the activity is usually assumed to be unity and the thermodynamic equilibrium constant ($K_{reaction}$) goes from

$$K_{reaction} = \frac{\prod_{i=1}^{\#ofproducts} a_i}{\prod_{i=1}^{\#ofreactants} a_i} \tag{B-4}$$

to

$$K_{reaction} = a_{gas} = P_{gas} \tag{B-5}$$

where

$$\ln K_{reaction} = \frac{RT}{\Delta G_{f,reaction}} \tag{B-6}$$

for a standard state of 1 bar with R the universal gas content and T the temperature in degrees Kelvin. Finally, the free energy of formation ($\Delta G_{f,}$reaction) for the minerals controlling the partial pressure is

$$\Delta G_{f,reaction} = \sum_{i=1}^{\#ofproducts} \Delta G_{f,i} - \sum_{i=1}^{\#ofreactants} \Delta G_{f,i} \tag{B-7}$$

Substituting the free energies for likely mineral reactions allows the determination of the controlling assemblege for a known partial pressure of gas. Giggenbach (1981) used this technique to develop mineral stability diagrams under natural state geothermal reservoir conditions, however, little is known about reaction rates within a producing reservoir.

Appendix C: Analytical Expression for Backflow to the Matrix

Consider a matrix element with time independant boundary conditions. The fluid in the matrix is initially at a temperature T_1, a total pressure P_1, and is without CO_2. The boundary element (fracture) is at a lower temperature T_2, an equal total pressure P_2, and has a CO_2 partial pressure of P_{c2}. In order to have total equilibrium between the two elements under two phase conditions the temperature, pressure, and partial pressure of CO_2 must be equal. As the matrix cools due to conduction, CO_2 is required in the matrix to maintain thermodynamic equilibrium. The amount of CO_2 necessary to equilibrate the partial pressure in the matrix is then

$$[\rho_{CO_2} S_g + \rho_l X_{cl}(1-S_g)]\phi V \tag{C-1}$$

where S_g is the final saturation in the matrix of volume V and the other terms are as defined in nomenclature. To determine how much fluid is required to supply this amount of CO_2 to the matrix, it is necessary to determine the fraction of each phase that is mobile. The mass fraction of the liquid phase is then

$$W_l = \frac{k_{rl}\rho_l}{\mu_l}\nu_t \tag{C-2}$$

and the mass fraction of the gas phase is

$$W_g = \frac{k_{rg}\rho_g}{\mu_g}\nu_t \tag{C-3}$$

where ν_t is the total kinematic viscosity and is defined as

$$\nu_t = \frac{1}{\frac{k_{rl}\rho_l}{\mu_l} + \frac{k_{rg}\rho_g}{\mu_g}} \tag{C-4}$$

The total flow of CO_2 is then

$$M_{c,tot} = MX_c \tag{C-5}$$

where M is the total mass of backflow and X_c is defined as

$$X_c = X_{cl} + X_{cg} = \frac{k_{rl}\rho_l}{\mu_l}\nu_t X_{cl} + \frac{k_{rg}\rho_g}{\mu_g}\nu_t X_{cg} \tag{C-6}$$

Dividing the total amount of CO_2 needed by the fractions of each phase that is mobile gives the total mass of backflow per unit pore volume as

$$\frac{M}{\phi V} = \frac{\rho_{CO_2} S_g + \rho_l X_{cl}(1.-S_g)}{\frac{k_{rl}}{\mu_l}\rho_l \nu_t X_{cl} + \frac{k_{rg}}{\mu_g}\rho_g \nu_t X_{cg}} \tag{C-7}$$

This report was done with support from the Department of Energy. Any conclusions or opinions expressed in this report represent solely those of the author(s) and not necessarily those of The Regents of the University of California, the Lawrence Berkeley Laboratory or the Department of Energy.

Reference to a company or product name does not imply approval or recommendation of the product by the University of California or the U.S. Department of Energy to the exclusion of others that may be suitable.

LAWRENCE BERKELEY LABORATORY
TECHNICAL INFORMATION DEPARTMENT
UNIVERSITY OF CALIFORNIA
BERKELEY, CALIFORNIA 94720